

# On Teleost Muscle Stem Cells and the Vertical Myoseptum as Their Niche

Dissertation

der Mathematisch-Naturwissenschaftlichen Fakultät  
der Eberhard Karls Universität Tübingen  
zur Erlangung des Grades eines Doktors der  
Naturwissenschaften (Dr. rer. nat.)

vorgelegt von  
Sören Alsheimer  
aus Frankfurt am Main

Tübingen  
2012

Tag der mündlichen Qualifikation: 23.07.2012

Dekan: Prof. Dr. Wolfgang Rosenstiel

1. Berichterstatter: Prof. Dr. Christiane Nüsslein-Volhard

2. Berichterstatter: Prof. Dr. Rolf Reuter

meiner Familie



— *Noch sind sie gleich bereit, zu weinen und zu lachen,  
Sie ehren noch den Schwung, erfreuen sich am Schein;  
Wer fertig ist, dem ist nichts recht zu machen;  
Ein Werdender wird immer dankbar sein.*—

Goethe, Faust

# 1

## Acknowledgements

THIS WORK IS THE RESULT of the single most fascinating and challenging scientific endeavor in my academic career. I could not have succeeded in conducting this research project without the help of numerous people. Their remarkable insight, gentle guidance and lasting support really is the foundation of this work. This is to say 'thank you':

In particular I want to thank my academic mentor Prof. Dr. Christiane Nüsslein-Volhard (Nobel Prize in Physiology or Medicine 1995) for giving me the opportunity to work in her lab at the Max-Planck-Institut für Entwicklungsbiologie in Tübingen. Her prudent and far-sighted advice has guided this project

from its inception to its end and her continuing trust has finally allowed it to come to fruition.

Further I want to thank the reviewers of my PhD thesis, Prof. Dr. Christiane Nüsslein-Volhard and Prof. Dr. Rolf Reuter, the members of PhD advisory committee Prof. Dr. Christiane Nüsslein-Volhard, Prof. Dr. Rolf Reuter, Prof. Dr. Gerd Jürgens, Dr. Jana Krauss, Dr. Gáspár Jékely, Dr. Mitchell P. Levesque, and Dr. Christian Söllner for their efforts and constructive criticism.

I want to thank Dr. Brigitte Walderich. Her sincere sympathy has helped me through difficult times. Her excellent organizational skills keep this lab running smoothly and render it a top-notch working environment. Apart from this I want to thank her and her 'crew' of animal care takers for the considerable effort they are undertaking to maintain our fish. In this regard, I want to particularly thank Mario Pezzuti for doing such a great job every day.

I wish to express my gratitude to Dr. Jana Krauss for supporting me in many ways. In particular I am grateful for the *myod* BAC transgenic line that she has generated, the *tnw in situ* hybridization that she has performed, for the support that she has given me with manuscript writing, and countless discussions that we had about this project.

Gratefully I want to acknowledge Dr. Mitchell P. Levesque's (a former member of the lab, presently working at UZH, Zurich, Switzerland) contributions to this project. His bioinformatic skills and deep understanding of the analysis of microarray data were instrumental to the success of this project.

Dr. Christian Söllner's and Dr. Gavin Wright's (Sanger, Cambridge, UK) contributions concerning the AVEXIS assay were likewise very important to the success of this project and have led into a number of fascinating scientific collaborations. Apart from this I want to thank Christian for his gentle and kind way of helping me and other scholars in the lab.

I want to thank Alessandro Mongera for his sincerity, collegiality, and dedication. Further I wish to record my gratitude to Dr. Heinz Schwarz, Dr. Dirk Linke, Thomas Arnold, and Carolin Ewers for helping me with protein purification and antibody raising.

Lending a few words from William Shakespeare, I wish to thank my friends: '*A friend is one that knows you as you are, understands where you have been, accepts what you have become, and still, gently allows you to grow.*' I am truly grateful for having friends like this. Alexandra Wigand, Pantelis Astrinidis, Arpita Kulkarni, Julia Noack, and Thomas Hörtig shall not remain unmentioned at this point. A special 'Thank you!' goes out to my number one ace, Dr. Martin Wigand, for being someone, that I can count on no matter what happens.

I wish to thank Ines Wolff for everything that we shared and all the support that she has given me throughout the years.

For giving me '*roots and wings*', I owe my deepest gratitude to my mom and dad, Jutta and Volker, my late grandmother, Irmgard Alsheimer, my grandfather, Helmuth Alsheimer, my sister, Ragna, and my brothers, Ingmar and Marvin. Their continuing faith in me, boundless patience, and caring love is

hardly deserved but warmly appreciated. These humble lines do not suffice to express my thankfulness. I dedicate this work to them.

Finally, I want to thank my girlfriend, Alessandra Romano, for her unwavering love and understanding.

# Contents

|          |  |           |
|----------|--|-----------|
| <b>1</b> | <b>Acknowledgements</b>  | <b>5</b>  |
| <b>2</b> | <b>Summary</b>   | <b>23</b> |
| <b>3</b> | <b>Highlights</b>  | <b>27</b> |
| <b>4</b> | <b>Zusammenfassung</b>   | <b>29</b> |
| <b>I</b> | <b>Introduction</b>  | <b>33</b> |
| <b>5</b> | <b>Stem cells</b>  | <b>35</b> |
| 5.1      | A definition of the term ‘stem cell’ . . . . .                     | 37        |
| 5.2      | Stemness, Potency, Differentiation and Cell Lineages . . . . .     | 38        |
| 5.3      | Existence of stem cells . . . . .                                  | 40        |
| 5.4      | Mechanisms of self-renewal . . . . .                               | 42        |
| 5.5      | The niche concept . . . . .  | 44        |
| 5.6      | Stem cell heterogeneity and landscape models . . . . .             | 46        |
| 5.7      | Identification of stem cells and stem cell heterogeneity . . . . . | 48        |

|           |   |           |
|-----------|---|-----------|
| <b>6</b>  | <b>Muscle development and growth in vertebrates</b>                                   | <b>53</b> |
| 6.1       | Gene regulatory networks governing myogenic differentiation . . . . .                 | 55        |
| 6.2       | Primary myogenesis and the developmental origin of satellite cells . . . . .          | 57        |
| 6.3       | Satellite cells of skeletal muscle . . . . .  | 60        |
| 6.4       | Notch signaling and MSC maintenance . . . . .   | 63        |
| 6.5       | Evidence for a possible role of Numb in asymmetric self-renewal of MSCs . . . . .     | 67        |
| <b>7</b>  | <b>Experimental strategy</b>  | <b>69</b> |
| <b>8</b>  | <b>Aim of this work</b>   | <b>75</b> |
| <b>II</b> | <b>Results</b>  | <b>79</b> |
| <b>9</b>  | <b>Intravital imaging-based reconstruction of the teleost myogenic lineage</b>        | <b>81</b> |
| 9.1       | Generation of a zebrafish <i>pax7::GFP</i> BAC transgenic line . . . . .              | 83        |
| 9.2       | Non-invasive intravital imaging of primary myogenesis in zebrafish . . . . .          | 83        |
| 9.3       | Three types of Pax7 <sup>+</sup> MPs during secondary myogenesis . . . . .            | 91        |
| 9.4       | DMPs give rise to the quiescent MSCs of secondary myogenesis . . . . .                | 93        |
| <b>10</b> | <b>Direct isolation and transcriptional profiling of teleost Pax7<sup>+</sup> MPs</b> | <b>99</b> |

|  |            |
|--|------------|
| <b>11 Morpholino screen</b>  | <b>107</b> |
| <b>12 Systematic screening for novel extracellular MSC-niche protein-protein interactions</b>                    | <b>113</b> |
| <b>13 Niche extracellular matrix component Tenascin W regulates muscle stem cell self-renewal</b>                | <b>119</b> |
| 13.1 Tenascin W is required for MSC maintenance . . . . .  | 120        |
| 13.2 Tenascin W interacts with Notch ligands DeltaA and B . . . . .  | 126        |
| <b>III Discussion</b>  | <b>131</b> |
| <b>14 Identification of teleost MSCs and their origin in the teleost dermomyotome</b>                            | <b>133</b> |
| 14.1 Teleost MSC maintenance may be governed by symmetric cell division and stochastic differentiation . . . . . | 137        |
| <b>15 The vertical myoseptum functions as the MSC niche in teleosts</b>  | <b>139</b> |
| 15.1 On the evolution and ontogeny of the vertical myoseptum . . . . .   | 142        |
| 15.2 Muscle stem cells construct their own niche . . . . .   | 143        |
| 15.3 Tenascin W, a niche molecule and novel regulator of Notch signaling . . . . .                               | 145        |
| <b>16 MSC/MP-secreted proteins with auto-/paracrine signaling function</b>                                       | <b>149</b> |

|  |            |
|--|------------|
| <b>17 Approaching a MSC gene expression signature conserved across the vertebrate subphylum</b>                                      | <b>153</b> |
| <b>IV Further Findings and Projects</b>  | <b>157</b> |
| <b>18 <i>thrombospondin 4B</i> morphants develop severe muscular dystrophy</b>   | <b>159</b> |
| <b>19 Teleost MSCs secrete known and <i>bona fide</i> novel components of the Hh signaling pathway</b>                               | <b>163</b> |
| 19.1 Wnt inhibitory factor 1(Wif1) deposited at the vertical myoseptum is essential for correct somite patterning . . . . .          | 164        |
| 19.2 A2CEY7 is a novel candidate component of the Hedgehog signaling pathway . . . . .   | 172        |
| <b>20 Auto- and paracrine Csf1-FMS signaling regulates <i>pax7</i> expression during teleost neural crest and muscle development</b> | <b>175</b> |
| 20.1 Functional and topological divergence of Csf1-FMS ligand-receptor genes . . . . .   | 177        |
| 20.2 Csf1-FMS signaling regulates Pax7 expression .  | 180        |
| <b>21 Concluding Remarks</b>   | <b>185</b> |
| <b>V Materials and Methods</b>   | <b>191</b> |
| <b>22 Experimental Procedures</b>  | <b>193</b> |
| 22.1 Fish strains . . . . .  | 193        |

|           |  |            |
|-----------|--|------------|
| 22.2      | Generation of Tg( <i>pax7</i> :EGFP) <sup>sa</sup> BAC transgenic line . . . . . | 194        |
| 22.3      | Non-invasive intravital 4D imaging . . . . .                                     | 194        |
| 22.4      | Direct Isolation of Pax7 <sup>+</sup> MSCs/MPs by FACS-sorting . . . . .         | 195        |
| 22.5      | Microarray Profiling . . . . .   | 197        |
| 22.6      | Raising and Affinity Purification of Zebrafish Pax7 Antibody . . . . .           | 197        |
| 22.7      | Antibody Staining . . . . .  | 198        |
| 22.8      | Histology . . . . .  | 199        |
| 22.9      | <i>in situ</i> Hybridization . . . . .   | 199        |
| 22.10     | Morpholino Injections . . . . .  | 199        |
| 22.11     | Extracellular protein-protein interaction screen (AVEXIS) . . . . .              | 200        |
| <b>VI</b> | <b>Supplemental Data</b>   | <b>203</b> |
| <b>23</b> | <b>Author contributions</b>  | <b>215</b> |
| <b>24</b> | <b>Bibliography</b>  | <b>217</b> |
| <b>25</b> | <b>Curriculum vitae</b>  | <b>247</b> |



# List of Figures

|      |  |    |
|------|--|----|
| 9.1  | Schematic of the zebrafish <i>pax7a</i> locus, BAC recombination and overview of transgene expression at 4dpf. . . . . | 82 |
| 9.2  | Myomeric organization of the axial musculature in teleosts. . . . .  | 84 |
| 9.3  | Timeline of myogenesis in zebrafish larvae. . . . .  | 85 |
| 9.4  | Intravital imaging of Pax7 <sup>+</sup> MPs during primary myogenesis and transition phase . . . . .                   | 87 |
| 9.5  | Intravital imaging of <i>pax7::GFP</i> ; <i>pfe/pfe</i> embryos during transition phase. . . . .                       | 90 |
| 9.6  | Anatomical and cell morphological classification of Pax7 <sup>+</sup> MPs during secondary myogenesis . . . . .        | 92 |
| 9.7  | Intravital imaging-based clonal analysis identifies DMPs as the actual MSCs in teleosts. . . . .                       | 93 |
| 9.8  | Live imaging Pax7 <sup>+</sup> MPs during secondary myogenesis. . . . .  | 95 |
| 9.9  | 4dpf dorsomedial trunk in inside-to-outside view and normal shading projection. . . . .                                | 96 |
| 9.10 | Early myoblasts (EMBs) give rise to fusion-competent myoblasts (FcMBs). . . . .  | 96 |

|      |  |     |
|------|--|-----|
| 9.11 | Intravital imaging and clonal analysis of early myoblasts (EMBs). . . . .  | 98  |
| 10.1 | Direct isolation of zebrafish Pax7 <sup>+</sup> MSCs/MPs.  | 100 |
| 10.2 | Transcriptional profiling of Pax7 <sup>+</sup> MSCs/MPs.   | 102 |
| 10.3 | Pax7 <sup>+</sup> MSCs/MPs secrete candidate niche components. . . . .   | 104 |
| 11.1 | Morphology of ATG MO-injected embryos during segmentation phase. . . . .   | 109 |
| 12.1 | AVEXIS Screening of Seraf and NLRP1 . . . . .  | 116 |
| 12.2 | AVEXIS Screening of Wfdc1 . . . . .  | 117 |
| 13.1 | Domain structure of Tenascin W and transcript expression at 4dpf. . . . .  | 120 |
| 13.2 | Tnw is essential for MSC maintenance . . . . .   | 121 |
| 13.3 | Quantification of Pax7 <sup>+</sup> DMP cells in <i>tnw</i> morphants vs. 5 mismatch morpholino (5MM)-injected controls. . . . .                           | 122 |
| 13.4 | Morphological and histological defects in <i>tnw</i> morphants at day 2. . . . .   | 124 |
| 13.5 | Muscle growth and vasculogenesis defects in <i>tnw</i> morphants. . . . .  | 125 |
| 13.6 | Aberrant cell morphology of DMPs in 4day-old <i>pax7::GFP tnw</i> morphants. . . . .   | 126 |
| 13.7 | Intravital imaging-based clonal analysis of DMPs in a 4day-old <i>tnw</i> morphant shows illegitimate activation of the quiescent MSC compartment. . . . . | 127 |
| 13.8 | AVEXIS screen of a Tnw deletion construct for extracellular protein-protein interaction partners identifies Notch ligands DeltaA and B. . . . .            | 128 |

|      |  |     |
|------|--|-----|
| 14.1 | Working model of the myogenic lineage in teleosts.   | 136 |
| 15.1 | Presence of Pax7 <sup>+</sup> MSCs at the vertical myoseptum in juvenile <i>wild type</i> and <i>pfeffer</i> mutant zebrafish. . . . . | 140 |
| 18.1 | Morphology of <i>thsb4b</i> ATG MO-injected embryos during segmentation phase. . . . .   | 160 |
| 18.2 | Hypomorphic <i>thsb4b</i> ATG morphant larvae display severe muscular dystrophy. . . . .   | 162 |
| 19.1 | Wnt inhibitory factor 1 (Wif1) is immobilized at the vertical myoseptum. . . . .   | 165 |
| 19.2 | The vertical myoseptum is a zone of low canonical Wnt signaling activity. . . . .  | 167 |
| 19.3 | Morphology of <i>wif1</i> ATG morphants at mid-segmentation stage and 48hpf. . . . .   | 168 |
| 19.4 | Somite patterning defects in 24hpf <i>wif1</i> ATG morphants. . . . .  | 170 |
| 19.5 | Anti-Pax7, Anti-MF20 immunohistochemistry reveals changes in MSC number and overall muscle histology in selected morphants. . . . .    | 173 |
| 20.1 | Divergent expression patterns of teleost <i>csf1</i> paralogs. . . . .   | 178 |
| 20.2 | Functional divergence of Csf1 ligand paralogs in teleost fish. . . . .   | 179 |
| 20.3 | Csf1-Csf1r/FMS signaling regulates Pax7 expression. . . . .  | 181 |
| 20.4 | Working model of the autocrine and paracrine Csf1-FMS signaling cross-talk between MSCs and xanthophores. . . . .                      | 183 |



# List of Tables

|      |  |     |
|------|--|-----|
| 9.1  | Estimated cell cycle duration for DMPs, CMPs, and EMBs in 4-6dpf zebrafish larvae. . . . . | 97  |
| 11.1 | Morpholino screen summary. . . . .   | 110 |
| 17.1 | Molecular signature of quiescent MSCs conserved throughout vertebrate evolution. . . . .   | 155 |
| 22.1 | Supplemental movies. . . . .   | 196 |
| 22.2 | Morpholinos used in this study. . . . .  | 201 |
| 22.3 | ‘Teleost MSC microarray profiling’ dataset . . .   | 205 |
| 22.4 | AVEXIS screen of Tnw(5xFn-FG) deletion construct vs. bait protein library. . . . .         | 210 |



# List of Abbreviations

|         |   |
|---------|---|
| 5MM     | 5 mismatch morpholino                             |
| A486nm  | absorption at 486nm                               |
| ACD     | asymmetric cell division                          |
| ATG     | start codon                                       |
| AVEXIS  | avidity-based extracellular interaction screening |
| BAC     | bacterial artificial chromosome                   |
| BrdU    | bromodeoxyuridine                                 |
| CMP     | committed myogenic progenitor                     |
| ComN    | commissural neuron                                |
| DMP     | dermomyogenic progenitor                          |
| ECM     | extracellular matrix                              |
| EMB     | early myoblast                                    |
| EMT     | epithelial-to-mesenchymal transition              |
| ES cell | embryonic stem cell                               |
| FACS    | fluorescence activated cell sorting               |
| FcMB    | fusion-competent myoblast                         |
| FfMB    | fibre-forming myoblast                            |
| FSC-A   | forward scatter-amplitude                         |
| GFP     | green fluorescent protein                         |
| HB      | hindbrain   |

|                 |       |                                    |
|-----------------|-------|------------------------------------|
| Hh              | ..... | hedgehog                           |
| MF              | ..... | muscle fibre                       |
| MO              | ..... | morpholino                         |
| MP              | ..... | myogenic progenitor                |
| MPI             | ..... | Max-Planck-Institute               |
| MRF             | ..... | myogenic regulatory factor         |
| MSC             | ..... | muscle stem cells                  |
| NICD            | ..... | Notch intracellular domain         |
| SCD             | ..... | symmetric cell division            |
| SSC-A           | ..... | side scatter-amplitude             |
| StDev, $\sigma$ | ..... | standard deviation                 |
| TA cell         | ..... | transit-amplifying cell            |
| TGF $\beta$     | ..... | transforming growth factor $\beta$ |
| Xph             | ..... | xanthophore                        |

— Solch ein Ragout es muss Euch glücken;  
Leicht ist es vorgelegt, so leicht als ausgedacht,  
Was hilft's, wenn Ihr ein Ganzes dargebracht,  
Das Publikum wird es Euch doch zerpfücken.—

Goethe, Faust

# 2

## Summary

**P**AX7<sup>+</sup> MUSCLE STEM CELLS (MSCs) drive muscle growth and repair in tetrapod muscle. A zebrafish *pax7::GFP* line was generated to study teleost MSCs by intravital imaging. This non-invasive, explorative and unbiased approach (A) allows muscle stem cells and their committed progeny to be monitored in their unperturbed tissue microenvironment, and (B) allows clonal relationships amongst Pax7<sup>+</sup> myogenic progenitors to be clarified by intravital imaging-based clonal analysis. In this way it was possible to reconstruct the myogenic lineage both qualitatively and quantitatively. This tool was further used to isolate teleosts MSCs and perform transcriptional pro-

filing. The data presented here show (A) that teleost MSCs derive directly from a population of Pax7<sup>+</sup> dermomyogenic progenitors, which form an epithelial sheet of cells - the teleost dermomyotome - covering the maturing somite, (B) that the niche for teleost MSCs is the vertical myoseptum, a thin sheet of extracellular matrix connecting neighbouring somites, and (C) that teleost MSCs contribute to the formation of their own niche by secreting a number of ECM components.

The use of zebrafish as a model system further allowed a systematic reverse genetics screen involving more than 20 genes equaling roughly 12,5% of the profiling candidate genes to be performed, using morpholinos, which provide a rapid and inexpensive way of assessing gene function. This led to the identification of muscle-related phenotypes for *csf1b*, *wfdc1*, *wif1*, which encode secreted signaling molecules and modulators, for *cdon*, *A2CEY7*, which are present on the cell surface, as well as for *fmod*, *thbs4b*, *tnw*, *olfml2Bb*, which are extracellular matrix components. While some of these knockdowns affect the myogenic lineage primarily at the level of the muscle stem cells, others seem to impact on myoblast function or perturb the attachment of muscle fibres to the extracellular matrix. The AVEXIS technology was exploited to screen a library of extracellular bait proteins for interaction with MSC-derived secreted proteins, including cell surface molecules, ligands and ECM components. The combination of functional and biochemical data has led to a number of distinct projects, whose core observations and conclusions are briefly summarized in the following:

- Tenascin W (Tnw) - an MSC-derived hexameric ECM

component, which is abundantly expressed in human glioblastoma as well as tumors of the brain, breast and colon - interacts with the Notch ligands DeltaA and B. Upon knockdown of Tnw MSC number declines dramatically as a result of illegitimate activation. These findings establish Tnw, one of the most specific markers of human cancer, as an MSC-derived niche molecule, and implicate Tnw in Notch signaling.

- Csf1b is one of most strongly upregulated genes in teleost MSCs. *csf1a* and *csf1b* as well as the *csf1r* receptor paralogs diverged in terms of function and expression pattern during the course of teleost evolution. *pax7* reporter activity is strongly reduced in *csf1ra* mutant (*pfef-fer*) xanthophores suggesting that Csf signaling regulates Pax7 expression in the neural crest and possibly also the myogenic lineage.
- The GPI-anchored cell surface molecule A2CEY7 is a *bona fide* novel, essential component of Hh signaling.
- Seraf, an EGF-type orphan ligand expressed in the dermo-myotome and later by MSCs, binds to FGFR4 receptor constituting an autocrine feedback-loop. Apart from its interaction with FGFR4 two further novel interactions with the extracellular hub protein Opticin and Kon-Tiki 3/Cspg4 were detected.



— Drei Jahr ist eine kurze Zeit,  
Und, Gott! das Feld ist gar zo weit,  
Wenn man einen Fingerzeig nur hat,  
Lässt sich's schon eher weiter fühlen. —

Goethe, Faust

# 3

## Highlights

- First intravital imaging of muscle stem cells (MSCs)
- Reconstruction of the teleost myogenic lineage by *in vivo* clonal analysis
- Identification of teleost MSCs, CMPs and EMBs inside the Pax7<sup>+</sup> MP compartment
- Estimation of mean cell cycle time for MSCs (120h) and their committed progeny (30-40h) in a 4-5dpf zebrafish larva
- The vertical myoseptum serves as the teleost MSC niche

- MSCs secrete candidate niche ECM components
- Discovery of novel MSC-niche interactions through biochemical (AVEXIS) and functional (morpholino) screening
- Tenascin W is an essential MSC-derived MSC niche component
- Tenascin W interacts with Notch ligands DeltaA and B
- Autocrine Csf1-FMS signaling regulates Pax7 expression

— Bescheidne Wahrheit sprech ich dir.  
Wenn sich der Mensch, die kleine Narrenwelt  
Gewöhnlich für ein Ganzes hält -

Goethe, Faust

# 4

## Zusammenfassung

**P**<sub>AX7</sub><sup>+</sup> MUSKELSTAMMZELLEN (MSCs) erlauben das Wachstum und die Regeneration der Muskulatur der Tetrapoda. Im Zuge der vorliegenden Studie ist eine *pax7::GFP* transgene Zebrafischlinie erzeugt worden, die es erlaubt MSCs durch intravitale Mikroskopie zu untersuchen. Dieser nicht-invasive, explorative und vorurteilsfreie Ansatz erlaubt es (A) MSCs und ihre Progenitoren im ungestörten Gewebekontext zu verfolgen und (B) die klonalen Beziehungen zwischen Pax7<sup>+</sup> myogenen Progenitoren durch intravitale klonale Analyse aufzuklären. In dieser Weise war es möglich die myogene Linie qualitativ und quantitativ zu rekonstruieren. Die *pax7::GFP* transgene Linie

wurde weiterhin benutzt, um MSCs zu isolieren und im Hinblick auf ihre Genexpression zu analysieren. Die hier präsentierten Daten zeigen (A) daß die MSCs der Knochenfische direkt aus einer Population Pax7<sup>+</sup> dermomyogener Progenitoren hervorgehen, die ein epitheliales Zellblatt – das Dermomyotom der Knochenfische – bilden, welches den reifenden Somiten überspannt, (B) daß das vertikale Myoseptum, eine dünne Schicht extrazellulärer Matrix zwischen den Somiten, die Nische für MSCs in Knochenfischen bildet, und (C) daß die MSCs der Knochenfische selbst zum Aufbau ihrer Nische beitragen.

Die Verwendung des Zebrafisches als Modellsystem erlaubte es im Weiteren eine systematische revers-genetische Suche durchzuführen, in die mehr als 20 Gene eingeschlossen wurden, die in etwa 12,5% der Kandidatengene des Transkriptionsprofils entsprechen. Zu diesem Zweck wurden Morpholinos verwendet, die es erlauben schnell und kostengünstig Rückschlüsse auf die Funktionen der jeweiligen Kandidatengene zu ziehen. Dies führte zur Identifizierung von muskelbezogenen Phänotypen für *csf1b*, *wif1*, welche sekretierte Signalmoleküle bzw. -modulatoren kodieren, für *cdon*, *A2CEY7*, die Zelloberflächenproteine kodieren, sowie für *fmod*, *thbs4b*, *tnw* und *ofml2b*, die Komponenten der extrazellulären Matrix (ECM) kodieren. Während einige dieser Knockdowns die myogene Linie primär auf der Ebene der Muskelstammzellen betreffen, scheinen andere hauptsächlich die Funktion der Myoblasten oder die Anheftung der Muskelfasern an die extrazelluläre Matrix zu beeinträchtigen.

Die AVEIXIS Plattform wurde genutzt, um durch eine sys-

tematische Suche neue extrazelluläre Protein-Protein-Wechselwirkungen zwischen MSC-sekretierten Proteinen und Zelloberflächenproteinen, Liganden und ECM-Komponenten zu finden. Die Kombination von funktionellen und biochemischen Daten führte zu unterschiedlichen Projekten, deren Kernbeobachtungen im Folgenden kurz umrissen werden sollen:

- Tenascin W (Tnw) – ein MSC-sekretiertes ECM-Molekül, welches stark in humanen Glioblastomen und anderen Tumoren des Gehirns, der weiblichen Brust und des Dickdarms exprimiert ist – interagiert mit den Notch-Liganden DeltaA und B. Knockdown von Tnw führt zu einem deutlichen Absinken der MSC-Zahl resultierend aus der illegitimen Aktivierung und vorzeitigen Differenzierung von MSCs. Diese Ergebnisse etablieren Tnw – einen der spezifischsten Marker menschlicher Krebserkrankungen als MSC-sekretiertes MSC-Nischenmolekül und implizieren Tenascin W als Komponente des Notch-Signalwegs.
- *csf1b* ist eines der am stärksten hochregulierten Gene in den MSCs der Knochenfische. Die Paraloge, die *Csf1a* und *Csf1b*, sowie den *Csf1r*-Rezeptor kodieren, sind im Verlauf der Evolution der Knochenfische in Bezug auf ihre Expression und Funktion divergiert. Die Aktivität des *pax7* Reporters ist stark reduziert in den Xanthophoren von *csf1ra* Mutanten (*pfeffer*), was daraufhinweist, daß *Csf1* die Expression von *Pax7* in Zellen der Neuralleiste und möglicherweise auch in Zellen der myogenen Linie steuert.

- Das GPI-verankerte Zelloberflächenmolekül A2CEY7 ist eine *bona fide* neue und essentielle Komponente des Hh-Signalwegs.
- Seraf, ein 'orphan ligand', der im Dermomyotom und später durch MSCs exprimiert wird, bindet an den FGF Rezeptor FGFR4. Die Interaktion mit FGFR4 konstituiert eine autokrine Schleife. Neben der Interaktion mit FGFR4 konnten zwei weitere Interaktionen mit dem extrazellulären 'hub protein' Opticin und dem Transmembranprotein Kon-Tiki 3/Cspg4 gefunden werden.

# Part I

## Introduction



— *Schon gut! Nur muß man sich nicht allzu ängstlich quälen  
Denn eben wo Begriffe fehlen,  
Da stellt ein Wort zur rechten Zeit sich ein.* —

Goethe, Faust

# 5

## Stem cells

**E**VEN UNDER physiological conditions vertebrate organs experience a continuous loss of differentiated cells due to cell death (Biteau et al., 2011; Pellettieri and Sanchez Alvarado, 2007). While some organs, such as the blood, intestine, or skin, lose and replace excessive amounts of cells each day other organs, such as the brain, heart or skeletal muscle, show very little tissue turnover and were thus regarded ‘postmitotic’ organs for most of the 20th century. In fact the paradigm that the human brain is essentially a fixed structure with no capability of postnatal neurogenesis was so strong that the initial demonstration that neurogenesis occurs in the mammalian

brain by Altman in 1963 was simply neglected by the scientific community (Altman and Das, 1965). Too strong was the impression that the intricate complexity of the adult brain, which had been characterized by Camillo Golgi and Santiago Ramón y Cajal (Nobel Prize in Physiology or Medicine 1906) at the turn of the 19th century (Cajal, 1906), could allow for integration of new cells. Work of the last decades has established that many, if not all, adult vertebrate organs including the brain and heart show at least some degree of physiological cell turnover. In a very elegant way tissue turnover rates have recently been determined for the human brain, heart and other organs, which exhibit very low cell turnover rates. These studies made use of the fact that nuclear bomb tests released a significant amount (pulse) of  $^{14}\text{C}$  isotope into the atmosphere until 1963, when the Partial Test Ban Treaty was signed, leading to a phase of exponential atmospheric  $^{14}\text{C}$  decay (chase). Annual renewal rates for human cells have been estimated for adipocytes (10%) and cardiomyocytes (1%-0.25%), based on the  $^{14}\text{C}$ -content of their genomic DNA (Bergmann et al., 2009; Spalding et al., 2008; Spalding et al., 2005).

Interestingly, physiological cell turnover rates do not necessarily mirror regenerative capacity of vertebrate organs. Skeletal muscle for instance displays robust regenerative potential, but only low physiological cell turnover. As such, big differences exist regarding the self-renewal rates and regenerative capacity amongst vertebrate organs. Likewise, for each particular organ these properties vary considerably between different vertebrate taxa. While the brain and heart of humans essentially do not regenerate after injury, zebrafish or axolotl show a remarkable capacity to regenerate these organs even after severe trauma

(Brockes et al., 2001; Tanaka and Reddien, 2011). Independent of the extent to which different adult vertebrate organs are capable of replacing lost or injured cells, this raises the question of how new cells can be generated in an adult organ and how they can functionally integrate into preexisting tissue context.

In principle these new cells could derive from the division of differentiated cells. Indeed hepatocytes of the liver (Fausto, 2000) or  $\beta$  cells of the pancreas are able to generate new cells by duplication (Dor et al., 2004). In these cases fully differentiated cells divide to generate new cells that in turn contribute to organ growth and regeneration. The vast majority of the more than 200 fully differentiated cell types found in adult mammals, including neurons, muscle fibres, cardiomyocytes, enterocytes, and so forth are, however, postmitotic cells (Buttitta and Edgar, 2007). This implies that newly generated cells must derive from a tissue resident population of cells, which retain the capacity to generate progenitor cells capable of differentiating into the appropriate cell type. These cells are known as stem cells.

## 5.1 A definition of the term ‘stem cell’

The term stem cell has been promiscuously used in the literature. A clear definition of the term therefore seems to be important: stem cells should be defined as the most upstream component of a particular cellular lineage capable of continuously giving rise to committed progenitors that will ultimately differentiate into one (i.e. unipotent) or more (i.e. oligo- or

multipotent) differentiated cell types. The defining characteristics of stem cells are thus ‘long-term’ self-renewal and potency. The former means that stem cells are maintained over extended periods of time, the latter that stem cells are less differentiated than their progeny. The combination of these two properties is referred to as stemness.

## 5.2 Stemness, Potency, Differentiation and Cell Lineages

The nature of stem cells as cells being equipped with stemness can only be understood involving other concepts of developmental biology, which are potency, differentiation and cell lineages (Leychkis et al., 2009). Ultimately all cells found in a metazoan body derive from the fertilized zygote. Soon after fertilization the zygote starts to undergo cleavage divisions generating blastomeres leading to the formation of what is generally referred to as the blastula. Through transplantation experiments in a wide variety of metazoan species it was found that blastomeres have the potency to give rise to all cells of the adult animal (Carlson, 2010). As development proceeds, the potency of embryonic precursors is gradually restricted. This means that precursors are channeled into distinct cell lineages, which fan out into the distinct terminal cell fates or cell types found in the adult animal. This process is referred to as differentiation. Differentiation is the result of patterning processes and inductive events, which lead initially equipotent cells to adopt divergent fates (Wolpert, 1971; Wolpert, 2002). Each of these distinct cell fates is associated with a distinct gene

expression signature. The key fate choices that precede terminal differentiation as well as the latter establishment of cell type-specific gene expression signatures is guided by small sets of transcription factors, which form gene regulatory networks that control large numbers of target genes (Betancur et al., 2010; Erwin and Davidson, 2009). Gene regulatory networks may be activated by as little as just one transcription factor, which is sufficient to activate a small set of cooperating further transcription factors thereby 'firmly' establishing a gene regulatory network, that orchestrates the activation of a large set of target genes needed to drive terminal differentiation. These particularly powerful transcription factors, sometimes referred to as master regulators, have profound influence on global gene expression patterns and hence cell fate choice. This raises the question whether or not there is a molecular regulatory network common to all adult stem cells. *A priori* this appears to be unlikely as adult stem cells of distinct cell lineages apparently underwent a number of critical cell fate choices, like allocation into ecto-, endo-, or mesodermal lineages, and consequently express distinct sets of 'master regulators'. This is illustrated by the prominent roles of transcription factors like Sox10 in the neural crest cell (Kelsh, 2006), Pax3/7 in the myogenic (Buckingham and Relaix, 2007), Gata 1/2/3 in the hematopoietic (Bresnick et al., 2012) and PU.1 in the myelopoietic lineage (Burda et al., 2010). Consistent with this view it has been argued that stemness may result from the inhibition of differentiation and not from the execution of a 'stemness program' (Casanova, 2012; Mikkers and Frisen, 2005). In this sense stemness is seen as the 'default state'. In 2002 two studies appeared reporting the identification of a molecular signature

of stemness by comparative transcriptomics of ES cells, hematopoietic stem cells and neural stem cells (Ivanova et al., 2002; Ramalho-Santos et al., 2002). A year later a similar study was published this time involving ES cells, neural stem cells, and retinal stem cells (Fortunel et al., 2003). To the surprise of the authors these three ‘stemness’ gene sets had only one gene in common encoding Integrin  $\alpha 6$ . Despite these results comparative transcriptomic or proteomic analysis of distinct adult vertebrate stem cell population are, in principle, suited to address the question. Currently, however, the precision with which adult stem cells can be defined in vertebrates does not allow distinct stem cell populations to be isolated with sufficient purity. Even for hematopoietic stem cells fluorescence activated cell sorting (FACS) based on as many as seven distinct molecular markers does not yield populations of more than 50% purity (Schroeder, 2010). Thus it remains an unresolved issue, whether or not there is a universal core regulatory network ensuring stemness in adult stem cell populations of distinct cellular lineages.

### 5.3 Existence of stem cells

The existence of stem cells was first demonstrated by bone marrow transplantation experiments, conducted in the 1960s. Following to the transplantation of bone marrow into lethally irradiated mice Till and McCulloch observed the formation of nodules in the spleen, which were later shown to derive from single cells that were called ‘colony forming units’ (Till and McCulloch, 1961). In parallel Donall E. Thomas (Nobel Prize in

Physiology or Medicine 1990) performed the first bone marrow transplantation to treat a leukemia patient with a bone marrow transplant from a healthy identical twin (Thomas, 2005). Likewise, George Mathé succeeded in performing the first allograft of bone marrow in an attempt to rescue workers that had received a lethal dose of radiation due to a criticality accident (Mathé, 1959). Taken together these studies demonstrated that bone marrow contains adult stem cells capable of long-term reconstituting complex adult tissues, i.e. tissues such as bone marrow and blood, which are made up of a number of distinct differentiated cell types. As such these experiments for the first time experimentally demonstrated the two principal traits of stem cells, the capability to self-renew (self-renewal) and to give rise to one or multiple types of differentiating progeny (potency). Cells, which are equipped with these remarkable properties, have been identified during the past decades in a number of invertebrate (Spradling et al., 2008) and vertebrate organs (Blanpain and Fuchs, 2006; Blanpain et al., 2007; Marshman et al., 2002; Morrison and Spradling, 2008; Potten, 1981; Snippert and Clevers, 2011; Weissman, 2000; Zhao et al., 2008). In *Drosophila* and *Caenorhabditis elegans* adult stem cells have been identified in the germline (germline stem cells) as well as in the soma (somatic stem cells). In these species the possibility to gain direct visual access to potential stem cells allowed the unequivocal identification of stem cells by intravital imaging-based clonal analysis. In mammalian vertebrates the existence of stem cells has been shown for a number of organs including the brain, blood, colon, intestine, skeletal muscle, and skin (Blanpain and Fuchs, 2006; Blanpain et al., 2007; Marshman et al., 2002; Morrison and Spradling, 2008; Potten,

1981; Snippert and Clevers, 2011; Weissman, 2000; Zhao et al., 2008). In light of these findings it seems reasonable to assume that most, if not all, vertebrate organs contain adult stem cell populations that enable life-long tissue homeostasis.

## 5.4 Mechanisms of self-renewal

The function of stem cells is to provide a long-term source of multi- or oligopotent progenitor cells, which drive tissue self-renewal and regeneration following tissue damage. This implies that stem cells must be able to maintain themselves (self-renew) either on the single cell or on the population level and retain some degree of potency (Ohlstein and Spradling, 2006; Simons and Clevers, 2011; Voog and Jones, 2010). Conceptually self-renewal can be achieved by at least two different modes:

- **hierarchical mode**, asymmetric cell division leads to self-renewal of the mother cell and at the same time generates a differentiating daughter cell (Knoblich, 2008; Morrison and Kimble, 2006).
- **population asymmetry or neutral drift**, in which proliferation and differentiation rates are balanced on the cell population level (Lopez-Garcia et al., 2010; Simons and Clevers, 2011; Snippert et al., 2010).

It is well established that asymmetric cell division ensures the maintenance of male and female germ line stem cells as well as neuroblasts in *Drosophila* (Knoblich, 2008). These observations have fueled the general expectation that somatic stem

cells of vertebrates, similarly, should rely on this mode of maintenance. Evidence for asymmetric cell division of vertebrate stem cells, however, is scarce and without exception indirect. Whether or not there are vertebrate stem cell populations that rely on this mode of maintenance is currently a matter of debate. In fact mathematical modeling of stem cell dynamics in the adult mouse small intestine has shown that neutral competition alone is sufficient to explain the observed cell proliferation and differentiation kinetics (Lopez-Garcia et al., 2010; Snippert et al., 2010). Recent modeling, however, suggests that during embryonic development intestinal stem cells amplify at maximal pace establishing a population of stem cells, which then switches to asymmetric cell division to maintain crypt homeostasis (Itzkovitz et al., 2012). Taken together this might indicate that stem cells may employ asymmetric cell divisions under particular developmental or physiological circumstances. Further measurements of *in vivo* stem cell and lineage dynamics are needed to resolve this issue. Similarly, reports on asymmetric DNA strand segregation in satellite cells of vertebrate skeletal muscle (Conboy et al., 2007; Rocheteau et al., 2012; Shinin et al., 2009) and other stem cell populations, such as intestinal stem cells (Potten et al., 2002) or hematopoietic stem cells (Cairns, 1975), are subject of intense controversy (Lansdorp, 2007). Recently, Multi-isotope imaging mass spectrometry (MIMS) enabled the precise quantification of  $^{15}\text{N}$  label retention in the mouse intestine. This study showed that intestinal cells do not segregate DNA template strands asymmetrically refuting the ‘immortal strand hypothesis’ for the mouse intestine (Steinhauser et al., 2012). Likewise, initial claims about asymmetric template strand segregation by

hematopoietic stem cells (Cairns, 1975) were challenged using label-retention assays (Kiel et al., 2007). Importantly, the mere detection of asymmetric cell division is not sufficient to invoke this mode of cell division as the mode of maintenance. Apart from these considerations, one has to bear in mind that asymmetry in the fate of two daughter cells can be a consequence of asymmetric cell division, i.e. *a priori* cell intrinsic asymmetry is inherited to the daughter cells, or result from the induction of different fates in two equal daughter cells (Knoblich, 2008). It thus remains an open question of how vertebrate stem cells self-renew.

## 5.5 The niche concept

The observation that stem cells fail to retain stemness once isolated from their endogenous context led to the formulation of the niche concept by Schofield in 1978 which invokes a locally defined microenvironment of special physicochemical properties generated by a support cell population (Schofield, 1978). The intrinsic propensity of stem cells to lose stemness in absence of appropriate signals seems to be a safe-guarding mechanism as cells with robust proliferative capacity are inherently dangerous to the organism. Studies on *Drosophila* and *C. elegans* germ line stem cells were the first to identify an anatomical correlate to this concept and confirmed the existence of a support cell type providing key niche factors (Kimble and White, 1981; Xie and Spradling, 1998, 2000). In vertebrates stem cell populations have been described in a number of organs. Identifying vertebrate stem cell niches, however, has

been hampered by the inability to follow single vertebrate stem cells in the living animal with sufficient spatial resolution. This problem has led to ambiguity in the distinction of stem cells from more committed progenitors. As a result vertebrate stem cell niches remain more vaguely defined in terms of their precise microanatomy, physicochemical properties, and ontogeny (Fuchs et al., 2004; Kuang et al., 2008; Morrison and Spradling, 2008; Voog and Jones, 2010). Likewise the identity of possible support cell types and the ways in which they interact with the somatic stem cell populations remain largely unclear. Recent evidence suggests that Paneth cells of the mouse intestine function as a support cell type providing key Wnt signals necessary for intestinal stem cell proliferation (Sato et al., 2011). In the following the term niche will be used for the properties of a stem cells microenvironment that ensure the maintenance of stemness, as it has become apparent that stem cell niches generally seem to be spatially defined and do not reflect a mere combination of humoral factors. This is a very stringent definition as it excludes factors, which control the activation of stem cells, but are not needed for their self-renewal.

What we would like to understand is, how stem cell niches arise during vertebrate development. Further we would like to know the key niche factors and their cellular sources. At this point it will remain a challenging task to enlighten the ways in which niche factors interact with themselves to create the particular properties of stem cell niches and to find out how these properties are perceived by stem cells. Eventually basic research in this direction will provide the necessary insight, which must precede the application of stem cells as therapeutic agents. Specifically, a deeper knowledge of niche properties

may allow niches to be emulated in cell culture, which in turn may allow stem cell self-renewal in cell culture opening the way to robust amplification of stem cells *in vitro*.

## 5.6 Stem cell heterogeneity and landscape models

Stem cells like other cells are complex adaptive systems, i.e. the system's properties emerge from the complex interactions of the system's components and the system is able to adapt to the environment. They can therefore be treated as a dynamical system, which can be described mathematically using rate equations. The solutions to these equations are called 'attractors', because of the system's tendency to be attracted to one of these 'equilibrium states'. In 'energy landscape' representations attractors correspond to the lowest points in local depressions, while the depression itself is called a 'basin of attraction', i.e. the 'set of initial conditions from which a dynamical system will tend to move' towards a particular attractor (Enver et al., 2009; Macarthur et al., 2009). It is an important corollary from this view that two systems (cells) might take completely different paths finally ending up in the same 'basin of attraction' (cell fate; Wang et al., 2011). Further this concept explains, why there is only a limited number of observable 'network states' or cell types and why transitions between different cell types appear discrete and not continuous. Another important implication, which is illustrated by these landscape models, is that cell fate choices are robust against noise deriving from environmental changes and fluctuations in the number of mo-

lecules for example. Likewise this interpretation suggests that, while lineage progression is theoretically reversible, the ‘energy costs’ associated with it are high and thus dedifferentiation is unlikely to occur without strong stimuli. This explains why in particular terminal cell fates are practically irreversible under physiological conditions. At the same time, however, it can be understood conceptually how particular naturally occurring or experimentally induced situations can trigger dedifferentiation. In this view it seems appropriate to replace the term ‘cell type’, which was coined owing to the histological observation of terminally differentiated cells, with ‘cell states’ referring to cells of a particular cellular lineage, which are moving towards the same attractor. In other words ‘cell states’ should be defined as the sum of those ‘network states’ which together constitute a basin of attraction. In such a nomenclature the term ‘cell type’ may be meaningfully used to refer to the terminally differentiated cells of a particular cellular lineage. These ‘network theory’-based concepts, which were championed by Conrad Hal Waddington (Slack, 2002) in his ‘The strategy of the genes’ (Waddington, 1957) and Stuart Kauffman (Kauffman, 1969) and are now the research focus of system biologists, have yet to penetrate the dominating thinking about stem cells and differentiation (Enver et al., 2009). Currently, the expression of only few molecular markers is used to distinguish stem cells, committed progenitors and differentiated cells. This is problematic as stem cells, which are in a common basin of attraction moving towards a common attractor, i.e. stemness, can adopt any of the ‘network states’ defining the basin of attraction. In other words a population of stem cells assessed for a number of molecular markers might display considerable

heterogeneity in the expression of these markers, despite the fact that all of these cells move towards the same attractor and thus constitute a homogeneous population of stem cells. For this reason molecular markers are of limited use in assessing the heterogeneity of stem cell populations. The question at this point is, whether the presence or absence of a given molecular marker has functional implication, i.e. can drive the system to move out of the basin of attraction and to move towards another. In fact the expression of single transcriptional master regulators is sufficient to bring about these radical changes. A key challenge in developmental systems biology is to define the ‘nodes’ and ‘network topologies’ of these ‘network states’, i.e. the genes expression signatures and the molecular interactions amongst the gene products that characterize stem cells and progenitor populations.

## **5.7 Identification of stem cells and stem cell heterogeneity**

While research of the past five decades has convincingly demonstrated the existence of stem cells in many organs of adult invertebrate and vertebrate species, the unequivocal identification of stem cells remains a challenging task (Morrison and Spradling, 2008; Simons and Clevers, 2011). For their anatomical simplicity, and high tissue turn-over rates the vertebrate skin and intestine have become powerful models to study adult vertebrate stem cells. The general picture that emerged from these studies is that adult stem cells comprise a small population of tissue resident cells which are able to give

rise to already committed, but not yet fully differentiated cells (Potten and Loeffler, 1990). These latter cells in turn divide more frequently as they gradually become more committed finally differentiating into the appropriate cell types. These cells have been termed transit-amplifying (TA) cells. In this stem cell/TA cell model, which was largely based on studies of tissue homeostasis in the mammalian epidermis and intestinal epithelium, the main proliferative load that rest upon the cellular lineage is carried by the TA cell compartment (Potten and Loeffler, 1990). This has been interpreted to be a particular feature which allows stem cells to support a cellular lineage for extended periods of time undergoing a minimal number of cell divisions. This might protect stem cells from replicative senescence or damages to the genetic material that may arise during replication. While these efforts allowed a conceptual framework of somatic cellular lineages to be developed, they fell short of identifying the actual stem cell population. This failure is rooted in the expectation that stem cells divide only very infrequently, a feature that is also referred to as quiescence. Based on this assumption numerous slow-cycling cell populations were identified as *bona fide* stem cells in the last 30 years using pulse-chase paradigms based on nucleotide analogs, such as  $^3\text{H}$ -thymidine and BrdU, or genetic labels. In the mouse intestine so called ‘+4 cells’ residing above the crypt-located Paneth cells were found in this way and were thus believed to correspond to the intestinal stem cell compartment (Potten et al., 1997). Work of Mario R. Cappecchi’s lab (Nobel Prize in Physiology or Medicine 2007) later showed that ‘+4 cells’ express Bmi, a component of the Polycomb repressing complex 1 (Prx1). Through genetic fate mapping it

could be established that  $Bmi^+$  cells give rise to all intestinal cell fates. Moreover, ablation of  $Bmi^+$  cells by inducible expression of diphtheria toxin was sufficient to provoke a complete breakdown of intestinal homeostasis and loss of intestinal crypts (Sangiorgi and Capecchi, 2008).

Genetic lineage tracing based on the Wnt target gene and orphan receptor *Lgr5*, however, suggested that crypt base columnar cells correspond to the actual intestinal stem cell compartment (Barker et al., 2007), as postulated before (Cheng and Leblond, 1974). Intriguingly, ablation of  $Lgr5^+$  cells by knock-in of diphtheria toxin receptor in the *lgr5* locus does not lead to break down of intestinal homeostasis, but expansion of  $Bmi^+$  cells, which are normally quiescent (Tian et al., 2011). This exemplifies that, in spite of more than 40 years of intense research on an anatomically simple model system, the true identity of intestinal stem cells is still a matter of debate (Yan et al., 2012), raising the concern that current strategies used to identify stem cells based on either cell cycle kinetics or molecular markers are limited systematically and hence will not suffice for separating stem cells from their already committed progeny.

In landscape models of differentiation, such as Waddington's 'epigenetic landscape', stem cells (Waddington, 1957) and various types of TA cells are represented by distinct depressions in the landscape ('basins of attraction'; Enver et al., 2009; Macarthur et al., 2009). An important corollary from this systems biology view on differentiation is that stem cells and their immediate committed progeny might not be distinguishable based on the expression of molecular markers. In fact there

is, currently, not a single molecular marker for which it would have been demonstrated that it reliably achieves this task. In other words a homogenous population of stem cells, i.e. cells in ‘network states’ constituting a single basin of attraction, might display considerable heterogeneity in terms of gene expression patterns or network topologies. At the same time a population of cells unanimously expressing a single or even many given molecular markers, may actually correspond to a heterogeneous assembly of cells in a variety distinct cell states. In their recent review Simons and Clevers state, that ‘there is increasing emphasis on developing novel experimental characterizations of stem cell function based on phenotypic behavior over time’ (Simons and Clevers, 2011). In fact it appears that by monitoring complex traits such as cell morphology, membrane dynamics, migratory behavior, cell division mode, cell division patterns and above all clonal relationships (potency) more relevant predictions about the existence and nature of ‘cell states’ can be made.



— Wie nur dem Kopf nicht alle Hoffnung schwindet,  
Der immerfort an schalem Zeuge klebt,  
Mit gier'ger Hand nach Schätzen gräbt,  
Und froh ist, wenn er Regenwürmer findet! —

Goethe, Faust

# 6

## Muscle development and growth in vertebrates

THE MUSCULATURE of adult vertebrates displays a remarkable capacity to regenerate as well as to grow and shrink in response to increases or decreases in physiological activity (Braun and Gautel, 2011; Charge and Rudnicki, 2004; Ciciliot and Schiaffino, 2010). The growth of skeletal muscle in vertebrates seems to be primarily governed by a single signaling pathway, which involves the extracellular TGF $\beta$  family ligand Myostatin and the cell surface Activin II B receptor. Inactivating mutations of the *myostatin* gene in dogs, cattle (Belgian

Blue breed) or the *myostatin* knockout in mice cause gigantic muscle growth (Lee and McPherron, 1999, 2001; McPherron et al., 1997; McPherron and Lee, 1997). Under normal circumstances Myostatin is released by the muscle fibre systemically and restricts the growth of skeletal muscle (Joulia-Ekaza and Cabello, 2006). This indicates that skeletal muscle has an inherent propensity to grow, which normally is restricted by Myostatin signaling. The biological function is thus to limit otherwise boundless growth of muscle mass. While the limitation of muscle growth might not seem to be a desirable trait at first sight, it is clear that skeletal muscle is a key determinant of total energy expenditure. Muscle mass therefore has to be tightly adapted to the actual needs. Apart from the restrictive influence of Myostatin signaling several factors positively regulate muscle growth including IGF-1, growth hormone and androgens (Goldspink et al., 2008; Velloso, 2008). In principle muscle can grow by an increase in muscle fibre number (hyperplasia) or increase in muscle fibre size, which is accompanied by an increase in fibre diameter, length and myonuclei number (hypertrophy), the latter being the strongly dominating form of postnatal muscle growth in humans. Teleosts instead display variable shares of hyperplastic and hypertrophic muscle growth in different areas of the body (Johnston et al., 2011). Either way muscle growth is always connected to cell proliferation, which generates myoblasts that ultimately form muscle fibres *de novo* or fuse with existing ones thereby providing additional myonuclei (Abmayr and Pavlath, 2012). The source for these postnatal myoblasts enabling muscle growth and regeneration remained elusive for most of the 20th century.

## 6.1 Gene regulatory networks governing myogenic differentiation

In 1987 Davis, Weintraub and Lassar published their landmark paper showing that ‘expression of a single transfected cDNA converts fibroblasts to myoblasts’ (Davis et al., 1987). The cDNA they used in these experiments had been identified by subtractive hybridization experiments using myoblast cDNA libraries and encodes the basic Helix-Loop-Helix (bHLH) transcription factor MyoD. These findings demonstrated that cell lineage reprogramming is indeed possible by expression of a single factor. In the following years the molecular regulation of myoblast specification and differentiation was intensively investigated and additional transcription factors of the same class were identified, which likewise are able to bring about conversion to a myogenic fate. Altogether these transcription factors - MyoD, Myf5, Mrf4, and Myogenin (Myog) - constitute a family that is referred to as the Myogenic Regulatory Factor (MRF) family (Berkes and Tapscott, 2005; Rudnicki et al., 1992; Rudnicki and Jaenisch, 1995; Rudnicki et al., 1993; Tapscott and Weintraub, 1991; Weintraub et al., 1991a; Weintraub et al., 1991b). These factors constitute a genetic regulatory network, which can be set up by the expression of a single factor that in turn activates the expression of the other ‘nodes’ of this subnetwork. The stability of this cell fate decision is then likely to depend on autoregulatory loops such as the direct autoactivation of MyoD (Lun et al., 1997; Weintraub et al., 1991b) or indirect autoactivation through more complicated positive feedback-loops (Edmondson et al., 1992). The Mrf family appears to have evolved from a single *myoD* gene, which

underwent duplication and diversification giving rise to the Mrf family of recent vertebrates (Zhang et al., 1999). Like other bHLH transcription factors MRFs form homo- or heterodimers with other bHLH transcription factors. MyoD-E protein (E12, E47, E2A) or MyoD-HEB/Tcf12 dimerization (Parker et al., 2006) leads to the activation of target genes containing the cognate consensus site so called E-boxes. Amongst these target genes are MyoD (autoactivation), Myog, and Mef2, which is a member of the Myocyte enhancer factor family of transcription factors. After their activation Myog and Mef2 synergize with MyoD to establish the expression of genes needed for myogenic differentiation like *troponin*, *a-actin*, *creatine kinase* (Berkes and Tapscott, 2005; Molkenin et al., 1995; Naidu et al., 1995). It is important to note that owing to its interaction with HEB/Tcf12, the primary downstream effector of canonical Wnt signaling in skeletal muscle, MyoD functions as an integrator of Wnt signaling (Parker et al., 2006). Opposed to these pro-myogenic Wnt signals (Anakwe et al., 2003; Borello et al., 1999; Brack et al., 2008) seem to be inhibitory Notch signals, which trigger the expression of Hey1, 2 and 3 (Buas et al., 2009; Buas and Kadesch, 2010; Tsivitse, 2010). Hey1 inhibits the activation of MyoD target genes and myogenic differentiation (Buas et al., 2010). Apparently, this does not depend on dimerization with MyoD, but on cooperation with other factors and direct DNA-binding in the promoter regions of myogenic differentiation genes. Apart from Hey1 other transcription factors such as MyoR (Lu et al., 1999), Id proteins (Melnikova et al., 1999), and Sox9 (Hernandez-Hernandez et al., 2009) are potent repressors of myogenic differentiation.

Despite the significance of MyoD, Myf5, Mrf4, and Myog mouse

mutants for either of these genes display only subtle defects of developmental myogenesis pointing to considerable redundancy between MRF factors (Berkes and Tapscott, 2005). In other words, the genetic regulatory network controlling myogenic differentiation appears to be relatively robust to removal of single nodes. The most severe phenotype of these mutants is the defect of muscle regeneration seen in *myod* mutant mice (Megeny et al., 1996). Interestingly, inactivating mutations of the single *myod* homolog in *Drosophila* (*nautilus*) (Keller et al., 1998) and *C. elegans* (*hlh-1*) do not abrogate muscle development indicating that myogenic differentiation is redundantly controlled by other transcription factors. Through a synthetic lethal RNAi screen in *C. elegans* *hlh-1* mutants, two loci were identified showing genetic interaction with the *hlh-1* locus. The first of these loci - *unc-120* - was identified before in screens for ‘uncontrolled movement’ and encodes the homolog to vertebrate Serum response factor (Srf). The second, *hmd-1*, encodes the homolog of vertebrate Hand transcription factors. From these results it was concluded that MyoD, Srf and Hand constitute the core of the genetic regulatory network that controls the formation of body wall muscles in invertebrates and the formation of skeletal muscle in vertebrates (Fukushige et al., 2006).

## 6.2 Primary myogenesis and the developmental origin of satellite cells

In vertebrates, myogenesis commences shortly after segmentation in which cells of the presomitic mesoderm become al-

located into epithelial blocks: the somites (Christ and Scaal, 2008; Holley, 2007; Ordahl and Christ, 1997). It is well established that in vertebrates of all major clades the transcription factor Pax7 and its paralog Pax3 are expressed in cells of the anterior somite (Bryson-Richardson and Currie, 2008). These Pax7<sup>+</sup> cells then relocate to the outside as a result of somite rotation movements, where they form the external cell layer of Pax7<sup>+</sup> cells in anamniote species (Hollway et al., 2007; Stellabotte et al., 2007) and the epithelial dermomyotome in amniote species. The dermomyotome is an epithelial sheet of cells, which forms by somite rotation from the anterior somite half (Afonin et al., 2006; Hollway et al., 2007; Youn and Malacinski, 1981) and constitutes a transient source of embryonic Pax3<sup>+</sup>/Pax7<sup>+</sup> myogenic progenitors (MPs). In mouse and chick, Pax3<sup>+</sup>/Pax7<sup>+</sup> cells in the dermomyotome divide and migrate towards the epaxial and hypaxial lip, from which they delaminate by epithelial-to-mesenchymal transition (EMT) to populate the underlying primary myotome and limb buds. While the former will give rise to all axial musculature, the latter population of Pax3<sup>+</sup>/Pax7<sup>+</sup> MPs will give rise to the muscle of the extremities as well as the superficial muscle of the body, such as the *M. pectoralis* and *M. abdominalis* (Bentzinger et al., 2012; Buckingham and Relaix, 2007).

The primary myotome corresponds to the first muscle fibres that appear in amniote embryos directly underlying the dermomyotome. The process of seeding the primary embryonic muscle masses with dermomyotome-derived Pax3<sup>+</sup>/Pax7<sup>+</sup> myogenic progenitors is referred to as primary myogenesis in amniotes. It continues for a species-specific time before the dermomyotome disintegrates leaving behind the muscles with an endogenous

progenitor population thereby setting the stage for the next phase which accounts for postnatal muscle growth and development and is referred to as secondary myogenesis.

The primary myotome in amniotes is thought to be derived from dermomyotome-derived myogenic progenitors (Buckingham and Vincent, 2009). In *zebrafish* and *Xenopus* it could be clearly shown, however, that the primary myotome is generated from medial somitic cells (Devoto et al., 1996; Gaspera et al., 2012; Weinberg et al., 1996). As the somite matures, these medial somitic cells start to express myogenic regulatory factors, such as MyoD, and differentiate directly into slow muscle fibres, while migrating towards the outer surface of the somite, where they form a layer of slow muscle fibres (Ingham and Kim, 2005). This indicates that in anamniotes an initial phase of myogenic differentiation precedes ‘primary myogenesis’. It is possible, that this phase might likewise exist in amniote species, but has been gone unnoticed so far as these species do not lend themselves easily to intravital imaging. Assuming that the aforementioned preceding phase of myogenic differentiation is indeed a vertebrate synapomorphy it seems plausible that this initial phase is needed to build a scaffold of muscle fibres in a highly stereotypic fashion ensuring the proper orientation of the primary myotome.

Secondary myogenesis in amniote species relies on a small fraction of Pax3<sup>+</sup>/Pax7<sup>+</sup> myogenic progenitors, which were set aside and kept from differentiation to become MSCs of the adult (Relaix et al., 2005). Both Pax3<sup>+</sup>/Pax7<sup>+</sup> myogenic progenitors of the embryo and adult satellite cells originate in the dermomyotome as demonstrated by quail-chick chimeras and

genetic lineage tracing and share important aspects of their physiology (Ben-Yair and Kalcheim, 2005; Chevallier et al., 1977; Christ et al., 1977; Gros et al., 2005; Lepper and Fan, 2010; Schienda et al., 2006). The singling-out of stem cells from a homogeneous population of Pax3<sup>+</sup>/Pax7<sup>+</sup> embryonic myogenic progenitors, i.e. the balancing of stem cell self-renewal with differentiation, critically depends on Notch signaling as discussed in the following sections. The transcription factors Pax3 and Pax7 function redundantly to confer a myogenic identity onto these cells and at the same time orchestrate genetic programs that ensure MSC maintenance and repress differentiation (Bismuth and Relaix, 2010; Bryson-Richardson and Currie, 2008). The expression of Pax7 in the amniote dermomyotome as well as the teleost external cell layer has led to the conclusion that both structures are homologous (Devoto et al., 2006), despite the fact that neither MSCs nor their developmental origin have been identified in fish.

### 6.3 Satellite cells of skeletal muscle

In 1961 electron microscopy of frog skeletal muscle led to the discovery of small mononuclear cells underneath the basal lamina, which surrounds each muscle fibre (Mauro, 1961). These companions (latin *satelles*) to the gigantic muscle fibres were named satellite cells. Since their discovery satellite cells were regarded as the potential source of postnatal myoblasts (Collins et al., 2005; Moss and Leblond, 1971). Definitive evidence that the satellite cell pool contains muscle stem cells was, however, only provided in 2008 through the transplantation of single

satellite cells (Sacco et al., 2008). Both terms satellite cell and muscle stem cell are used interchangeably in the literature, despite the fact that the former is anatomically defined, while the definition of the latter is based on function. Satellite cells express the transcription factor Pax7 and include the adult muscle stem cell (MSC) population of amniote skeletal muscle (Kuang et al., 2007; Sacco et al., 2008). Lineage tracing studies have shown that about 10% of the satellite cell pool are Pax7<sup>+</sup>, Myf5<sup>-</sup> cells and display robust engraftment efficiency. The remaining 90% of the satellite cell pool are Pax7<sup>+</sup>, Myf5<sup>+</sup> cells and display only limited engraftment efficiency. These observations indicated that only 10% of the Pax7<sup>+</sup> satellite cells are actual MSCs, while the remaining 90% correspond to already committed myogenic progenitors, which are also Pax7<sup>+</sup> (Kuang et al., 2007). This observation represents a landmark in the field as it demonstrated that the previously documented heterogeneity inside the satellite cell compartment does not only reflect random fluctuations in marker expression, but is indeed functionally relevant. Further support for the notion that only a minor fraction of satellite cells are actual muscle stem cells is provided by a study, in which single genetically labelled satellite cells were isolated and transplanted into adult mouse muscle. In this study only 3 out of 72 single satellite cell transplantations led to engraftment (Sacco et al., 2008). Further along this line, the finding that a small fraction of satellite cells is Pax7<sup>+</sup>, Myf5<sup>-</sup>, which was originally based on lineage tracing experiments involving a *myf5::Cre* transgenic line, has been corroborated by immunohistochemistry using an  $\alpha$ Myf5 antibody (Gayraud-Morel et al., 2012). Apart from these findings a number of studies reported heterogeneity inside

the satellite cell compartment with respect to the expression of molecular markers and performance in engraftment assays (Gayraud-Morel et al., 2012). Taken together it appears that roughly the following percentages of satellite cells are positive for the following markers on the protein level 100% Pax7, 95% Myf5, 94% NCAM, 80% CXCR4, 12% Pax3, 1% Myog (Bir-essi and Rando, 2010; Cerletti et al., 2008; Gayraud-Morel et al., 2012; Kuang et al., 2007; Lindstrom et al., 2010; Sacco et al., 2008). This heterogeneity is not surprising, while skeletal muscle is a tissue with very low tissue turn over, it seems reasonable to assume that the myogenic lineage is made up of a stem cell and one or more transit-amplifying compartments as it is the case for other cellular lineages (Potten and Loeffler, 1990).

So far satellite cells have been identified in anuran amphibians (Mauro, 1961), birds (Gros et al., 2005), and mammals (Relaix et al., 2005). The presence of satellite cells in the musculature of adult teleost fish is widely assumed, but has not been demonstrated unequivocally. The fact that in adult urodele amphibian skeletal muscle Pax7<sup>+</sup> cells are found in a supralaminal position, i.e. above the basal lamina, which surrounds the muscle fibre, demonstrates that the ‘satellite location’ of MSCs is not a universal trait amongst vertebrates (Morrison et al., 2006).

## 6.4 Notch signaling and MSC maintenance

Owing to the problems mentioned before that relate to the unequivocal identification of vertebrate MSCs, few genuine niche factors whose activity is essential for MSC maintenance have been identified (Kuang et al., 2008). What has become apparent, though, is that the Notch signaling pathway is of central importance to vertebrate myogenesis controlling key aspects of MSC self-renewal and myogenic differentiation (Bjornson et al., 2012; Fukada et al., 2011; Luo et al., 2005; Mourikis et al., 2012; Schuster-Gossler et al., 2007; Vasyutina et al., 2007; Wen et al., 2012). The Notch signaling pathway is one of a small number of highly conserved signaling pathways, which arose with the evolution of metazoans (Gazave et al., 2009). Notch signaling has been implicated in a broad variety of biological processes including asymmetric cell division (e.g. asymmetric division of neuroblasts in *Drosophila*), cell fate control through lateral inhibition (e.g. *Drosophila* sensory organ precursor development), biological oscillators (e.g. vertebrate segmentation clock), boundary formation (e.g. *Drosophila* wing and vertebrate mid-hindbrain boundary) and stem cell maintenance (Artavanis-Tsakonas and Muskavitch, 2010; Artavanis-Tsakonas et al., 1999). Deregulation of Notch signaling has been associated with a number of human pathologies (Louvi and Artavanis-Tsakonas, 2012) including T-cell acute lymphoblastic leukemia, a highly aggressive cancer, which is caused by chromosomal rearrangements that disrupt the human *notch1* gene (Ellisen et al., 1991). Taken together these lines of evidence establish Notch as a tumor suppressor.

The discovery of this pathway began in 1914 when John S. Dexter found fruit flies that had notches at their wings. Only three years later Thomas Hunt Morgan (Nobel Prize in Physiology or Medicine 1933) identified alleles of the *Notch* locus. He went on to demonstrate that the serration of wings found in *Notch* mutants is a sex-linked dominant phenotype, whereas the homozygous condition causes lethality (Morgan, 1917). The analysis of homozygous *Notch Drosophila* mutants revealed a strong increase of the neural fate at the expense of the alternative epidermal fate in the neurogenic region of the ectoderm (Poulson, 1937, 1940). For this reason the mutation of *Notch* is said to be a 'neurogenic mutation'. This nomenclature is somewhat misleading as the function of Notch signaling in this context is to promote the epidermal fate. Chris Doe and Corey Goodman studying neurogenesis in grasshoppers performed elegant laser ablation experiments, which suggested that 'lateral inhibition' ensures the development of 'a highly stereotyped pattern' of neuroblasts in the neurogenic region (Doe and Goodman, 1985). Additional zygotic neurogenic loci including *Delta (Dl)*, *Enhancer of split [E(spl)]*, *mastermind (mam)*, *big brain (bib)*, and *neuralized (neu)* were later discovered through forward genetic screens in *Drosophila* (Jürgens, 1984; Nüsslein-Volhard, 1984; Wieschaus, 1984). Only a year later the molecular sequence of the *Notch* locus was published (Wharton et al., 1985). Notch 1 is type I transmembrane protein with extracellular domain (ECD) constituted by 36 EGF-type repeats followed by a negative regulatory region and a Notch intracellular domain (NICD, Chillakuri et al., 2012). Maturation of the Notch receptor involves proteolytic cleavage at the S1 cleavage site and subsequent heterodimer-

ization. In flies two ligands namely Delta and Serrate were shown to bind the Notch receptor (Rebay et al., 1991). The vertebrate homologs to these genes are referred to as Delta-like and Jagged. Like their receptor, Delta/Delta-like and Serrate/Jagged are single pass-transmembrane proteins, suggesting that the generic mode of Notch signaling activation involves direct contact between the signal-sending and signal-receiving cell (juxtacrine signaling). It is important to bear in mind, however, that cells may extend long filopodia allowing them to contact cells, which are multiple cell diameters apart. Such 'long-range' Notch signaling through filopodia has indeed been described (De Jossineau et al., 2003) and appears to be important for the robustness of patterning (Cohen et al., 2010). Upon binding to one of its ligands, Notch is cleaved by ADAM metalloproteases at the S2 cleavage site, liberating the extracellular domain. This allows the  $\gamma$ -secretase complex to cleave Notch at the S3 cleavage site releasing NICD (Chillakuri et al., 2012). In turn NICD is free to move into the nucleus and associate with a transcriptional repressor - referred to as SUH in flies or CBF-1/RBPJ in vertebrates - turning it into a transcriptional activator (Fortini and Artavanis-Tsakonas, 1994; Jarriault et al., 1995). The involvement of  $\gamma$ -secretase in the proteolytic processing and activation of Notch signaling explains why  $\gamma$ -secretase inhibitors can be used to block Notch signaling. It is important to note at this point that while ligand binding in *trans* leads to Notch receptor activation, *cis* interaction is known to inhibit receptor activation (Yaron and Sprinzak, 2012).

Notch signaling leads to the activation of generic Notch target genes, such as the Hey transcription factors (Leimeister et

al., 1999; Sasai et al., 1992), as well as tissue-specific Notch target genes. While there is only one *Notch* gene in *Drosophila*, mammalian genomes contain four *notch* genes encoding Notch1, 2, 3, and 4 receptors, which display divergent expression patterns and functions. In teleost species, paralogs of some of these genes are found owing to the teleost-specific genome duplication. Likewise, gene duplication led to the presence of more than one Delta-like or Jagged paralog in vertebrate genomes. Three Delta-like ligands, Dll1, Dll3, Dll4, and two Jagged ligands, Jag1 and Jag2, are encoded by mammalian genomes. Zebrafish Delta ligands are referred to as Dla, Dlb, Dlc, Dld and Dll4. It is important to note that *dla* and *dld* arose from gene duplication of the *dll1* gene, similarly *dlb* and *dlc* diverged from a single *dll3* gene. Interestingly the *dll4* gene is only present as one copy in the zebrafish genome (Gazave et al., 2009). In the context of neurogenesis and myogenesis in flies and vertebrates Notch signaling is long known to repress differentiation (Kopan et al., 1994; Nye et al., 1994; Sasai et al., 1992). Overexpression of Delta-like1 in cell culture of myogenic cells or *in vivo* in the chick limb suppresses the activation of MyoD and commitment to myogenic differentiation. Further to this point Notch signaling positively regulates *pax7* expression in C2C12 myoblasts and in satellite cells *in vivo* (Sun et al., 2008; Wen et al., 2012). The capability of Notch signaling to repress myogenic differentiation and activate *pax7* might explain why Notch signaling is in fact essential for the maintenance of embryonic Pax7<sup>+</sup> myogenic progenitors and adult MSCs (Mourikis et al., 2012). Severe muscle growth defects in the fetal phase resulting from premature differentiation of the embryonic Pax3<sup>+</sup>/ Pax7<sup>+</sup> myogenic progenitor

population are observed in Delta-like1 hypomorphic mutants and after conditional inactivation of the Notch downstream effector RBP-J (Schuster-Gossler et al., 2007; Vasyutina et al., 2007). Downstream of RBP-J two generic Notch target genes *hey1/hesr1* and *hey1/hesr3* encoding the transcription factors, Hey1 and Hey3, seem to be particularly important for MSC self-renewal as in *hesr1/hesr3* double knockout mice satellite cells fail to establish a population of quiescent MSCs and eventually decline in number during postnatal development (Fukada et al., 2011). Interestingly, 10% of the satellite cell pool which are Pax7<sup>+</sup>, Myf5<sup>-</sup> and display robust engraftment efficiency are *notch1*<sup>+</sup>, *notch3*<sup>+</sup>, *delta-like1*<sup>-</sup>, whereas 90% are Pax7<sup>+</sup>, Myf5<sup>+</sup> and *notch1*<sup>+</sup>, *notch3*<sup>-</sup>, *delta-like1*<sup>+</sup> and display only limited engraftment efficiency (Kuang et al., 2007). A number of open questions regarding the role(s) of Notch signaling in myogenesis remain to be addressed. So far studies have largely focussed on Delta-like 1 and Notch1. As mentioned before, the Notch 3 receptor appears to be specifically expressed in Pax7<sup>+</sup>, Myf5<sup>-</sup> MSCs. Regarding the role of Notch signaling in this process, a number of questions remain unresolved. These pertain to possible divergent functions of Notch1 and 3 in this context as well as to the roles of distinct Delta-like and Jagged ligands.

## 6.5 Evidence for a possible role of Numb in asymmetric self-renewal of MSCs

Numb is an endogenous cytoplasmic inhibitor of Notch signaling that was discovered in a forward genetic ‘bristle’ screen

for sensory organ development in *Drosophila* (Uemura et al., 1989). Binding of Numb to the intracellular domain of the Notch receptor triggers ubiquitination leading to receptor endocytosis and degradation (Gulino et al., 2010). Numb has a key role in asymmetric cell divisions in invertebrates (Knoblich, 2008). A classic example of this is the asymmetric distribution of Numb in *Drosophila* neuroblasts, which represses Notch signaling in one daughter cell, destined to differentiate into a ganglion mother cell, while leaving Notch signaling active in the other that self-renews the neuroblast fate. Of the three vertebrate Notch receptors Numb binds only to Notch1 and 2 targeting them for endocytosis and degradation leaving Notch3 unaffected (Beres et al., 2011). This is an important observation, as Notch3 is specifically expressed in Pax7<sup>+</sup>, Myf5<sup>-</sup> MSCs. This might mean that previously reported asymmetric distribution of Numb in isolated adult satellite cells (Shinin et al., 2009) may not pertain to the actual stem cells, but to a downstream committed progenitor compartment. As stated before it remains to be seen whether asymmetric cell division of adult satellite cells occurs *in vivo* and if so whether this is essential to MSC self-renewal. If this would indeed be the case, it still would remain a matter of debate whether asymmetric inhibition of Notch signaling by Numb is key to MSC self-renewal. Currently, the direct transfer of concepts derived from the self-renewal of invertebrate stem cells to vertebrate stem cells remains problematic due to the lack of unequivocal identification of MSCs and the lack of direct evidence for asymmetric segregation of Numb by satellite cells *in vivo*.

— *Wie schwer sind nicht die Mittel zu erwerben,  
Durch die man zu den Quellen steigt!  
Und eh man nur den halben Weg erreicht,  
Muß wohl ein armer Teufel sterben.* —

Goethe, Faust

# 7

## Experimental strategy

MOST OF WHAT we know about developmental biology in general and stem cells in particular has been derived from work with a small number of model systems including *Drosophila*, *Caenorhabditis elegans*, *Xenopus*, chick, and mouse. More recently, the zebrafish has joined this company. As experimental model systems each of these species offers a set of specific advantages and drawbacks. Mouse as a model system, for instance, offers the possibility to make changes to the genome at precise positions making use of homologous recombination and ES cell technology. This possibility represents a dedicate advantage for stem cell research mainly for two reas-

ons: (A) gene function can be analysed by generating knockout mice and (B) the fate of cells expressing certain markers can be analysed by lineage tracing making use of the Cre-loxP system (Kretzschmar and Watt, 2012; Pittet and Weissleder, 2011). Most importantly, mouse embryos develop inside the mother and exhibit considerable growth during embryonic development, whereas zebrafish embryos develop externally in the egg and grow only modestly during embryonic development. A significant problem of the mouse as a model system is thus the difficulty to perform intravital imaging (Pittet and Weissleder, 2011). This is the reason why most intravital studies performed in mice deal with cell populations. This means that differences between individual clones are blended into a population average, which represents a significant problem for vertebrate stem cell research, as stem cells are rare and molecular markers that would reliably distinguish them from their committed progeny are not available. The zebrafish offers a set of unique advantages over traditional vertebrate model systems. Zebrafish are easily maintained and breed throughout the year. A typical clutch size ranges from 200-300 eggs. The large number of offspring, which can be obtained from a single cross, is a specific advantage for a variety of experiments that rely on the analysis of large numbers of individuals, such as forward or reverse genetic screens as well as screening of chemical compound libraries. Apart from this the transparency of embryo and larva allows direct visual access to development. The combination of these features enables minute changes to the animal's morphology to be easily detected by stereomicroscopy many times without requiring special staining or contrasting methods, substantially reducing the time, effort and cost of re-

verse or forward genetic screens (Dooley and Zon, 2000; Kari et al., 2007). Another key advantage of the zebrafish, as opposed to the mouse, is the availability of morpholinos, which are ribonucleotide-analog based knockdown reagents (Summer-ton et al., 1997; Summerton and Weller, 1997). Morpholinos can be injected into zebrafish zygotes to block either the translation or splicing of particular mRNAs. They provide the opportunity to perform whole organism reverse genetic screens involving a large number of genes at a pace and cost which is unparalleled by any other vertebrate model (Bill et al., 2009; Eisen and Smith, 2008). Most importantly for this project, which aimed at the unequivocal identification of stem cells by intravital imaging, are the particular features of the zebrafish that render it so amenable to this direct and unbiased way of observation and set the zebrafish apart from all other vertebrate model organisms, in which true *in vivo* imaging is very difficult or impossible to achieve.

The rapid external development and comparably low number of cells with respect to other vertebrate embryos greatly facilitate the analysis of morphogenetic processes and organ development, as the number of cells, their clonal relationship and their location can be precisely tracked by intravital microscopy. This offers the remarkable opportunity to study stem cells and cell lineage dynamics in qualitative and quantitative terms. Specifically, parameters such as cell number, cell division rate, cell cycle phase, clonal relationships, migratory behavior, and differentiation rate can be directly read out by the intravital imaging of suitable transgenic reporter lines. These transgenic reporter lines as well as other transgenic tools are easily obtained using Tol2-mediated or BAC transgenesis (Suster et al.,

2011; Suster et al., 2009).

In spite of these undisputed advantages, working with zebrafish is connected to certain drawbacks. Two of these seem to be particularly important obstacles to a more widespread use of the zebrafish as model for vertebrate specific biological questions. First, the lack of zebrafish ES cells and/or homologous recombination technology precludes gene targeting and thus the establishment of conditional knockout strains. For this reason gene function can many times not be assessed in a tissue- or time-specific fashion. Second, the considerable divergence between teleost and mammalian, i.e. mouse and human, proteins renders the vast majority of commercially available antibodies useless, which hinders the analysis of cell populations based on molecular markers and likewise aggravates cell biological studies.

The use of zebrafish as a model system raises the question of how extendable conclusions derived from work with model organisms are to human biology or pathophysiology. In other words, what are the aspects of human biology, which are conserved since the last common ancestor of humans and zebrafish, which lived around 350 million years ago? Despite this long time, however, the genetic makeup of vertebrates is largely identical, i.e. orthologs for the vast majority of human genes can readily be identified in other vertebrates including teleost fish and *vice versa*. For example out of 29 genes, which are associated with muscular dystrophy in humans, 28 zebrafish orthologs have been identified (Steffen et al., 2007). Mutations in the zebrafish *dystrophin* gene (*sapje* mutant) or *mdx* mice lead to muscle fibre attachment defects and muscle de-

generation similar to the situation in humans. The devastating course of human Duchenne Muscular Dystrophy is, however, not reflected by zebrafish *sapje* mutants (Bassett et al., 2003) or the *mdx* mouse (Im et al., 1996; Sacco et al., 2010). The reason for this discrepancy seems to be the vastly different life spans of zebrafish, mice and humans. In the former two, life span might simply be too short to allow MSCs to undergo proliferative exhaustion, which is likely to be a key factor of the pathology of Duchenne and other Muscular Dystrophies (Sacco et al., 2010). Likewise, the vast difference in body size might limit the predictive power of *small* model organisms in certain context. Summing up it seems fair to say that the use of model systems has revolutionized modern biology and contributed most of what we know about the development, physiology and diseases of humans. Nevertheless, one has to be careful, when extrapolating experimental data derived from model system to human biology. For this project, it appears justified to use the zebrafish to find general principles and factors underlying the maintenance of MSCs in teleosts and humans. In particular this study will enable cross-phylogenetic comparisons between teleost and mammalian MSCs and their respective niches to be made, which is likely to reveal further features that are conserved between fish and man.



— *Der Geist der Medizin ist leicht zu fassen;  
Ihr durchstudiert die groß, und kleine Welt,  
Um es am Ende gehn zu lassen,  
Wie's Gott gefällt.*—

Goethe, Faust

# 8

## Aim of this work

THIS WORK'S INTENT is to contribute to our understanding of stem cells and their niche regarding their ontogeny and the molecular interactions between the two entities that underly the maintenance of stemness. It is the aim to exploit the particular aptitude of the zebrafish to (A) unequivocally identify teleost MSCs and their niche, (B) study stem cell dynamics in the living animal and (C) identify novel niche factors and cell surface molecules, which are essential for MSC maintenance. To this end a suitable reporter line labeling MSCs was generated and a combination of explorative approaches was undertaken. As a first step a qualitative description of

the myogenic lineage was derived from a significant body of intravital imaging data. In the following intravital imaging-based clonal analysis led to the identification of the actual teleost MSC compartment, the clear separation from already committed progenitors and strongly suggested that the vertical myoseptum functions as the teleost MSC niche. These embryological studies were then complemented by transcriptional profiling yielding a ‘teleost MSC’ dataset containing candidate genes with very specific expression in MSCs/MPs. By morpholino-mediated reverse genetics screening these candidates were then scrutinized for a possible function in the maintenance of stemness. In parallel the first systematic survey for extracellular protein-protein interactions was conducted by screening these candidates against a library of extracellular proteins taking advantage of the AVEXIS assay. This method stands out from other protein-protein interaction assays, in that it allows the high-throughput screening for extracellular protein-protein interactions, which are not accessible to standard high throughput protein-protein interaction methods, such as yeast-two-hybrid. The combination of gene expression, functional and protein-protein interaction data then formed an objective base to prioritize candidate genes and suggested that a number of MSC-derived proteins are in fact components of the MSC niche.

Gaining deeper insight into the molecular underpinnings of stemness is not only a fascinating basic science endeavor, but has to precede application of stem cells as therapeutic agents. The motivation for MSC research in general and this project in particular is therefore multifold. The existence of MSCs has fueled the hope that cytotherapies for several devastat-

ing hereditary diseases of human skeletal muscle can be developed. A number of loci have been associated with these human muscular dystrophies. The most prominent forms of muscular dystrophies (MD), such as Duchenne MD, Limb-girdle MDs, Fukuyama MD are caused by mutations in genes that directly or indirectly affect the function of the Dystrophin-Dystroglycan-Complex, which transmits the force from the intracellular actin cytoskeleton to the extracellular basal lamina (Bertini et al., 2011). A small number of genes encoding cytoplasmic proteins, e.g. nuclear lamins, or membrane proteins, e.g. Dysferlin, have been associated with other forms of muscular dystrophies (Han and Campbell, 2007). Despite the complex human genetics of these diseases, all of them appear to be accessible to the same therapeutic rationale (Meregalli et al., 2012; Vilquin et al., 2011). In simple terms it is the idea to use autologous genetically ill MSCs, isolate, expand and genetically correct them in cell culture and then transplant them back into the patient, where they will establish a long lasting source of genetically healthy myoblasts. This strategy, which was conceived in the early 1970s (Friedmann and Roblin, 1972), therefore is a combination gene and cell therapy and has been employed to treat hereditary immunological disorders (Cavazzana-Calvo et al., 2000). In these cases hematopoietic stem cells were transfected using retrovirus carrying a 'healthy' copy of the defect causing gene. A fundamental problem with gene or combined gene/cell therapy using viral vectors is the inherent danger that viral integration itself may cause oncogenic transformation through transactivation of oncogenes or disruption of tumor suppressor genes (Hacein-Bey-Abina et al., 2003). In fact four out of nine patients, which re-

ceived gene/cell therapy for severe combined immunodeficiency (SCID)-X1 in course of the 'Paris' trial run by Alain Fischer and colleagues, developed T-cell acute lymphoblastic leukemia (T-ALL; Hacein-Bey-Abina et al., 2008). Stable genetic correction should thus be achieved using homologous recombination protocols, which allow precise changes to the genome to be made. The most basic problem in proceeding along this avenue is the fact that MSCs do not retain stemness in cell culture (Montarras et al., 2005). The reason for this failure is that essential endogenous niche factors are currently unknown and hence cannot be added to the cell culture medium. The simplicity of the embryonic axial musculature of the zebrafish and a variety of specific further advantages have raised the hope, that the zebrafish might be a particularly suitable model to study the ontogeny and chemical composition of the MSC niche. It is the hope of the author that the results of these efforts may be useful in the development of therapeutics for human disease.

# Part II

# Results



— *Der Worte sind genug gewechselt,  
Laßt mich auch endlich Taten sehn!  
Indes ihr Komplimente drechselt,  
Kann etwas Nützliches geschehn.* —

Goethe, Faust

# 9

## Intravital imaging-based reconstruction of the teleost myogenic lineage

THE UNEQUIVOCAL IDENTIFICATION of stem cells remains a key problem in stem cell research. Zebrafish offers the fascinating opportunity to directly monitor MSCs and their progeny in their unperturbed endogenous context by intravital confocal microscopy. In mouse, chicken, and zebrafish, Pax7 is expressed in the central nervous system, neural crest cells and myogenic progenitors (Mansouri and Gruss, 1998; Mansouri

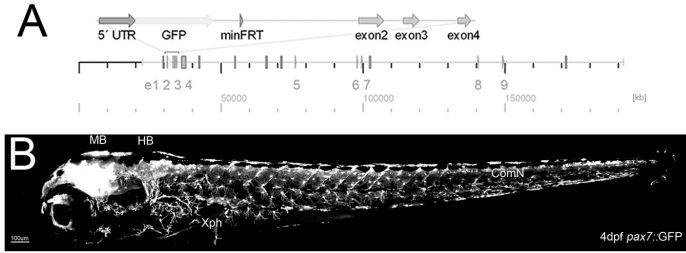


**Figure 9.1:** Schematic of the zebrafish *pax7a* locus, BAC recombination (A) and overview of transgene expression in a 4day-old transgenic zebrafish larva (B). MB - midbrain, HB - hindbrain, Xph - xanthophore, ComN - commissural neurons.

et al., 1996; Otto et al., 2006). As detailed in the introduction Pax7 is a paired-box transcription factor with key roles in myogenic lineage specification and muscle stem cell maintenance. Despite its expression in non-myogenic cell types Pax7 remains the most specific marker for vertebrate embryonic and adult MSCs known so far. Based on these grounds *pax7* was chosen to attempt the generation of transgenic GFP reporter line that would label teleost MSCs. The zebrafish genome contains two *pax7* genes - *pax7a* and *b* - a fact that was unknown, when this project was undertaken, and only became apparent with the latest assembly of the zebrafish genome.

## 9.1 Generation of a zebrafish *pax7::GFP* BAC transgenic line

To this end a BAC library screen was performed with a probe for *pax7*. The identified BAC CH211-287M7, which is now known to span approx. -30kb to +90kb of the *pax7a* locus, was then modified using BAC recombination as to replace the proteogenic part of exon1 with a GFP-SV40 polyA-tail cassette (Figure 9.1A) and used to generate a zebrafish *pax7::GFP* BAC transgenic line which reports the expression of *pax7* consistent with published expression data (Figure 9.1B; Seo et al., 1998). In contrast to a previously published line (Seger et al., 2011), this line drives robust GFP expression and allows Pax7<sup>+</sup> MPs to be followed over several days by intravital imaging. In order to reduce the prominent GFP expression in neural crest derived xanthophores, most imaging experiments were performed in *pfeffer* (*pfe*) mutants, which carry a mutation in *csf1ra/fmsA*, one of two paralogs of the Csf1 receptor in teleosts. *Pfe* mutants display an almost complete absence of xanthophores, but are otherwise indistinguishable from *wild type* (Odenthal et al., 1996; Parichy et al., 2000).

## 9.2 Non-invasive intravital imaging of primary myogenesis in zebrafish

The axial musculature of teleosts is divided into myotomes or myomeres, which correspond to individual somites and are separated from each other by vertical myosepta and cut into

a dorsal and ventral half by the horizontal myoseptum (Johnston, 2000). Myosepta are thin sheets of extracellular matrix and essential for proper force transmission (Figure 9.2). Based on the observations presented in the following, zebrafish muscle development may be divided into primary and secondary myogenesis, two phases that are connected by a transition phase (Figure 9.3). It is important to note at this point, that primary myogenesis is preceded by an initial wave of myogenesis during which the most medial somitic cells directly start to express MyoD and undergo differentiation into muscle fibres.

Within the myogenic lineage GFP expression commences in somitic cells around 20hpf (Figure 9.4A, Movie S1). As a result of somite rotation these Pax7<sup>+</sup> somitic cells come to lie on the outer surface of the somite (Hollway et al., 2007; Stellabotte et al., 2007), where they form a transient epithelial layer of cuboidal cells (Figure 9.4A, Movie S1). These cells adhere to the vertical myosepta on both sides. Soon after its emergence this epithelial sheet of cells disintegrates and cells in the layer divide and get dragged apart as the growth of the myotome enlarges the distance between the myosepta (Figure 9.4A, right panel, Movie S1).

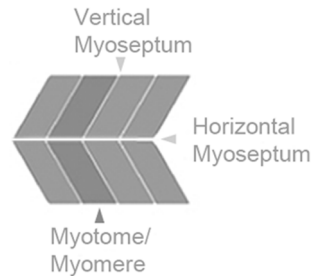


**Figure 9.2:** The axial musculature of teleosts is organized into chevron-shaped myotomes, which are separated from each other by vertical myosepta.

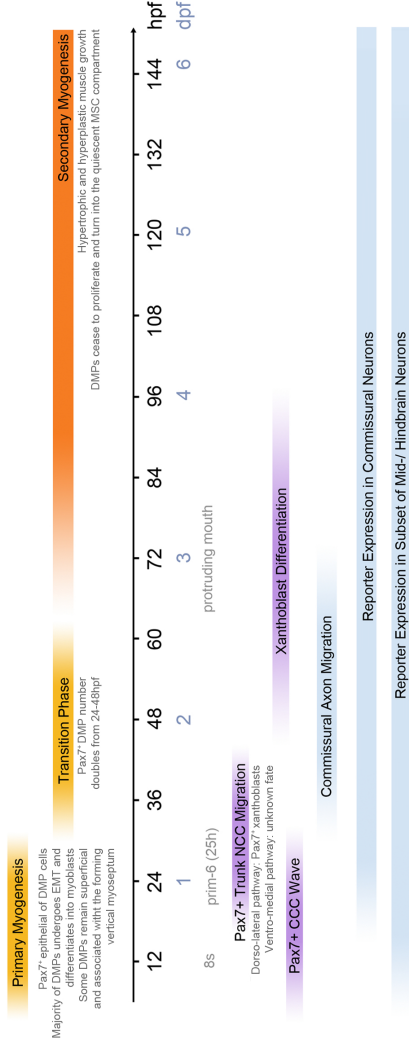
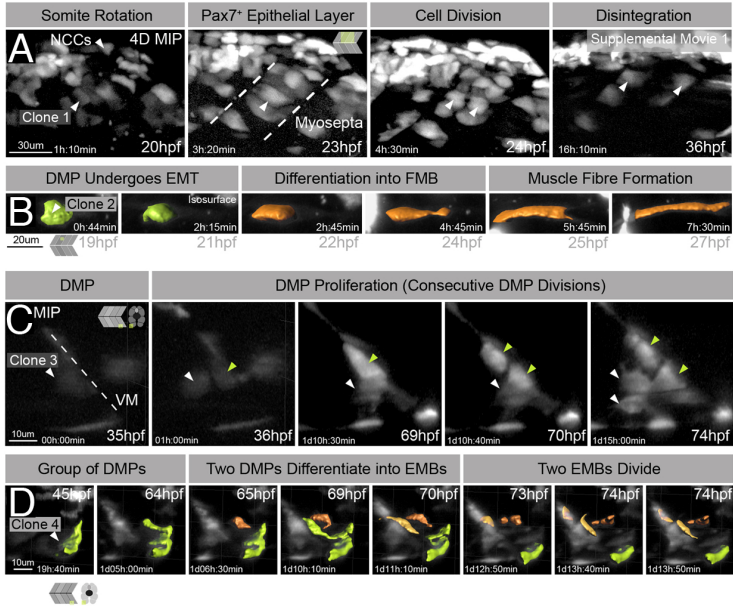


Figure 9.3: Timeline of myogenesis in zebrafish larvae.

The vast majority of their descendants leave their superficial position, migrate into the underlying myotome and differentiate into myoblasts that give rise to muscle fibres directly (Figure 9.4B, Movie S2). Importantly, during this phase no fusion events between myoblasts and myofibers were observed. A small fraction of Pax7<sup>+</sup> cells, however, is kept from differentiation. These cells stay in their superficial position and remain attached to the vertical myosepta (Figure 9.4A, right panel, 36hpf). In the following these cells will be referred to as dermomyogenic progenitors (DMPs). By the end of primary myogenesis around 26hpf the differentiation of the first wave of Pax7<sup>+</sup> myoblasts leads to the clearance of Pax7<sup>+</sup> cells from the myotome.



**Figure 9.4:** Live imaging of the medial trunk of *pax7::GFP* transgenic embryos during primary myogenesis and transition phase. (A) Selected scenes of Movie S1 showing the onset of reporter expression in somitic cells (20hpf) and dorsal neural crest cells (NCCs), the formation of a Pax7<sup>+</sup> epithelial layer on top of the myotome (23hpf), the cell divisions in this layer (24hpf) as well as its disintegration until 36hpf. (B) Isosurface rendering showing a DMP cell (green, 19hpf) undergoing EMT (21hpf), migration into the underlying myotome and differentiation into a myoblast (orange), which ultimately gives rise to a muscle fibre (Movie S2). (C) Live imaging of a DMP cell clone located in a ventral myotome from 35-74hpf. (D) Live imaging of a group of DMP cells (green isosurfaces) starting at 45hpf, which shows that the first Pax7<sup>+</sup> MPs (yellow and orange isosurfaces) that reappear inside the myotome at the onset of secondary myogenesis are descendants of DMP cells (see also Figure 9.5). EMT - epithelial-to-mesenchymal transition.

Consequently, DMPs are the only remaining Pax7<sup>+</sup> cells of the myogenic lineage between approximately 30-65hpf (Figure 9.4C). During this transition phase (Figure 9.3) the number of DMPs per somite approximately doubles from 20 (24hpf) to 40 (48hpf). DMPs continue to divide until approximately 3dpf at a rate of 1 division/day (Figure 9.4C, Figure 9.5, Movie S3). Notably the external cell layer, which has been described before, corresponds to this DMP cell pool. Intravital imaging, however, shows that the external cell layer of DMPs is no longer an epithelium during these development stages.

Around 72hpf two key events mark the transition to secondary myogenesis:

- DMPs cease to proliferate and become mitotically quiescent (Movie S3);
- Pax7<sup>+</sup> MPs reappear inside the myotome. Live imaging shows that these cells derive from a small fraction of DMPs that leave their superficial position (Figure 9.4D, Figure 9.5D, Movie S3).

Following DMPs with single cell resolution allows migratory behavior and clonal relationships to be monitored (Figure 9.5 and Movie S3). Clone 1 shows that DMPs are able to divide symmetrically. Clone 2 indicates that following symmetric division (61hpf) one of daughter cells remains in the DMP state, whereas the other leave the superficial position (69hpf) and differentiates into an EMB. This EMB divides again (79hpf) and finally both EMB daughter cells differentiate into fusion-competent myoblasts (FcMB), that ultimately fuse with pre-existing muscle fibres (MF, 84hpf) as evidenced by the spread

of GFP in receiving fibres. Clone 2 and similar clones obtained during transition phase and during secondary myogenesis demonstrate that EMBs derive from DMPs.

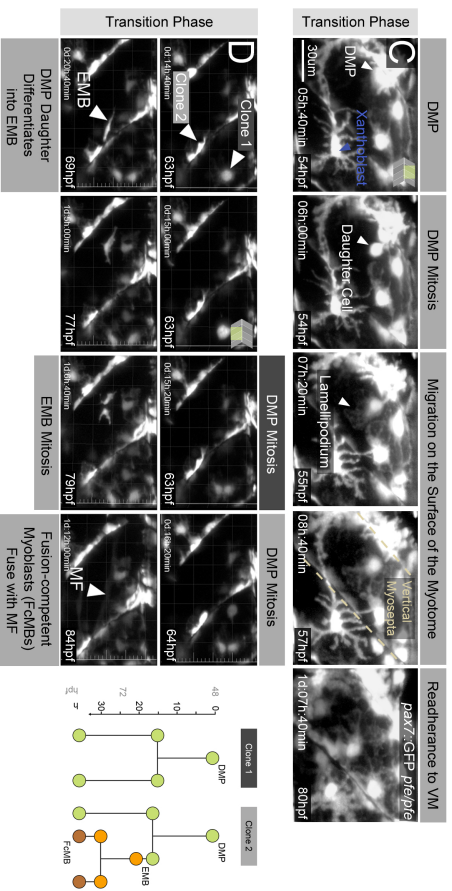
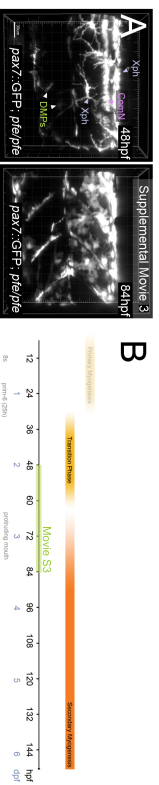


**Figure 9.5:** Intravital imaging of *par7::GFP*; *pfe/pfe* embryos during transition phase. (A-D) Live imaging of the medial trunk of a *par7::GFP*; *pfe/pfe* transgenic embryo from 48-84hpf Movie S3. (A) Start and end timepoint of Movie S3. (C-D) Clonal analysis of DMPs during transition phase.

### 9.3 Three types of Pax7<sup>+</sup> MPs during secondary myogenesis

In 4-7 day-old larvae, corresponding to the first days of secondary myogenesis, Pax7<sup>+</sup> MPs can be subdivided based on anatomical and morphological criteria into the following classes (Figure 9.6A-D):

- **Dermomyogenic progenitors (DMPs)**. DMPs are associated with the vertical myosepta (Figure 9.6B) lying above the slow muscle fibre layer. They have large kidney-shaped nuclei and extend long digitated cytoplasmic processes that bestow these cells a stellate morphology (Figure 9.6A-D, Animation S1).
- **Committed Myogenic Progenitors (CMPs)**. CMPs adhere to the vertical myosepta, but in contrast to DMPs are located underneath the slow muscle fibre layer. They have spindle-shaped cell bodies and nuclei (Figure 9.6A-D, Animation S1). CMPs display varying degrees of polarization towards the vertical myoseptum. Depending on the angle between the vertical myoseptum and mitotic spindle CMPs undergo symmetric (SCD, Figure 9.8 and Movie S4) or asymmetric cell division (ACD, Figures 9.8B and 9.9). While symmetric cell division leads to an increase in CMP number, following asymmetric division one daughter cell loses contact with the myoseptum and enters the myotome (Animation S2).
- **Early Myoblast (EMB)**. EMBs are freely moving inside the myotome. Their cell morphology is flexible and

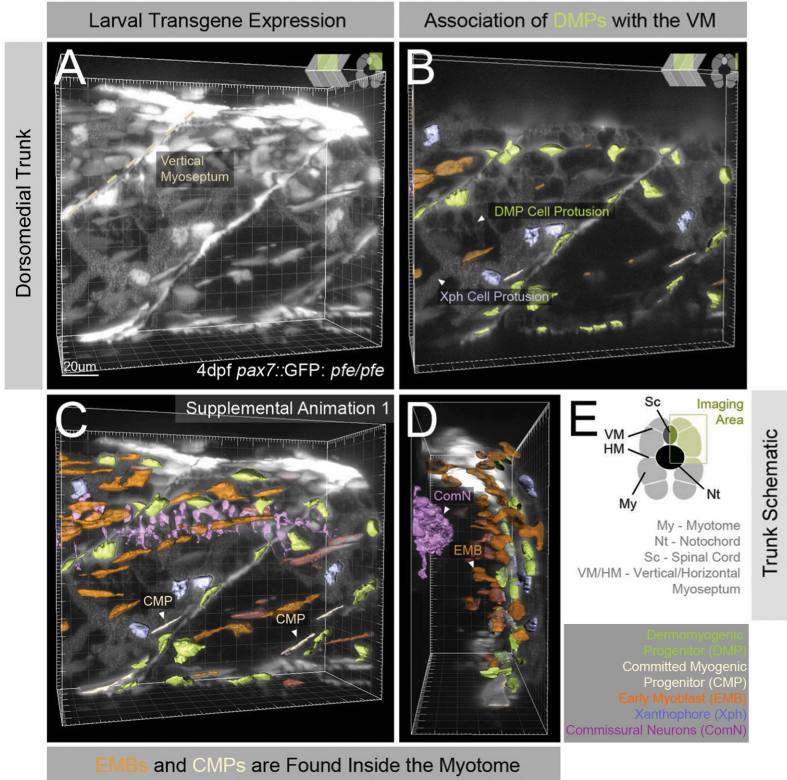


**Figure 9.6:** Anatomical and cell morphological classification of Pax7<sup>+</sup> MPs during secondary myogenesis. (A-D) Selected scenes (Animation S1) showing the dorsomedial trunk of a 4dpf *pax7::GFP; pfe/pfe* larva. (A) Maximum intensity projection of the whole volume. (B) Volume with orthoslicer to display the lateral cells including DMPs (central soma -green isosurfaces) and xanthophores, which are present in *pfeffer* mutants in very low numbers compared to *wt* (central soma - blue isosurfaces). Note the thin processes of DMP cells, which are not rendered. (C-D) Lateral and transverse view of (A) including isosurfaces. EMBs (orange) are found inside the myotome, while CMPs (light green) still adhere to the vertical myoseptum. Note that CMPs are deeper in the tissue in comparison to the superficial DMPs (dark green).

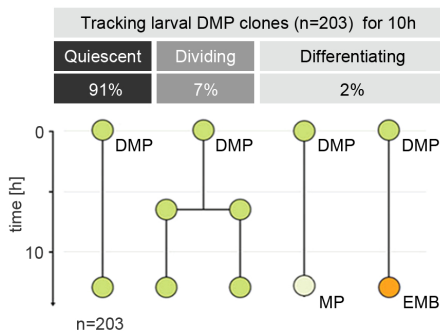


**Figure 9.7:** Intravital imaging-based clonal analysis identifies DMPs as the actual MSCs in teleosts. For details see text.

highly dynamic (Figures 9.6, 9.8C, 9.11A, and Movie S4). Note that Figures 9.8C and 9.11 display the same EMB cell at slightly different timepoints and altered display adjustment to enhance the visibility of thin cytoplasmic protrusions. EMBs divide symmetrically (Figure 9.8C) and are able to give rise to fusion-competent (Figure 9.10) or fibre-forming myoblasts (Figure 9.11C-D).

## 9.4 DMPs give rise to the quiescent MSCs of secondary myogenesis

To resolve whether these three classes correspond to functionally distinct progenitor compartments of the teleost myogenic lineage, more than 200 DMPs in 4-6dpf zebrafish larvae (secondary myogenesis) were tracked by intravital imaging for at least 10h and analyzed for migratory behavior, cell division

patterns and differentiation. As depicted in Figure 9.7 91% of DMP cells observed, did not divide, migrate or differentiate indicating that these cells turn to quiescence at this stage. 7% of DMP cells showed no migratory activity but divided symmetrically thereby generating two DMP daughter cells, while only 2% were found to leave their superficial position, enter the myotome through the vertical myoseptum and differentiate into either CMP or EMB.

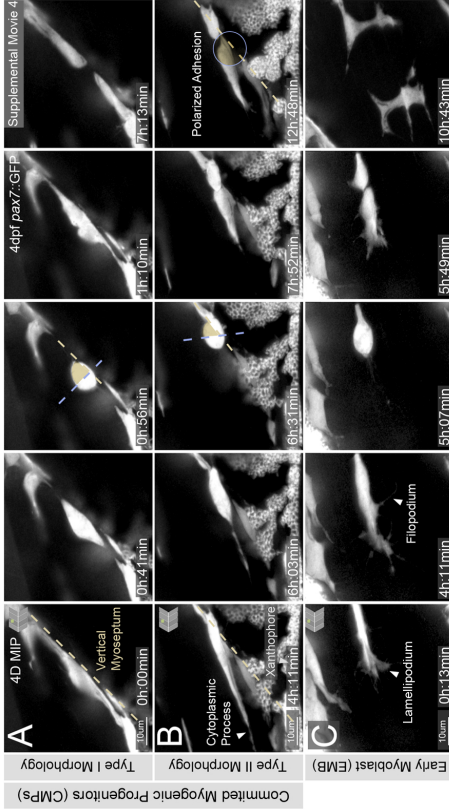


**Figure 9.8:** Live imaging Pax7<sup>+</sup> MPs during secondary myogenesis. (A-C) Live imaging of Pax7<sup>+</sup> MPs in a 4dpf *pax7::GFP wt* larva. (A, B) CMPs are associated with the vertical myosepta. (A) Symmetric cell division of a CMP. The plane of cell division is perpendicular to the vertical myoseptum (type I morphology). (B) Asymmetric cell division of a CMP as result of polarized adhesion (type II morphology) leads to the generation of EMBs.

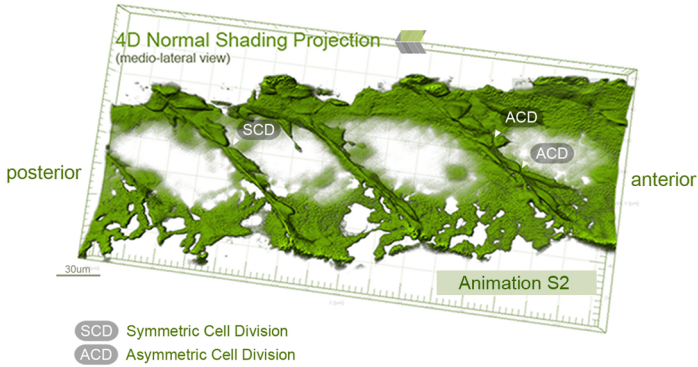


**Figure 9.9:** 4dpf dorsomedial trunk in inside-to-outside view and normal shading projection. Selected scene from Animation S2, showing CMP cells located at the vertical myosepta undergoing symmetric and asymmetric cell division.

By following CMP clones it turned out that CMPs give rise to EMBs either by direct differentiation or through asymmetric cell division (Figure 9.9 and Animation S2). The analysis of EMB clones showed that these cells are capable to become fusion-competent myoblasts or give rise to new myotubes directly. Importantly, no EMB giving rise to a CMP or DMP, nor a CMP giving rise to a DMP, was observed indicating that DMPs, CMPs, and EMBs form hierarchically connected Pax7<sup>+</sup> MP classes. Based on the assumption that cell divisions

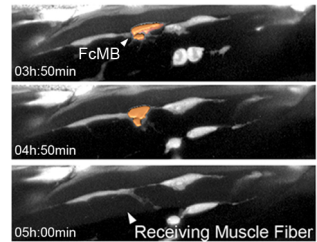


**Figure 9.10:** Early myoblasts (EMBs) give rise to fusion-competent myoblasts (FcMBs).

**Table 9.1:** Estimated cell cycle duration for DMPs, CMPs, and EMBs in 4-6dpf zebrafish larvae

|                    | DMP | CMP | EMB |
|--------------------|-----|-----|-----|
| n=                 | 173 | 22  | 51  |
| Standard Deviation | 17  | 3   | 6   |
| Mean duration [h]  | 127 | 37  | 29  |

of MPs are asynchronous the mean cell cycle times for these distinct progenitor types at 4-6dpf can be estimated (Table 9.1).

These results show that DMPs enter quiescence at the onset of secondary myogenesis (Movie S5) and demonstrate that DMPs form the most upstream MP compartment in larval teleosts. For this reason these cells will be henceforth referred to as muscle stem cells (MSCs). Further these observations show that CMPs and EMBs form intermediate transit-amplifying progenitor compartments, which exhibit considerably higher cell division rates and thus carry the bulk proliferative load, which rests on the myogenic lineage during phases of intense muscle growth or regeneration. Importantly, clonal analysis shows that, downstream of the EMB compartment the myogenic lineage bifurcates into fusion-competent and fibre-forming myoblasts (Figure 9.10 and 9.11C,D).

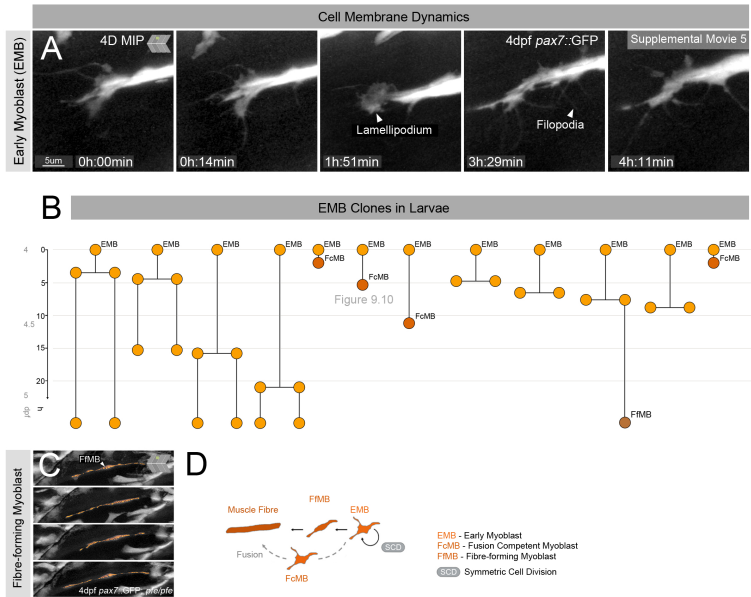


**Figure 9.11:** Intravital imaging and clonal analysis of early myoblasts (EMBs) indicate that this compartment serves as a transit-amplifying progenitor compartment. (A) Additional selected scenes of Movie S4 showing the same EMB as in Figure 9.8C depicting the highly flexible cell morphology of an EMB during migration. (B) Examples of EMB clones observed in 4-5dpf zebrafish larvae. (C) *De novo* muscle fibre formation by a fibre-forming myoblasts (FfMB) at 4dpf. (D) Clonal analysis indicates that EMBs amplify in a number by symmetric cell division (SCD) and are able to give rise to fusion-competent myoblasts (FcMB, Figure 9.10) or fibre-forming myoblasts (FfMB Figure 9.11C,D).

— *Nicht Kunst und Wissenschaft allein,  
Geduld will bei dem Werke sein.  
Ein stiller Geist ist jahrelang geschäftig,  
Die Zeit nur macht die feine Gärung kräftig.*—  
Goethe, Faust

# 10

## Direct isolation and transcriptional profiling of teleost Pax7<sup>+</sup> MPs

OF CONSIDERABLE interest to vertebrate stem cell research in general and muscle stem cell research in particular is the identification of a transcriptional signature that characterizes vertebrate muscle stem cells. Appropriate cell surface markers or transgenic lines, that would allow the isolation of vertebrate MSCs were not available when this project was started. Therefore it seemed prudent to directly isolate Pax7<sup>+</sup> MPs from zebrafish larval tissue (4dpf). This timepoint right after the onset of secondary myogenesis was chosen, because

MSCs already started to become quiescent at this point, but downstream committed progenitors did not yet have the time to expand strongly in number. Based on the quantification of imaging data from 4dpf, it can be expected that DMPs/MSCs account for 57% and that CMPs/EMBs account for 43% of the sorted GFP<sup>+</sup> population, which is a very favorable ratio of stem cells to committed progeny.

Cells were purified from decapitated and partially dissociated larvae to reduce contamination with Pax7<sup>+</sup> neurons. Small cells with low granularity (gate P1), which excludes Pax7<sup>+</sup> xanthophores, were sorted by fluorescence activated cell sorting (Figure 10.1). Gated cells (P1) were split into GFP<sup>+</sup> (P2) and GFP<sup>-</sup> (P4) cell populations as evident from the histogram in Figure 10.1. GFP<sup>-</sup> cells from outside P1 (P3) were unified with P4 and served as the GFP<sup>-</sup> reference population (P3+P4), which was compared with P2. This means, that the fraction containing GFP<sup>+</sup> MPs was compared (Figure 10.1; P2) with GFP<sup>-</sup> cells from inside and outside P1, which includes GFP<sup>-</sup> cells not only from musculature but all other trunk

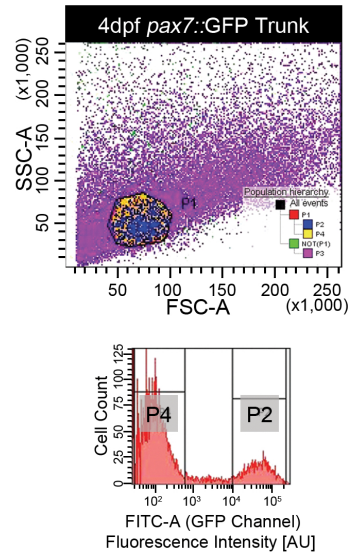


**Figure 10.1:** Direct isolation of zebrafish Pax7<sup>+</sup> MSCs/MPs. Upper panel: FSC-A/SSC-A gating. Lower panel: Fluorescence gating.

tissues. This experimental design was chosen to find genes, which are specifically expressed by Pax7<sup>+</sup> MPs, as it compares Pax7<sup>+</sup> cells of the myogenic lineage with all other cells present in the trunk of the animal, including cells deriving from the skin, muscle tissue, inner organs and blood.

By transcriptional profiling, which was performed in collaboration with Dr. Mitchell Paul Levesque, who conducted the statistical analysis of the microarray data, 152 unique genes were found to be significantly upregulated in Pax7<sup>+</sup> MPs (Table 22.3). Based on False Discovery Rate statistics the dataset is expected to contain less than one false-positive. The Top 30 genes of this ‘teleost MSC profiling’ are shown in Figure 9.2. Amongst these Top 30 roughly 60% have been implicated in the muscle development before.

These genes include *myog* (23,0x, rank 1), *pax7* (11,1x, rank 3), *myf5* (8,3x, rank 7), *meox1* (6,0x, rank 13), and *pax3* (5,6x, rank 15), which encode well established transcriptional regulators of myogenesis (Bryson-Richardson and Currie, 2008; Mankoo et al., 2003). Strikingly, 85% of the transcription factors that were found have been implicated in myogenesis before. In addition to the transcriptional regulators that were identified potent transcriptional repressors of myogenic differentiation including the Notch signaling mediator *hey1* and *hey2* (Buas et al., 2010; Fukada et al., 2011) as well as *sox9a* are contained in the dataset (Hernandez-Hernandez et al., 2009). Consistent with this observation, the dataset is basically devoid of genes characteristic of muscle fibre differentiation, e.g. *alpha actinin*, *troponin*, or *creatine kinase* (Gautel, 2011; Tai et al., 2011). The large share of genes specifically involved

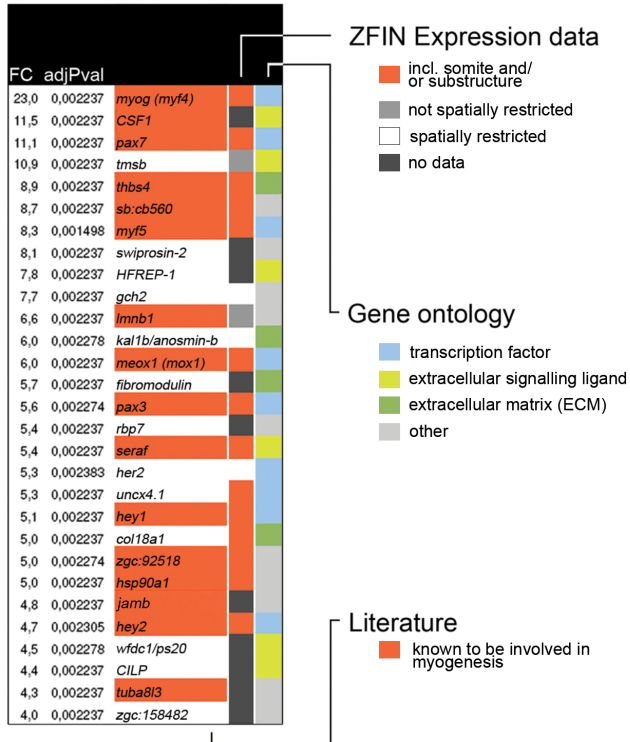


**Figure 10.2:** Transcriptional profiling of Pax7<sup>+</sup> MSCs/MPs. Top 30 of 152 unique genes upregulated in zebrafish MSCs/MPs based on a false-discovery rate of less than 1. All data will be made available through the ArrayExpress expression repository <http://www.ebi.ac.uk/arrayexpress/>.

in muscle development but not muscle differentiation confirms the strong enrichment of MSCs/MPs in the sorted Pax7<sup>+</sup> population. This ‘teleost MSC profiling’ dataset can therefore be expected to contain a significant share of genes, whose function is essential for the regulation of a number of different aspects of MSC physiology such as the maintenance of stemness as well as the regulation of their activation and differentiation.

**Teleost Pax7<sup>+</sup> MPs secrete candidate niche components** This study focussed on secreted proteins, which are very specifically expressed by teleost MSCs. A number of such genes, corresponding to roughly 10% of the dataset, encoding for secreted proteins were identified and are listed in Figure 10.3 containing also schematic representations of the respective PFAM domain structure as well as a summary of known protein-protein interaction partners, which are listed in the String 8.3 database. These include growth factors such as Csf1b, the orphan ligands Seraf, Hfrep/Hepassocin and Wfdc1, as well as Wnt inhibitory factor 1 (Wif1). Interestingly, a number of non-collagenous extracellular matrix (ECM) components such as Thrombospondin 4b (Thbs4b), Kalman 1b/Anosmin-b (Kal1b), Fibromodulin (Fmod), Lumican (Lum), Olfactomedin-like 2Bb/Photomedin 2b (Olfml2Bb), and Tenascin W (Tnw) were found to be upregulated in teleost MSCs/MPs. In addition three collagens Col5a, Col6a and Col18a1 are contained in the ‘teleost MSC profiling’ dataset (Figure 10.2, 10.3 and Table 22.3). Many of these secreted proteins have already been implicated in myogenesis and/or tendon formation. Taking into account that MSCs and MPs are associated with the vertical myoseptum, these findings suggest that these ECM molecules

**A**

| Non-Collagenous ECM Components                                      |      |  |  |
|---|------|--|--|
| Gene  | FC   | Domain Structure   | STRING 8.3                                       |
| Uniprot Acc.  |      | Size (aa) & Oligomeriz.  | Human Homolog Interactors                        |
| <i>thbs4b</i><br>QBJGW0   | 8.9x | TSPN EGFP 8xTSP3 TSPC<br>949aa Pentamer                                | Fibrogen<br>Fibronectin<br>Type V Col<br>Laminin |
| <i>kal1b</i><br>Q9LAR3  | 6.0x | WAPdS core<br>633aa  | Syndecan 2                                       |
| <i>fmod</i><br>Q4V5E0   | 5.7x | LRRNT 4x LRR 1<br>342aa  | Myostatin<br>TGFβ1,2,3                           |
| <i>col18a1</i>  | 5.0x | Frizzled Domain LamG 4x Col Collagenase NC10/<br>Endostatin<br>1,645aa | KDR, GPC1/4,<br>MMP2, CTSL1,<br>ITGA5, FBLN2     |
| <i>tnw</i>  | 3.3x | EGFP FN3 FG<br>932aa   | None   |
| LOC792773<br><i>similar to adiclan</i><br>A7MBS5 (protein fragment) | 3.2x | LRR 1 2x Ig I-set<br>861aa (protein fragment)                          | None   |
| <i>lumican</i><br>Q6IQG7  | 3.0x | LRRNT LRR 1<br>344aa   | ACAN<br>Col1A2<br>MMP14                          |
| <i>olfm21B</i><br>B0UXR7  | 2.8x | OLF<br>645aa   | None   |

**B**

| Extracellular Signalling Molecules & Modulators |       |                         |                           |
|---|-------|-------------------------|---------------------------|
| Gene  | FC    | Domain Structure        | STRING 8.3                |
| Uniprot Acc.                                    |       | Size (aa) & Oligomeriz. | Human Homolog Interactors |
| <i>csf1b</i><br>B0UYR0                          | 11.5x | M-CSF1<br>284aa         | CSF1R<br>CBL              |
| <i>fgl1/hfrep</i><br>Q1RLR4                     | 7.8x  | FG C<br>378aa           | None                      |
| <i>seraf</i><br>Q0BCG4                          | 5.4x  | 5x EGF 2<br>210aa       | None                      |
| <i>wfdc1</i><br>A5WVP3                          | 4.5x  | WAPdS core<br>220aa     | None                      |
| <i>wif1</i><br>A5WVP3                           | 3.1x  | WIF 4x EGF 2<br>378aa   | None                      |

**Figure 10.3:** Pax7<sup>+</sup> MSCs/MPs secrete candidate niche components. (A) Non-collagenous ECM components and (B) extracellular signaling molecules and signaling modulators, which were identified to be significantly upregulated in teleost MSCs/MPs. A schematic of domain organisation according to domains annotated in PFAM database as well as known protein interactions listed in String 8.3 database were included in the figure. FC - Fold change

are components of the vertical myoseptum. As the vertical myoseptum functions as the MSC niche in embryonic and larval teleosts, it seemed reasonable to assume that at least some of these candidates are genuine niche components. As the molecular composition of vertebrate stem cell niches remains largely enigmatic, it was the focus of this work to assess these MSC-secreted proteins for a possible function as niche molecules. Working with zebrafish offers the dedicated advantage to prioritize the candidates in an unbiased way by systematic reverse genetics screening using morpholino-mediated knockdown (see Chapter 11). Concomitantly, these MSC-derived extracellular proteins were included in the ‘Tübingen AVEXIS’ screen for extracellular protein-protein interactions (see Chapter 12), as part of a collaboration with Dr. Christian Söllner (MPI für Entwicklungsbiologie, Tübingen). This allowed candidate genes to be prioritized based on the phenotypes elicited by their knockdown and protein interaction partners.



— *Wie glücklich würde sich der Affe schätzen,  
Könnte er nur auch ins Lotto setzen!* —

Goethe, Faust



## Morpholino screen

THE PRIORITISATION of candidate genes is a key step in every profiling experiment and is typically based on prior knowledge and fold change. While fold change is a poor indicator of the relevance of a particular gene, prior knowledge allows educated guesses about the function of a particular gene to be made, which increases the odds of picking a gene, whose functional perturbation leads to a relevant phenotype. By necessity this way of picking reduces novelty. The use of zebrafish as a model system offers the strong advantage at this point to go the other way round, i.e. prioritize candidate genes by the phenotypes, which are elicited by their knockdown. This

possibility was exploited to systematically screen candidates, which were identified by the ‘teleost MSC profiling’ described in Chapter 10. The focus of the MO screen was on secreted proteins, including candidate niche components, i.e secreted non-collagenous ECM components (Figure 10.3A) as well as signaling molecules/modulators (Figure 10.3B), and cell surface molecules, which were upregulated in teleost MSCs such as *Prtga*, *Rgmb*, *Cdon*, *Gas1b*, *A2CEY7*, and *CD81*.

From the profiling dataset a subset of genes were selected, and MO translation ( $MO^{ATG}$ ) or splice blocking MOs ( $MO^{GT}$ ) were designed and then injected directly into the zygote using the doses indicated in Table 22.2. The effective dose range was determined for each morpholino in pilot experiments. It is important to note that the use of translation blocking MOs is connected to the problem, that the knockdown efficacy can only be controlled directly on the protein level which necessitates the use of appropriate antibodies. Such antibodies are, however, typically not commercially available for zebrafish proteins. In a first step all morphants were inspected in the stereomicroscope during 16-18hpf, 24hpf, 48hpf, 72hpf, and 4dpf. In this way a small number of early embryonic lethal phenotypes as well as morphological phenotypes arising later during development were identified. A selection of interesting examples is presented in this chapter.

As evident from Figure 11.1 several candidate gene morphants display clearly visible morphological defects already during mid-segmentation. With few exceptions these phenotypes are relatively mild and the corresponding morphants are viable and can thus be analyzed also for possible phenotypes during second-

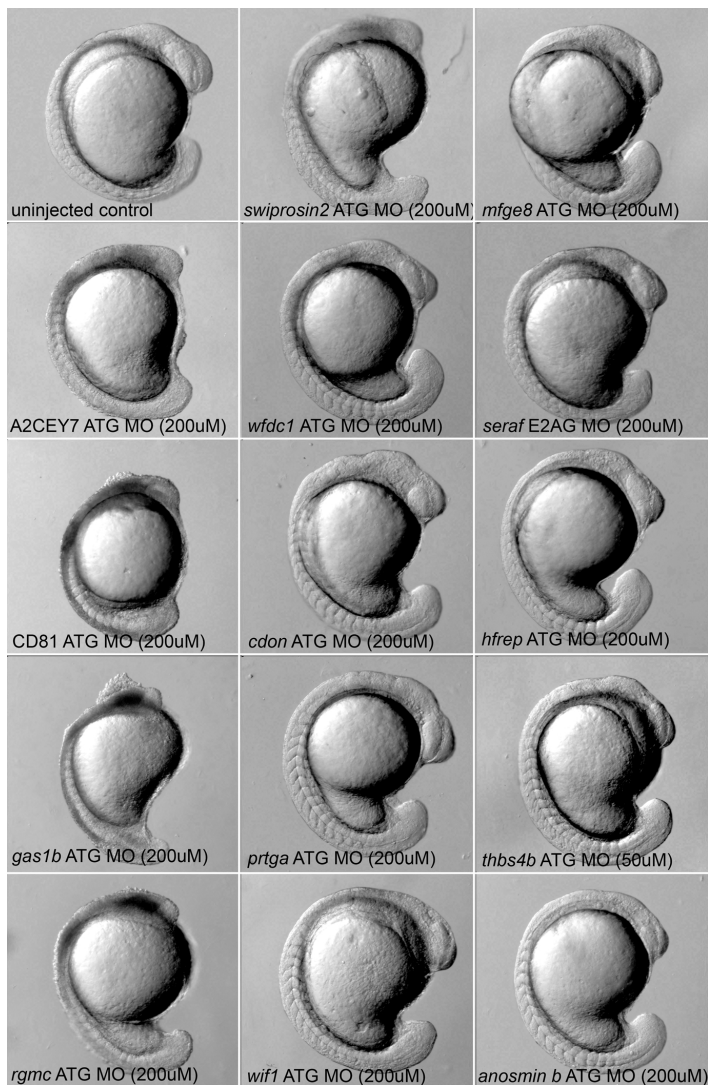


**Figure 11.1:** Morphology of ATG MO-injected embryos during segmentation phase (14-16 somite stage). A small number of candidate gene morphants displays severe early embryonic phenotypes. For a summary see Table 11.1 (Note that the *thbs4b* ATG morphant is hypomorphic. Compare Figure 18.1).

**Table 11.1:** Morpholino screen summary.

| Morpholino                       | Morphant Phenotype   |
|----------------------------------|--|
| <i>A2CEY7</i> <sup>ATG</sup>     | 16s: blocky somites, cranial development severely retarded, cranial necrosis (see Chapter 11)  |
| <i>A2CEY7</i> <sup>GT</sup>      | 2dpf: somites with absent horizontal myoseptum, strong hypomorphants display blocky somites (see Chapter 19)   |
| <i>CD81</i> <sup>ATG</sup>       | 16s: blocky somites, cranial development severely retarded, cranial necrosis, cluster of cells above midbrain (see Chapter 19)   |
| <i>gas1b</i> <sup>ATG</sup>      | 16s: blocky somites, cranial necrosis, abnormal somite shape (see Chapter 11)  |
| <i>cdon</i> <sup>ATG</sup>       | 1dpf: cranial phenotype; 2dpf: blocky somites, absent horizontal myoseptum, reduced MSC number (see Chapter 19)  |
| <i>wif1</i> <sup>ATG</sup>       | 1dpf: blocky somites, dysmorphic cranium, somite patterning defects, curly tail, absent horizontal myoseptum, (see Chapter 19)   |
| <i>wif1</i> <sup>GT1&amp;2</sup> | no phenotype detected (see Chapter 19)   |
| <i>csf1b</i> <sup>ATG</sup>      | early embryonic lethal   |
| <i>csf1b</i> <sup>GT</sup>       | 2dpf: xanthophore apoptosis very similar to <i>csf1ra</i> mutant ( <i>pfeffer</i> )  |
| <i>csf1a</i> <sup>GT</sup>       | 2dpf: xanthophores cluster on the dorsal hemisegment and fail to cross the horizontal myoseptum  |
| <i>hfrep</i> <sup>ATG</sup>      | no phenotype detected  |
| <i>seraf</i> <sup>ATG</sup>      | no phenotype detected  |
| <i>seraf</i> <sup>GT</sup>       | no phenotype detected  |
| <i>rgmb</i> <sup>GT</sup>        | 2dpf: primary motor axon guidance defective; 4dpf: ca.1-5% of morphants develop focal dystrophic lesions, which are characterized by very low number of Pax7 <sup>+</sup> MSCs/MPs                   |
| <i>rgmc</i> <sup>ATG</sup>       | 1dpf: dysmorphic cranium and trunk   |
| <i>prtga</i> <sup>ATG</sup>      | 1dpf: shortened myotomes, possibly reduced myonuclei number  |
| <i>kal1b</i> <sup>ATG</sup>      | 1dpf: aberrant somite formation  |
| <i>olfml2b</i> GT                | 2dpf: overall normal morphology, histology reveals occasional muscle detachment;<br>3dpf: severe muscular dystrophy, caused by muscle fibre attachment defect  |
| <i>fmod</i> <sup>ATG</sup>       | 1dpf: shortened myotomes, possibly reduced myonuclei number  |
| <i>swiprosin</i> <sup>ATG</sup>  | no phenotype detected  |
| <i>thbs4b</i> <sup>ATG</sup>     | early embryonic lethal; hypomorphant 4dpf: severe muscular dystrophy, for further information (see Chapter 18)   |
| <i>tnw</i> <sup>e111</sup>       | 1dpf: strongly reduced MSC number, 2dpf: myosepta defective, angiogenesis defects, Notch reporter activity downregulated; 4dpf: muscular dystrophy, illegitimate activation of MSCs (see Chapter 13) |
| <i>wfdc1</i> <sup>ATG</sup>      | 2dpf: slightly irregular vertical myosepta   |

ary myogenesis. For candidate genes whose knockdown elicits strong early embryonic phenotypes such as *A2CEY7*, *thbs4b*, *CD81*, and *gas1b* either injection of sublethal morpholino doses or splice blocking morpholinos were used, which allow for maternal rescue, to analyze later phenotypes. In the following these will be referred to as hypomorphic morphants. A selection of non-embryonic lethal morphants was assessed for obvious changes in MSC number at 48hpf and muscle morphology using whole mount immunofluorescence for Pax7 and Myosin light chain (Figure 19.5). The results of the morpholino screen are summarized in Table 11.1. Particularly interesting phenotypes that were discovered in the screen are discussed in Chapters 13, 18, 19, and 20.



— *Ich bin zu alt, um nur zu spielen,  
Zu jung, um ohne Wunsch zu sein.*—

Goethe, Faust

# 12

## Systematic screening for novel extracellular MSC-niche protein-protein interactions

AS MENTIONED before the scarcity of intravital imaging data has led to ambiguity in the identification of vertebrate stem cells and consequently also their niches. The chemical composition of stem cell niches is therefore largely unknown. Even more enigmatic remain the interactions of niche molecules with other components of the extracellular matrix or receptors, coreceptors and adhesion molecules, which are present on the

cell surface of the stem cell of interest and/or possible support cell populations. This stem cell-niche interaction space is basically unexplored. The identification of interaction partners for the MSC-secreted molecules, however, appears to be a promising avenue to find novel MSC niche components. The detection of interactions amongst extracellular proteins-proteins is, however, no mean feat as these interactions are typically transient, i.e. of low affinity, and hence difficult to access by classical protein-protein interaction assays. This is particularly true for protein-protein interaction assays, which are commonly used for high throughput screening such as yeast-two-hybrid. The recent development of the AVEXIS technology, an ELISA-style assay, which relies on the artificial oligomerization of prey proteins through fusion with the pentamerization domain of Thrombospondin 5, also known as Comp, allowed screening for molecular interaction partners of MSC-secreted proteins in a high throughput fashion. The oligomerization of prey proteins leads to an increase in avidity and renders even low affinity interactions detectable (Bushell et al., 2008). The AVEXIS assay is therefore a key advance in the field of extracellular matrix biology. In collaboration with Dr. Christian Söllner the recently developed AVEXIS assay has been exploited to screen for extracellular protein-protein interactions in a high-throughput fashion (Bushell et al., 2008). To this end 25 MSC-secreted proteins identified by the teleost MSC profiling were screened against a library of more than 200 extracellular proteins. 16 of these were newly added to the library. Thus far this represents the largest systematic screen for vertebrate stem cell-niche protein-protein interactions. In this way 4 high-confidence interactions were found. These interac-

tions are rated 'high confidence', because they are  $3\sigma$  above the average of all bait proteins tested and were found in both orientations. This appears to be a comparably low number. The current AVEXIS library size of around 200 proteins, however, corresponds to less than 10% of the secretome. Apart from this it could be argued that the threshold is too conservative. Likewise, requiring bi-directionality of the interaction is problematic as proteins which interact homotypically might display strongly reduced function as prey proteins. While these latter restraints exist, the major limiting factor right now is the small library size. An increase in library size though possible will, however, necessitate a miniaturization of the assay as the number of tests increase with  $n!$ . The data are therefore insufficient to construct extended interaction networks, which would allow the analysis of MSC-niche network motifs. Despite these limitations the efforts made led to the identification of a number of novel interactions, which might turn out to be of key importance to stem cell biology and human cancer.

- Tenascin W an hexameric ECM glycoprotein binds to Notch ligands DeltaA and B (described in Chapter 13; Figure 13.8)
- Seraf/Vdwe an EGF-type ligand secreted by teleost MSCs, binds to FGFR4 and Kon-Tiki 3/Cspg4 (Figure 12.1A)
- Nlrr1/Lrrn1, the vertebrate homolog of *Drosophila* Capricious binds to Notch ligands, DeltaA, B and C (Figure 12.1B)
- Wfdc1, an orphan ligand, binds to Ephrin kinase 1 (Figure 12.2)

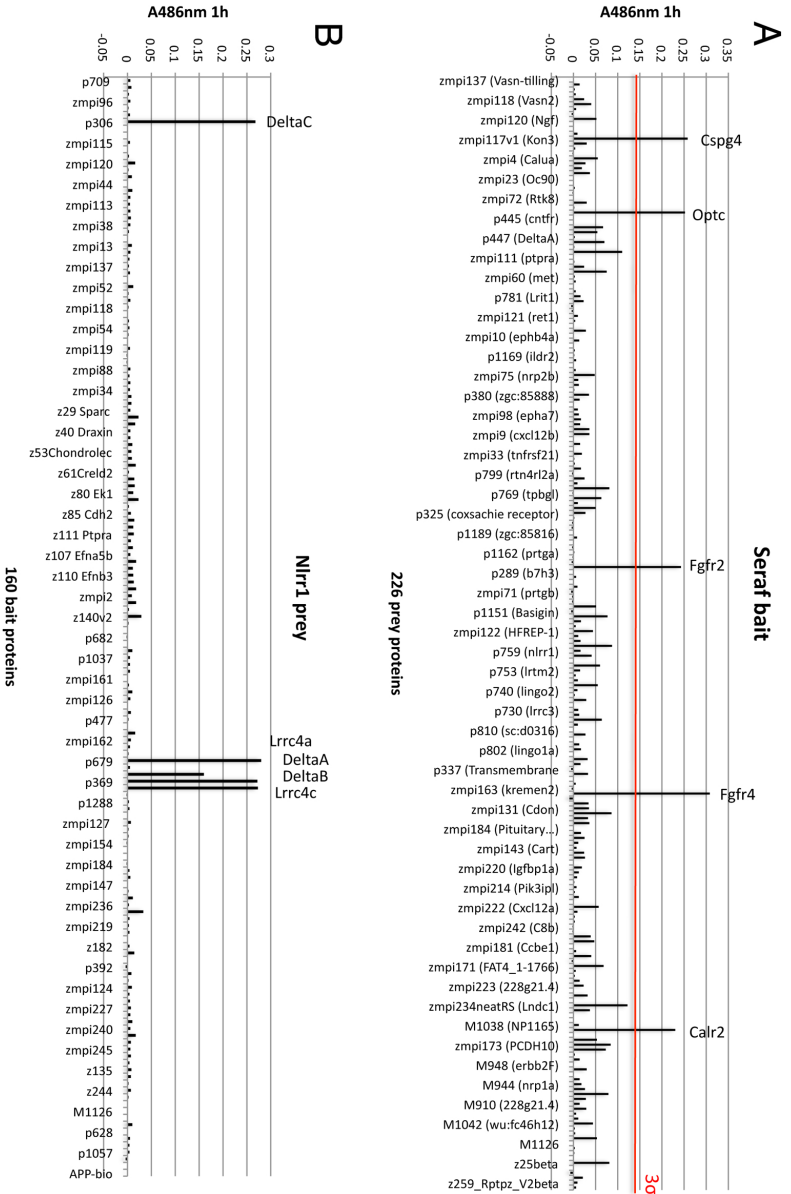
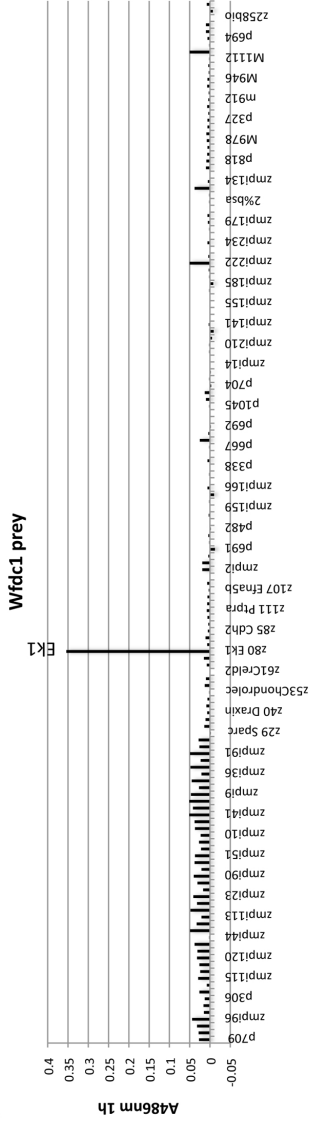
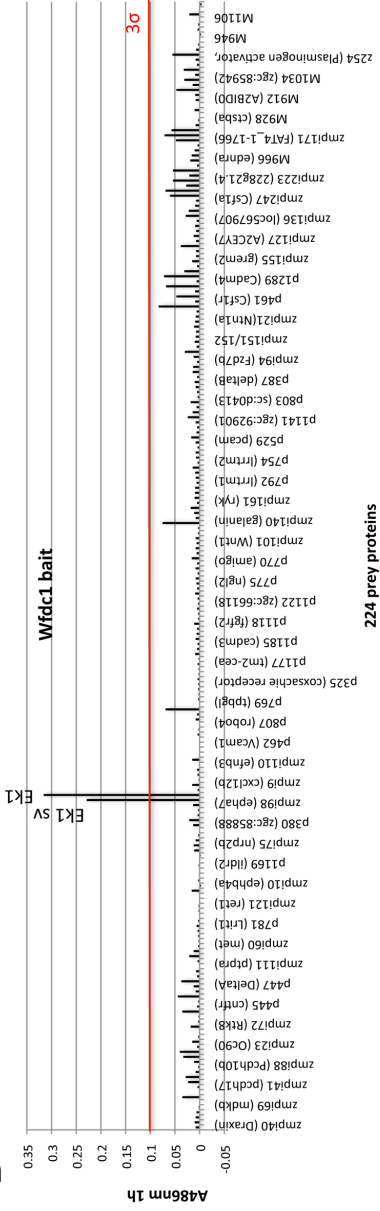


Figure 12.1: AVEXIS screening Seraif and Nlrr1 against the AVEXIS library.

**A****B****Figure 12.2:** AVEXIS screening of Wfdc1 against the AVEXIS library.



— *Man sieht sich leicht an Wald und Feldern satt;  
Des Vogels Fittich werd ich nie beneiden.  
Wie anders tragen uns die Geistesfreuden  
Von Buch zu Buch, von Blatt zu Blatt!* —

Goethe, Faust

# 13

## Niche extracellular matrix component Tenascin W regulates muscle stem cell self-renewal

OWING TO THE results of these pilot experiments, Tenascin W (Tnw), which belongs to a family of hexameric ECM glycoproteins, seemed to be a particularly promising candidate for being a MSC-derived MSC niche component. Its paralog Tenascin C (Tnc), was originally identified as a myotendinous antigen (Chiquet and Fambrough, 1984a, b).

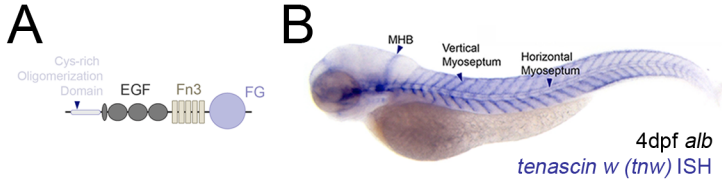


**Figure 13.1:** Domain structure of Tenascin W and transcript expression at 4dpf. (A) An N-terminal oligomerization domain mediates dimerization of Tnw trimers. This domain is followed by 3,5 EGF-type repeats (EGF), 5 fibronectin repeats (Fn) and a C-terminal fibrinogen domain (FG). (B) *tnw* *in situ* hybridization showing expression in cells, which are located at the vertical myoseptum (ISH performed by Dr. Jana Krauss, MPI für Entwicklungsbiologie, Tübingen).

### 13.1 Tenascin W is required for MSC maintenance

Tenascin W (Tnw) and Tenascin C (Tnc) share common domain architectures. An N-terminal domain mediating the dimerization of homotrimers is followed by epidermal growth factor-like (EGF) repeats, fibronectin (FN III) type III domains, and a C-terminal globular fibrinogen (FG) domain (Figure 13.1A).

Consistent with published results (Weber et al., 1998), *tnw* is transcribed in cells located at the vertical myoseptum at 48hpf and 4dpf (Figure 13.1B, provided by Dr. Jana Krauss, MPI für Entwicklungsbiologie, Tübingen). In conjunction with the profiling results this strongly suggests that *tnw* is indeed expressed by zebrafish MSCs. *tnw* knockdown experiments were

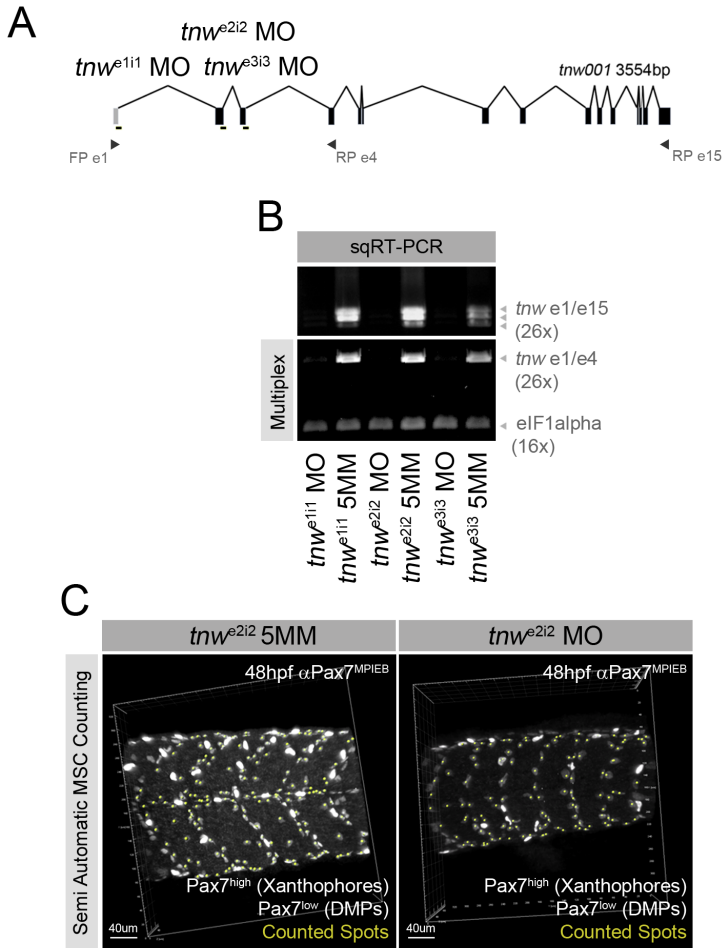


**Figure 13.2:** *Tnw* is essential for MSC maintenance. (A) *tnw* exon-intron structure indicating the placing of morpholinos and primers used. (B) semi-quantitative RT-PCR showing the absence of detectable *tnw* message in response to *tnw* MO injection. (C) Representative examples of whole-mount Pax7 antibody stainings of 24hpf *tnw* morphants and 5 mismatch morpholino (5MM)-injected controls used for quantification of DMPs (compare Figure 13-3). Note that DMPs express Pax7 at much lower level than xanthophores.

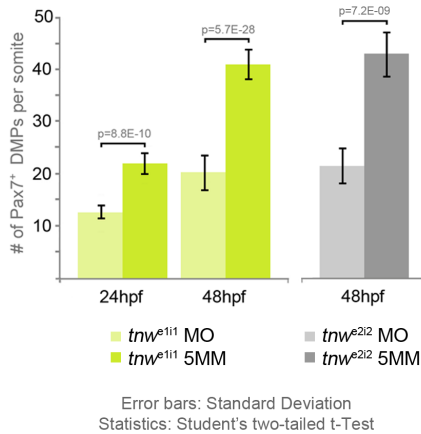


**Figure 13.3:** Quantification of Pax7<sup>+</sup> DMP cells in *tnw* morphants vs. 5 mismatch morpholino (5MM)-injected controls.

performed using morpholinos (MOs) that target the exon1-intron1 (*tnw*<sup>e1i1</sup> MO), exon2-intron2 (*tnw*<sup>e2i2</sup> MO) or exon3-intron3 (*tnw*<sup>e3i3</sup> MO) splice donor site (Figure 13.2A). All MOs effectively block splicing and exhibit negligible toxicity. Different splicing defects such as intron retention, exon skipping, activation of a cryptic splice or multiple splice defects can be triggered by the use of a MO. A number of primers were placed in the *tnw* locus (Figure 13.2A) to directly observe the consequences of *tnw* MOs on *tnw* mRNA by semiquantitative RT-PCR. It was found that in *tnw* morphants irrespective of the actual MO used *tnw* mRNA is virtually absent (Figure 13.2B).

To assess the possible effect of Tnw's depletion on MSC maintenance the number of DMPs at the end of primary myogen-

esis (24hpf) and during the transition phase (48hpf) was determined by whole mount immunofluorescence (Figures 13.2C and 13.3) using a Pax7 antibody, which was raised against the zebrafish Pax7c C-terminus with the help of Dr. Heinz Schwarz (MPI für Entwicklungsbiologie, Tübingen). Strikingly, *tnw* morphants show a 50% reduction in DMP number as early as 24hpf, in the absence of morphological defects (Figure 13.3). This pronounced reduction is also evident at 48hpf and later developmental stages, when morphological defects in the cranium (Figure 13.4A) as well as histological defects in the trunk musculature (Figure 13.4B) and vascularisation (Figure 13.5A) become apparent in *tnw* morphants. These abnormalities are accompanied by impaired force muscular transmission, as evident from the aberrant swimming motions of *tnw* morphants. As development proceeds, these defects become more prominent leading to the clearly visible phenotype of *tnw* morphants at 4dpf, which display severely reduced myotome growth, muscle fibre disorganization, defects of the vertical and horizontal myosepta, (Figure 13.5B), defects of the vasculature as well as dysgenesis in the cranium.

The response of myogenic lineage dynamics to the depletion of Tnw was monitored by intravital imaging of 4day old *tnw* morphant larvae. These imaging experiment demonstrated that the strong reduction of MPs is not caused by cell death, but by altered cell cycle and differentiation kinetics. In response to *tnw* knockdown, quiescent MSCs lose their normal digitated cell morphology (Figure 13.6), become mitotically active, and differentiate into CMPs or EMBs, which in turn frequently divide again (Figure 13.7 and Movie S6). Based on clonal analysis the mean cell cycle duration of MSCs in *tnw*

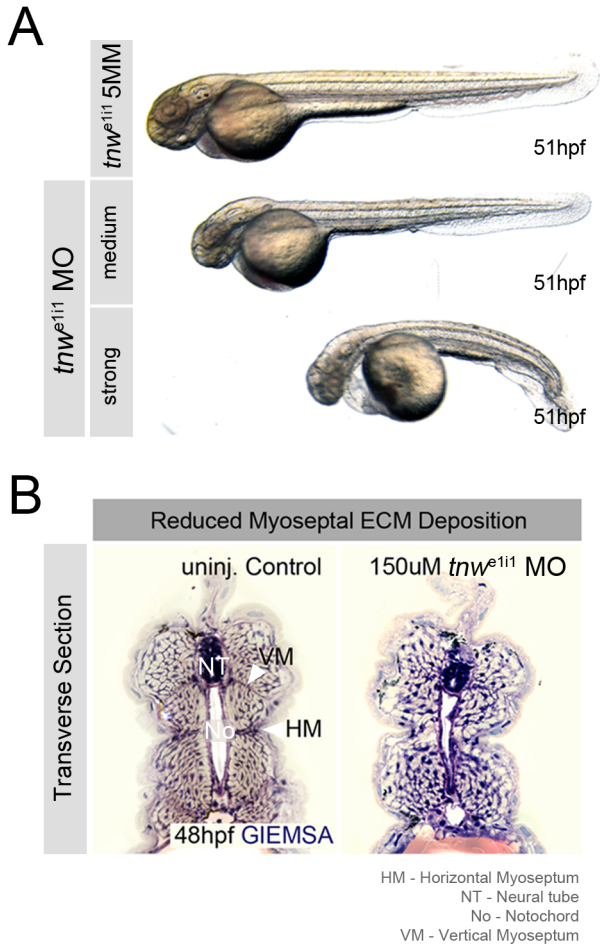


**Figure 13.4:** Morphological and histological defects in *tnw* morphants at day 2. (A) Morphological defects including shortening of the trunk, generally reduced growth and cranial defects are seen in 2day-old *tnw* morphants. (B) Transverse GIEMSA-stained plastic sections showing muscle fibre disorganization and reduced ECM deposition at the vertical and horizontal myoseptum.

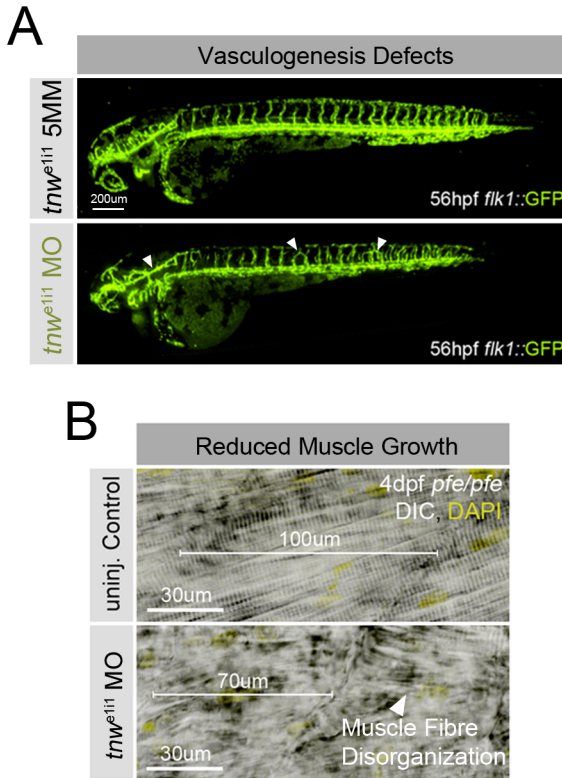


**Figure 13.5:** Muscle growth and vasculogenesis defects in *tnw* morphants. (A) Knockdown of *tnw* leads to defective vasculogenesis as evidenced by injection of *tnw* MOs in a *flk1::GFP* background. (B) Growth defects and muscle fibre disorganization are also easily visualized using Nomarski optics in 4-day old *tnw* morphants.

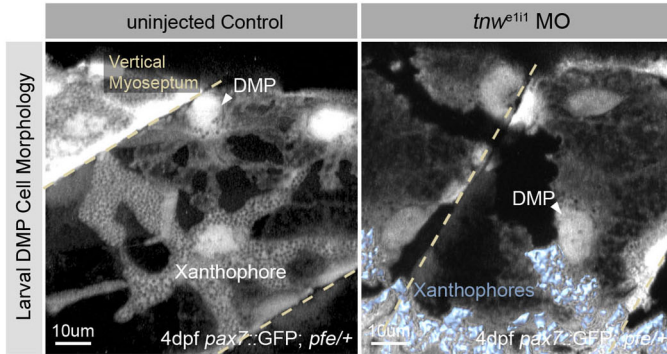


**Figure 13.6:** Aberrant cell morphology of DMPs in 4day-old *pax7::GFP tnw* morphants. In response to *Tnw*'s depletion, DMPs lose their digitated cell morphology.

morphants can be estimated to be around 30h as compared to more than 120h in uninjected controls (Table 9.1). The strong reduction of MSC number suggests that MSC proliferation in *tnw* morphants fails to compensate for the loss of MSCs due to illegitimate differentiation. These results indicate that *Tnw*, secreted by the MSCs, is an essential niche component needed to ensure MSC maintenance.

## 13.2 Tenascin W interacts with Notch ligands DeltaA and B

The finding that *Tnw* is an MSC-derived MSC niche component as well as the strong biomedical interest in Tenascins raised the interest in the interactions that *Tnw* might have with other

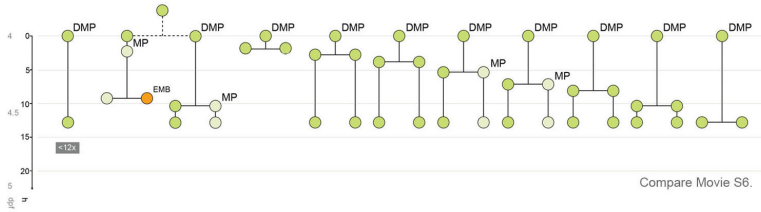


**Figure 13.7:** Intravital imaging-based clonal analysis of DMPs in a 4day-old *tnw* morphant shows illegitimate activation of the quiescent MSC compartment.

collagenous and non-collagenous ECM, signaling molecules as well as proteins present on the MSC's cell surface. In collaboration with Dr. Christian Söllner (MPI für Entwicklungsbiologie, Tübingen) the AVEXIS technology was exploited to screen a *Tnw* deletion construct lacking the N-terminal oligomerization domain as well as the EGF-type repeats against a library of more than 120 bait extracellular proteins. The screen was performed with a truncated form of *Tnw* as the expression levels of the full-length form were not sufficient for a complete library screen. Future efforts might circumvent this limitation and uncover more interaction partners, whose interaction with *Tnw* is mediated by the EGF-type repeats. While more interaction partners remain to be identified, the small set of interacting proteins found in this screen includes a number of interesting interactions. Most importantly, this screen detected interactions of *Tnw* with DeltaA and B, which are ligands of the Notch receptor (Figure 13.8A, Table 22.4). These results establish a direct link between the extracellular matrix glycoprotein, *Tnw*, and Notch signaling. By rescreening a panel of *Tnw* deletion constructs against zebrafish DeltaA,

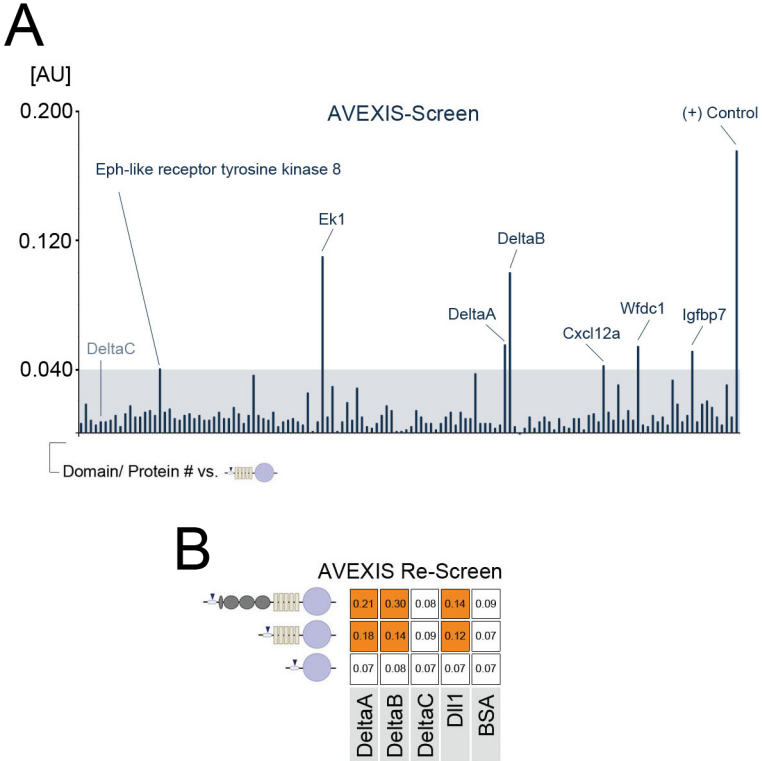


**Figure 13.8:** AVEXIS screen of a Thw deletion construct for extra-cellular protein-protein interaction partners identifies Notch ligands DeltaA and B. (A) Primary AVEXIS screen of Thw deletion construct against a library of more than 120 bait proteins (see also Table 22.4) identifies a very small set of interaction partners including Delta A and B, which are ligands of the Notch receptor. (B) AVEXIS-rescreen of Thw deletion constructs against a panel of Delta ligands including human Delta-like 1 (Dll1) reconfirms the hit in the primary screen and maps the interaction to the Fn type 3 repeats in Thw. Bovine serum albumin (BSA) serves as negative control.

B, C as well as Delta-like 1 (DLL1), the human homolog of DeltaA, the screening result was validated and the interaction was mapped to the Fibronectin-repeats in Tnw (Figure 13.8B). These observations indicate that Tnw, an MSC-derived MSC niche component, which is essential for MSC self-renewal interacts with Delta ligands of the Notch pathway and strongly suggest that Tnw's function as a niche molecule lies in the regulation of Notch signaling. Apart from the DeltaA and B a number of further interaction partners for Tnw were identified by the AVEXIS screen. According to the 'behavior' of these proteins in the AVEXIS screen (unpublished observation of Dr. Christian Söllner, MPI für Entwicklungsbiologie) these proteins are classified as 'frequent binders', i.e. they were found to interact with a large number of proteins in the screen. This raised the concern that the interactions detected involving these proteins might be false-positives. For this reason these proteins were not subject to further analysis.



## Part III

# Discussion



— *O! glücklich! wer noch hoffen kann.  
Aus diesem Meer des Irrthums aufzutauchen.  
Was man nicht weiß das eben brauchte man,  
Und was man weiß kann man nicht brauchen.* —  
Goethe, Faust

# 14

## Identification of teleost MSCs and their origin in the teleost dermomyotome

THE UNEQUIVOCAL IDENTIFICATION of stem cells remains a key problem in stem cell research (Morrison and Spradling, 2008). While lineage tracing allows the self-renewal and multi-/unipotency of small cell populations to be assessed *in vivo*, it does not allow stem cells to be discerned from their committed progeny, as there are no molecular markers whose expression would distinguish the two (Snippert and

Clevers, 2011). Using zebrafish as a model system provides the unique possibility to monitor progenitors with single cell resolution in the living animal by intravital imaging. From a significant number of such progenitor clones a particular cellular lineage can be reconstructed, which allows the actual stem cells to be identified based on their position in the lineage. This paradigm was exploited to reconstruct the myogenic lineage in teleost larvae (Chapter 9) and to obtain a fine-grained sub-classification of the Pax7<sup>+</sup> MP compartment into DMPs, CMPs and EMBs based on differences in their anatomical position, cell morphology (Figure 9.6 and Animation S1), migratory behavior (Figure 9.8 and Movie S4), mode of cell division (Figures 9.8, 9.9, Movie S4, and Animation S2), mean cell cycle time (Table 9.1) and clonal relationship (Figures 9.5, 9.7, 9.11). Their close association with the vertical myoseptum and the fact that MSC maintenance relies on self-secreted myoseptal components (Chapter 10), such as Tnw (Chapter 13), indicates that the vertical myoseptum serves as the teleost MSC niche. Teleost MSCs are able to self-renew by symmetric cell division generating a pool of equipotent MSCs from which a small fraction is singled out. In this way it could be shown that DMPs correspond to the most upstream MP of the teleost myogenic lineage. They derive directly from anterior/medial somitic cells, which start to express Pax7 prior to somite rotation (Figure 9.4A) and form a highly transient epithelial cover - the teleost dermomyotome - on top of the myotome around 23hpf. Soon after this the DMP cell division and the growth of the myotome leads to a disintegration of the teleost dermomyotome (24-30hpf) leaving behind a pool of DMP cells, from which the majority will differentiate into

myoblasts driving primary myogenesis, while a fraction will remain undifferentiated and associated with the vertical myoseptum. These cells will then undergo strong amplification during the consequent transition phase, which lasts approximately until 3dpf (Figures 9.3, 9.4 and 9.5). At the end of transition phase the majority of DMPs become progressively quiescent, while a small fraction leaves their superficial position and enter the myotome thereby giving rise to either CMPs or EMBs, which correspond to two transit-amplifying progenitor compartments (Figure 14.1). While EMBs are freely moving inside the myotome, CMPs still adhere to the vertical myoseptum (Figures 9.8 and 9.9). CMPs are able to divide symmetrically or asymmetrically (Figures 9.8, 9.9, Movie S4, and Animation S2). The latter mode allows CMPs to renew themselves and at the same time to generate an EMB (indirect myotome entry). Alternatively CMPs can directly lose their adhesivity towards the vertical myoseptum, enter the myotome and differentiate into an EMB (direct myotome entry). EMBs amplify in number by SCD and are able to differentiate into either fibre-forming myoblasts or fusion-competent myoblasts (Figures 9.10 and 9.11C,D). Importantly, none of the observed early embryonic Pax7<sup>+</sup> DMP cells undergoing differentiation during primary myogenesis underwent myoblast fusion. Instead these cells exclusively formed muscle fibres *de novo* (compare Movies S1 and S2). The lack of fusion-competent myoblasts during primary myogenesis is an important difference in the topology of the myogenic lineage during primary and secondary myogenesis. The fact that DMPs derive from the teleost dermomyotome, are the topmost myogenic progenitor of the teleost myogenic lineage, become quiescent with the on-

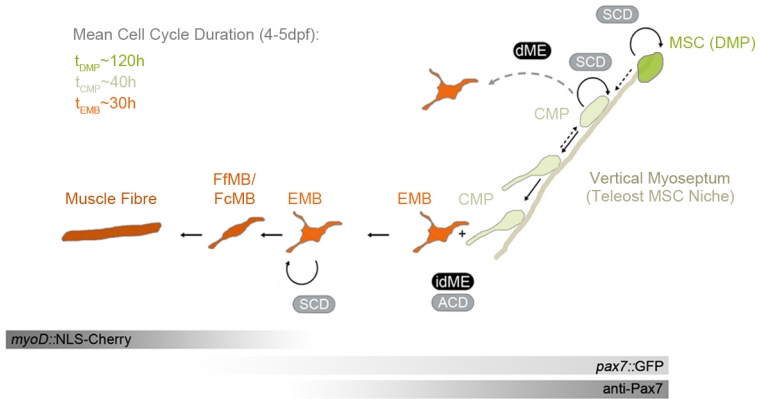


**Figure 14.1:** Working model of the myogenic lineage in teleosts. FcMB - fusion-competent myoblast. FfMB - fibre-forming myoblast, id/dME - in-/direct myotome entry, SCD - symmetric cell division, ACD - asymmetric cell division. For further explanation see text.

set of secondary myogenesis around 3dpf, and serve as a continuous source for Pax7<sup>+</sup> transit-amplifying cells (i.e. CMPs, EMBs), that will ultimately differentiate into fusion-competent or muscle fibre-forming myoblasts identifies the DMPs as the actual MSCs in teleost embryos and larvae (Figures 9.7, 14.1, and Table 9.1).

The developmental origin of DMPs in the Pax7<sup>+</sup> epithelial layer, which covers the myotome around 23hpf (Figure 9.4A), indicates that this somitic compartment is homologous to the dermomyotome of amniotes, as proposed before (Devoto et al., 2006; Hammond et al., 2007; Hollway et al., 2007; Marschallinger et al., 2009; Steinbacher et al., 2006; Stellabotte et al., 2007).

This indicates that the dermomyotome arose before the split of the teleost and amniote lineages and strengthens the notion that the principles governing MSC physiology are highly conserved within the vertebrate subphylum. Although the intravital imaging analysis performed for these earlier stages was not extended to adult teleosts, it can be expected that the model of the myogenic lineage provided here also applies to juvenile and adult teleost myogenesis (see Chapter 15). In conjunction with this, it can be hypothesized that also during secondary myogenesis teleost MSCs do not adopt a satellite location, but rather stay associated with the vertical myosepta, which would represent a clear difference between teleost and amniote MSC niches.

## 14.1 Teleost MSC maintenance may be governed by symmetric cell division and stochastic differentiation

Self-renewal and multi-/unipotency are the defining characteristics of stemness. Self-renewal can be achieved on the single cell-level through asymmetric cell division, which generates a stem cell and a differentiating progenitor daughter cell, or on the population level by stochastic singling out from a pool of equipotent stem cells. While adult mouse satellite cells have been shown to undergo asymmetric cell division in *in vitro* muscle fibre explant assays (Kuang et al., 2007) it is not clear whether mammalian MSC maintenance relies on this hierarchical mode of self-renewal and differentiation *in vivo*. Recently, elegant fate mapping experiments suggested that the stem cell

maintenance in the mouse intestine relies on neutral competition between symmetrically dividing stem cells (Lopez-Garcia et al., 2010; Snippert et al., 2010). Along this line *in vivo* clonal analysis of radial glia-like neural stem cells demonstrated that these stem cells are able to self-renew by asymmetric or symmetric cell division (Bonaguidi et al., 2011).

Clonal analysis suggests that self-renewal and maintenance of teleost MSCs, similarly, does not rely on asymmetric cell division. Rather it appears that teleost MSCs amplify symmetrically to generate a pool of MSCs from which a small fraction is singled out stochastically to undergo differentiation. In fact no differentiation event was observed being directly related to prior cell division (Figure 9.7). While this does not rule that previous asymmetric cell divisions deems a subfraction of MSCs prone to differentiation, the simpler explanation remains that MSCs self-renewal is ensured on the population-level.

— *Wer will was Lebendigs erkennen und beschreiben,  
Sucht erst den Geist heraus zu treiben,  
Dann hat er die Teile in seiner Hand,  
Fehlt leider! nur das geistige Band.* —

Goethe, Faust

# 15

## The vertical myoseptum functions as the MSC niche in teleosts

THE OBSERVATION that (A) quiescent MSCs display a strong association with the vertical myoseptum and (B) Tnw, which is secreted by MSCs, is both a component of the vertical myoseptum as well as an essential niche factor necessary for MSC maintenance, led to the conclusion that the vertical myoseptum is not merely a myotendinous junction connecting neighbouring myotomes, but also serves as the niche for MSCs in teleost larvae and possibly also in juveniles and adults. Importantly, Tnw is not the sole MSC-derived component of the

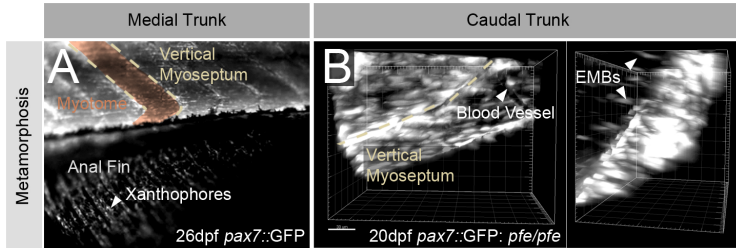


**Figure 15.1:** Presence of Pax7<sup>+</sup> MSCs at the vertical myoseptum in juvenile *wild type* (A) and *pfeffer* mutant (B) zebrafish.

vertical myoseptum evidently connected to key signaling functions pertaining to the regulation of MSC physiology. The soluble factor Wnt inhibitory factor 1 - the vertebrate homolog of *Drosophila shifted* (Glise et al., 2005; Gorfinkiel et al., 2005) - was likewise found to be strongly upregulated in MSCs and by immunofluorescence could be shown to be anchored to the vertical myoseptum (Figure 19.1). Preliminary functional data from the morpholino screen and prior knowledge about the implication of Wif1 in facilitating the mobility of lipid-modified morphogens of the Wnt and Hh families (Glise et al., 2005; Gorfinkiel et al., 2005) suggest that MSC-derived Wif1 might be required to facilitate the mobility of notochord derived Hh signals along the vertical myoseptum and thereby influence somite patterning (see Chapter 19). The view that the vertical myoseptum in addition to its importance for force transmission functions as the MSC niche in teleosts is supported by the preliminary observation, that in juvenile zebrafish MSCs are found at the vertical myoseptum (Figure 15.1). It is important to note at this point that the presence of these Pax7<sup>+</sup> cells in *pfeffer* mutants which lack xanthophores strongly sug-

gests that these cells are indeed MSCs. Thus the picture of the myogenic lineage provided here for larval teleosts may well hold true in qualitative terms for juveniles and adults as well. In quantitative terms it appears

- that the number of MSCs and EMBs increases proportional to the increase in muscle fibre number and
- that the mean cell cycle time of MSCs in juveniles and adults may exceed the time that was derived for 4-6dpf larvae.

## 15.1 On the evolution and ontogeny of the vertical myoseptum

Myosepta are the evolutionary predecessors of tendons and other types of myotendinous junctions. They are found in the cephalochordate *Amphioxus* (*Branchiostoma*), whose axial musculature is organized into myomeres (Summers and Koob, 2002). While it is unclear whether *Amphioxus* has MSCs, several lines of evidence point to this possibility: (A) the *Amphioxus* genome contains single *pax3/7*, *six1/2*, *six4/5* and *dach* genes (Holland et al., 1999; Kozmik et al., 2007), (B) these homologues to key regulators of vertebrate myogenesis are expressed in the presumptive somites of *Amphioxus*, (C) proliferating cells have been found on top of the somite in *Amphioxus* larva (Holland and Holland, 2006), (D) muscle growth continues throughout life.

The evolutionary origin of the dermomyotome and/or MSCs and the acquisition of MSC niche function by the myoseptum might therefore predate the split of the cephalochordate from the vertebrate lineage. As such the myoseptal MSC niche of zebrafish would reflect a more ancestral state of the MSC niche. In this regard it is very interesting to see that a number of myoseptal components including *thbs4*, *fmod*, *lumican*, and *olfml2B*, which were found to be strongly expressed by larval zebrafish MSCs (see Chapter 10), were recently also shown to be highly upregulated in quiescent vs. activated Pax7<sup>+</sup> mouse MSCs (Fukada et al., 2007). Taken together these findings suggest that MSCs play a pivotal role in the ontogeny of the vertical myoseptum. Likewise these findings indicate that the

vertical myoseptum, which functions as the MSC niche in teleosts, shares a number of components with the niche of adult mammalian MSCs. This is an important point as it indicates that principles derived from the study of teleost MSCs and their niche can be extrapolated to mammals.

## 15.2 Muscle stem cells construct their own niche

Recent work indicates that somatic support cells might not be a general property of stem cell niches. Intestinal stem cells in *Drosophila* for instance do not seem to rely on a niche that is provided by support cells (Ohlstein and Spradling, 2006). Similarly, in adult vertebrate skeletal muscle MSCs are found dispersed throughout the tissue with no apparent regularity. A prepatterned microanatomical site does not seem to exist for the MSCs of adult vertebrate muscle, which contrasts with other vertebrate organs in which stem cells are found in particular locations.

The fact that satellite cells are closely associated with the muscle fibre has led to the interpretation that the muscle fibre represents the niche support cell (Gopinath and Rando, 2008). While muscle fibres influence the activation of MSCs, it is not clear whether they provide signals that in a strict sense can be seen as niche signals, i.e. signals necessary for the maintenance of MSC stemness. Strikingly, isolated mouse satellite cells do not lose engraftment efficiency when cultured on a substrate that mimics the matrix elasticity of skeletal muscle (Gilbert

et al., 2010). It seems unlikely however, that matrix elasticity alone is sufficient to instruct MSC self-renewal. In conjunction with the results presented here and the profiling data of Pax7<sup>+</sup> mouse MSCs/MPs (Fukada et al., 2007; Pallafacchina et al., 2010), it seems reasonable to assume that adjusting this physical parameter renders the substrate permissive for MSCs to produce niche factors *in vitro*, which in turn allows for a higher rate of MSCs self-renewal. Most molecules known to regulate MSC quiescence, inhibition of differentiation or maintenance are MSC-derived (e.g. bFGF, Myostatin, BDNF, Delta-1, BMP4; Fukada et al., 2007; Kuang et al., 2008) Taken together, these and the results presented here show that MSCs in mouse and zebrafish produce niche factors themselves. While signals from the muscle fibres (e.g. nitric oxide, Hepatocyte growth factor), macrophages, the vasculature and the motor nerve guide the activation of MSCs, in particular during regenerative myogenesis (Boonen and Post, 2008), neither of these cell populations seem to function as a support cell similar to the niche forming somatic support cell in the *Drosophila* germarium (Xie and Spradling, 1998, 2000). Apart from Tenascin W, which was found to be an MSC-derived MSC niche component (see Chapter 13), other MSC-secreted candidate genes are very likely to be niche factors as well. These include Fibromodulin, which is known to bind Myostatin, the most potent suppressor of muscle growth (Miura et al., 2010).

### 15.3 Tenascin W, a niche molecule and novel regulator of Notch signaling

Tenascins comprise a small family of extracellular matrix (ECM) glycoproteins (Chiquet-Ehrismann and Tucker, 2004). The most intensively studied member of the Tenascin family is Tenascin C (Tnc). Both Tnc and Tnw are expressed in a wide variety of tissues with a large overlap in the expression domains of both molecules (Scherberich et al., 2004). Similar to its paralog *tnc*, *tnw* was found to be expressed in the majority of human breast tumors, colon carcinoma as well as oligodendroglioma, astrocytoma and glioblastoma, which contrasts with the absence of Tnw from healthy breast, colon or brain tissue (Martina et al., 2010). The expression of *tnc* has been shown to correlate with poor prognosis in a variety of human cancers. Tenascin C is expressed in the SVZ, the hair bulge, by stromal cells in the bone marrow, the presumptive niches of neural stem cells, hair follicle stem cells, and hematopoietic stem cells (von Holst, 2008). In light of the finding that MSC-secreted Tenascin W constitutes a key component of the MSC niche in zebrafish (see Chapter 13) it is very interesting that the source of Tenascin C expression in the hair bulge are hair follicle stem cells (Tumbar et al., 2004). The molecular function of Tenascin molecules is only beginning to be understood. Both Tenascin C and W share the same general domain architecture with variations in the number of EGF and fibronectin repeats. The overall weak phenotype of *tnc* knockout mice, as well as the still moderate phenotype of *tnw* morphants in zebrafish, might hence be attributable to redundancy between the two homologues. Molecules known to bind Tenascin C

include the EGF receptor, Fibronectin, Heparin, several Integrins, Nidogen, and Smoc-1. Strikingly, Tenascin C induced the expression of myogenesis-related transcriptional regulators Id2, Hey1 and Tcf12 in T98G cells (Ruiz et al., 2004). Id2 is a potent inhibitor of myogenic differentiation, which binds to myogenic regulatory factors such as Myf-5, Mgn, MyoD as well as to Tcf12 (Langlands et al., 1997) thereby suppressing their myogenic activity (Benezra et al., 1990; Jen et al., 1992), and is a known transcriptional target of Pax7 (McKinnell et al., 2008). In this regard it is important to know that aside from Tenascin W also Tenascin C is a component of the vertical myoseptum in zebrafish. Therefore it seems reasonable to assume that both Tenascin C and Tenascin W induce the expression of Id proteins in MSCs thereby regulating their quiescence. Furthermore the induction of Hey1 and Tcf12 (Ruiz et al., 2004) points to a possible involvement of Tenascin C in Notch and Wnt signaling, whose balance is known to regulate MSC self-renewal (Brack et al., 2008; Brack et al., 2007; Kuang et al., 2007; Schuster-Gossler et al., 2007; Vasyutina et al., 2007). In this regard it is important to note that both Hey1 (5,1x up) and Tcf12 (2,5x) were found to be strongly up-regulated in zebrafish MSCs/MPs. Moreover, the interaction that was detected between Tenascin W and Delta ligands suggests that the positive regulation of Notch signaling is a key function of Tenascin W and possibly other Tenascins as niche molecules. In this regard it is interesting to know that mouse MSCs are able to shed Dll1 (Sun et al., 2008). The clustering of shed Delta ligands on hexameric Tenascin W offers an attractive explanation for its function as a niche molecule. In this scenario Tenascin would positively regulate Notch signaling by

creating microenvironments of high Delta ligand concentration and/or increasing the avidity of Delta ligands by multimerization. Alternatively, Tenascin W might elevate Notch signaling by binding to membrane-bound Delta ligands thereby attenuating *cis*-inhibition between Delta and Notch. Importantly, since Tenascin W is a tumour stroma marker expressed in a wide variety of human cancers it seems reasonable to assume that also in this context Tenascin W functions as a niche molecule for cancer stem cells possibly by enhancing their Notch signaling activity (Martina et al., 2010). Along this line it has been reported recently that breast cancer cells rely on Tnc expression to be able to colonize lung tissue and that this dependency could be circumvented by up regulation of Notch signaling (Oskarsson et al., 2011). This suggests that apart from Tnw, Tnc also interacts with Delta-Ligands of the Notch receptor and that these protein-protein interactions represent promising novel drug targets for cancers of various origins including *glioblastoma multiforme*.



— *Drei Jahr ist eine kurze Zeit,  
Und, Gott! das Feld ist gar zo weit,  
Wenn man einen Fingerzeig nur hat,  
Lässt sich's schon eher weiter fühlen.* —

Goethe, Faust

# 16

## MSC/MP-secreted proteins with auto-/paracrine signaling function

THROUGH TRANSCRIPTIONAL PROFILING a number of signaling molecules were shown to be secreted by teleost MSCs/MPs. These include the cytokine Csf1b, the EGF-repeat containing ligand Seraf, and the WAP-disulfide core-containing protein Wfdc1/ps20. While the former is known to be the prototypical ligand for the FMS receptor tyrosine kinase (Pixley and Stanley, 2004), the latter were thus far orphan ligands (Wakamatsu et al., 2004). Using the AVEXIS screening platform these ligands could be deorphanized identifying an in-

teraction between Seraf and FGFR4 as well as Wfcd1/ps20 with Ephrin-Kinase 1 (Figures 12.1A and 12.2). These data suggest that MSC-derived Seraf binds to the FGFR4 receptor, which likewise was found to be strongly upregulated in teleost MSCs/MPs (Table 22.3). Taken together this indicates that Seraf-FGFR4 interaction is part of an autocrine feedback-loop. In light of these findings it is interesting to note that Seraf also interacts with Kon-Tiki 3, a type I transmembrane protein, which is also known as Cspg4 (Figure 12.1A). Whether Kon-Tiki 3/Cspg4 has a signaling function on its own or operates as a Seraf coreceptor facilitating Seraf-mediated FGFR4 signaling is currently not clear. A role for Seraf in FGFR4 signaling is, however, consistent with published expression data for *seraf*, which found expression of this ligand in the presumptive dermomyotome in rainbow trout (Dumont et al., 2008), as well as with the demonstration that Seraf-AP fusion protein binds to an unidentified receptor expressed in the chick primary myotome - a site of FGFR4 expression (Wakamatsu et al., 2004). Apart from this Wfcd1's interaction with Ephrin-Kinase 1 (Figure 12.2), which is primarily expressed in neurons of the CNS (Thisse et al., 2004), suggests that MSC-derived Wfcd1 has a paracrine function. It seems possible that via Wfcd1 teleost MSCs/MPs communicate with motor neurons, whose axons follow the vertical myosepta and thus are in close proximity to teleost MSCs. While in contrast to these novel interactions, the binding of Csf1b to FMS was known before, it is an important observation of this study that Csf1b is in fact expressed in cells of the myogenic lineage *in vivo*. Moreover, the demonstration that Csf1-FMSa signaling regulates *pax7* expression in xanthophores is a key finding of this study as it

suggests that Csf1-FMSa/b signaling likewise regulates *pax7* expression in the myogenic lineage constituting an autocrine feedback-loop. The fact that Csf1 was also found to be upregulated in satellite cells of adult mice further strengthens the view that Csf1 signaling is of essential importance for MSC physiology in teleosts and mammals (Table 17.1).



— *Vergebens dass Ihr ringsum wissenschaftlich schweift,  
Ein jeder lernt nur, was er lernen kann;  
Doch der den Augenblick ergreift,  
Das ist der rechte Mann.*—

Goethe, Faust

# 17

## Approaching a MSC gene expression signature conserved across the vertebrate subphylum

THE GENETICS of myogenic commitment (Baugh and Hunter, 2006; Seipel and Schmid, 2005), fusion (Rochlin et al., 2010), and muscle fibre differentiation (Cleto et al., 2003; Shaffer and Gillis, 2010; Vandekerckhove and Weber, 1984) are highly conserved. It is not known, however, how far the genetics of MSC physiology are conserved inside the vertebrate subphylum. Several experiments have interrogated the gene

expression signatures of mouse satellite cells, which comprise a heterogeneous mixture of MSCs and committed MPs. These experiments compared quiescent (i.e. directly isolated from healthy muscle), with activated satellite cells. The latter activated satellite cells in these studies were either isolated from dystrophic muscle (i.e. *mdx* mice) or satellite cells that were taken into cell culture (Fukada et al., 2007; Pallafacchina et al., 2010). This experimental setup hence uncovers genes that undergo differential regulation during the course of satellite cell activation, but does not select for genes whose expression is very specific to satellite cells.

In contrast to these existent profiling experiments, which aim at the characterization of the satellite cell's transcriptome in different development stages or physiological conditions, the approach chosen here was designed to detect the genes that are very specifically upregulated in MSCs. The rationale behind this decision was that genes, which are more strongly expressed in muscle stem cells than in other parts of the body are more likely to have muscle stem cell specific functions. Apart from this it is important to keep in mind that 'satellite cell' is an anatomically defined term, and that the satellite cell compartment contains only about 10% muscle stem cells and 90% committed myogenic progenitors/myoblasts (Kuang et al., 2007). Consequently, mouse satellite cell profiling datasets are strongly biased for already committed progenitors and have little contribution of the actual stem cell compartment. For the 'teleost MSC profiling' performed at 4dpf, however, it appears from simple counting that MSCs account for 57% of Pax7<sup>+</sup> MPs. For this reason the 'teleost MSC dataset' can be expected to contain a strong MSC signature. With this

**Table 17.1:** Molecular signature of quiescent MSCs conserved throughout vertebrate evolution.

| Gene           | Compartment  | Comment                                 |
|----------------|--------------|---|
| <i>pax7</i>    | Nucleus      | Transcription factor                    |
| <i>eya1</i>    | Nucleus      | Transcription factor                    |
| <i>myf5</i>    | Nucleus      | Transcription factor                    |
| <i>hey1</i>    | Nucleus      | Transcription factor                    |
| <i>mcm5</i>    | Nucleus      | DNA replication                         |
| <i>lmb1</i>    | Nucleus      | Nuclear lamina                          |
| <i>asf1b</i>   | Cytoplasm    | Histone chaperone                       |
| <i>lpl</i>     | Cytoplasm    | Enzymatic activity                      |
| <i>lrig</i>    | Cell Surface | Transmembrane protein                   |
| <i>fgfr4</i>   | Cell Surface | Transmembrane protein                   |
| <i>jamb</i>    | Cell Surface | Transmembrane protein                   |
| <i>csf1</i>    | Cell Surface | Transmembrane protein/possible shedding |
| <i>rgmb</i>    | Cell Surface | GPI-anchored protein                    |
| <i>gas1b</i>   | Cell Surface | GPI-anchored protein                    |
| <i>tspan13</i> | Cell Surface | Multipass-Transmembrane protein         |
| <i>thbs4</i>   | ECM          | Non-collagenous ECM                     |
| <i>olfml2b</i> | ECM          | Non-collagenous ECM                     |
| <i>fmod</i>    | ECM          | Non-collagenous ECM                     |
| <i>lumican</i> | ECM          | Non-collagenous ECM                     |

dataset, inter-class comparisons (e.g. osteichthyes to mammalia) within the vertebrate subphylum have become feasible. While a large intersection cannot be expected due to differences in the experimental designs, it can be expected that the identified conserved signature of vertebrate MSCs comprises a small list of genes (Table 17.1), whose expression in MSCs has been conserved over more than 300 million years of vertebrate evolution, because of their particular importance for MSC physiology.

## Part IV

# Further Findings and Projects



— Dass sollt Ihr mir nicht zweimal sagen!  
Ich denke mir wieviel es nützt;  
Denn, was man Schwarz auf weiß besitzt,  
Kann man getrost nach Hause tragen.—

Goethe, Faust

# 18

*thrombospondin 4B* morphants  
develop severe muscular dystrophy

THROMBOSPONDIN 4B is one the non-collagenous ECM components secreted by MSCs and was included in the MO screen. *thrombospondin 4B* (*thbs4b/tsp4b*) and *tnw* morphants (Chapter 13) both developed severe even though distinct forms of muscular dystrophy. Thbs4b is one of two paralogs of the *thbs4/tsp4* gene in teleosts and belongs to the B subgroup of Thrombospondins, which form pentamers. Beststudied member of the family is Tsp1, which belongs to the A subgroup of trimeric Thrombospondins (Adams and Lawler, 2011; Bent-

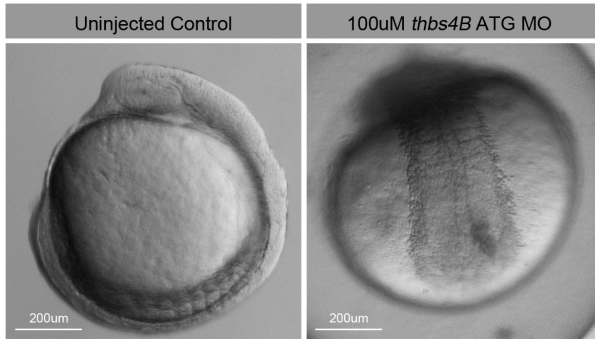


**Figure 18.1:** Morphology of *thbs4b* ATG MO-injected embryos during segmentation phase.

ley and Adams, 2010; Mosher and Adams, 2012). Knowledge about Tsp4's biological function and molecular interaction partners is scarce. Studies in mice have shown that Tsp1 and more weakly also Tsp4 serve as an adhesive substrate for skeletal myoblasts in cell culture (Adams and Lawler, 1994). The expression of *thbs4b*, initially widespread in the early somite during segmentation stage, soon begins to disappear from the center of myotome around 24hpf and becomes restricted to the vertical myoseptum and the dorsal and ventral muscle growth zones between 36-48hpf (Thisse, 2004). Upon knockdown using an ATG morpholino, *thbs4b* morphants display a very strong early embryonic lethal phenotype (Figure 18.1) indicating that Thbs4b is required early during development. Polarization contrast imaging shows that the 'partial knockdown' (hypomorphic)-*thbs4b* morphants have reduced muscle growth, disorganized muscle fibres and develop severe muscular dystrophy during larval development (Figure

18.1A and B). As evident from differential interference contrast images, the musculature of 7dpf *thbs4b* morphants is characterized by void spaces (Figure 18.2 C and D). These defects do not seem to be caused by muscle fibre detachment, as no detaching muscle fibres could be observed in living *thbs4b* morphants. It seems possible that in the context of muscle development and growth Thrombospondin 4, in agreement with its predominant expression in the dorsal and ventral muscle growth zones, facilitates myoblast proliferation, motility and/or fusion. This interpretation is supported by the observation that Thbs1 and more weakly also Thbs4 facilitate the adhesion of C2C12 myoblasts in cell culture (Adams and Lawler, 1994). AVEXIS screening of Thbs4 might contribute to our understanding of Thrombospondin function in this and other contexts.

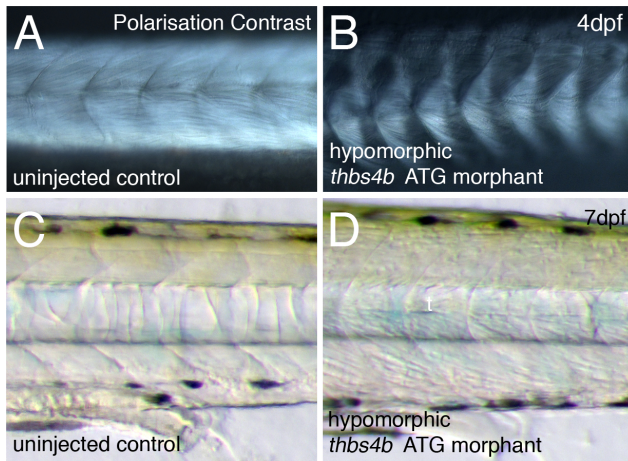


**Figure 18.2:** Hypomorphic *thbs4b* ATG morphant larvae display severe muscular dystrophy. (A, B) Polarisation contrast imaging shows reduced muscle mass and muscle disorganization in 4dpf *thbs4b* ATG morphant larvae. (C, D) Differential interference contrast imaging highlights the 'void spaces' in the musculature of 7dpf *thbs4b* ATG morphant larvae.

— Geheimnisvoll am lichten Tag  
Läßt sich Natur des Schleiers nicht berauben,  
Und was sie deinem Geist nicht offenbaren mag,  
Das zwingst du ihr nicht ab mit Hebeln und mit Schrauben.—

Goethe, Faust

# 19

## Teleost MSCs secrete known and *bona fide* novel components of the Hh signaling pathway

THE ‘TELEOST MSC DATASET’ contains a number of genes with known implication in vertebrate Hh signaling *gas1b* (Martinelli and Fan, 2007a, b), *cdon* (Sanchez-Arrones et al., 2012) and *wif1* (Glise et al., 2005; Gorfinkiel et al., 2005). This finding raised the interesting possibility that the specification, maintenance or activation of MSCs might depend on Hh signaling. The importance of Hh signaling for somite patterning,

i.e. the coordinated development of distinct muscle fibre types such as medial fast, fast and slow muscle fibres, and the formation of the horizontal myoseptum, is well established and has been recently reviewed (Ingham and Kim, 2005). Defects in Hh signaling are therefore associated with somite patterning and horizontal myoseptum defects.

### **19.1 Wnt inhibitory factor 1 (Wif1) deposited at the vertical myoseptum is essential for correct somite patterning**

Wnt inhibitory factor 1 (Wif1), the vertebrate homolog of *Drosophila shifted*, is an EGF-repeat and WIF domain containing extracellular matrix component. Wif1 has been identified in *Xenopus* as a soluble inhibitor of Wnt signaling (Hsieh et al., 1999). Structural studies further revealed that Wif1's WIF domain is able to accommodate acyl chains in a deep binding pocket as predicted previously by docking and the analysis of Wif1's NMR structure (Liepinsh et al., 2006; Malinauskas, 2008; Malinauskas et al., 2011). Interaction with Wnt ligands seems to be further enhanced by EGF repeats, which likewise contain a heparan-sulfate proteoglycan (HSPG)-binding site (Malinauskas et al., 2011).

Elegant experiments using the fly unveiled that *wif1/shifted* is not a mere inhibitor of Wnt signaling, but also involved in facilitating the mobility of lipid-modified morphogens such as Wnt and Hh ligands (Glise et al., 2005; Gorfinkiel et al., 2005). This observation is explained by the fact that lipid moieties on

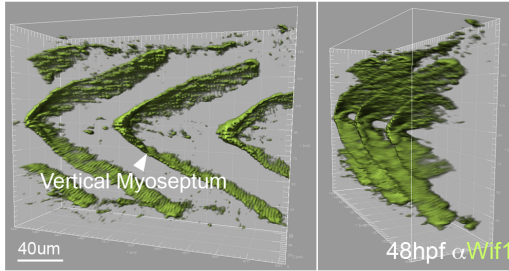


**Figure 19.1:** Wnt inhibitory factor 1 (Wif1) is immobilized at the vertical myoseptum.

Wnt or Hh ligands strongly favor their association with the cell membrane, as the extracellular milieu is hydrophobic. Through association with large multimeric assemblies or through interaction with Wif1 the lipid moiety can be shielded allowing lipid-modified morphogens to travel through a hydrophilic environment. This view is corroborated by the finding that in *shifted* mutants Hh gradients in the wing are steeper than normal (Glise et al., 2005; Gorfinkiel et al., 2005). In *Xenopus wif1* RNA was found to be strongly expressed in maturing somites (Hsieh et al., 1999). Whole-mount antibody staining of 48hpf zebrafish embryos, however, showed that Wif1 protein is deposited along the full medial-lateral extent of the vertical myoseptum (Figure 19.1).

Interestingly, *wif1* is one of the genes upregulated by MSCs/MPs at 4dpf (Figure 10.3B). It seems reasonable to assume that Wif1 is derived from MSCs and possibly other sources during larval development and becomes immobilized by an as yet unidentified interaction with a component of the vertical my-

oseptum and renders this structure a zone of suppressed Wnt signaling activity. In line with this hypothesis intravital imaging of a transcriptional Wnt reporter line in *pax7::GFP* background shows that the vertical myoseptum is indeed a zone of low canonical Wnt signaling activity (Figure 19.2). This observation is consistent with the general view of canonical Wnt signaling during myogenesis. Furthermore this shows that during primary myogenesis Pax7<sup>+</sup> MPs which leave the vertical myoseptum display strong Wnt signaling activity. During secondary myogenesis, however, Wnt signaling reporter activity is barely detectable in either DMPs, CMPs, or EMBs. The upregulation of Wnt signaling during the course of myogenic regulation is a well-documented phenomenon and leads to the activation of downstream transcription factor *tcf12/heb*, which dimerizes with MRF transcription factors leading to the activation of myogenic differentiation genes (Parker et al., 2006). The rapid differentiation of FfMBs during primary myogenesis might thus explain the observed colocalization of *pax7* and Wnt signaling reporter activity. The very low activity of the Wnt signaling reporter in DMPs, CMPs, and EMBs of secondary myogenesis speaks for the fact that these MPs are not undergoing myogenic differentiation.

For this reason *Wif1* seemed to be an interesting candidate for an MSC-derived MSC niche molecule. The functional analysis of *Wif1* as a potential MSC niche component using morpholino-mediated knockdown is, however, complicated by a very strong phenotype that develops between 1-2dpf in *wif1*<sup>ATG</sup> morphants (Figure 19.3). While these morphants display only moderate irregularities in the head and somites during somitogenesis, somite patterning and notochord development defects lead

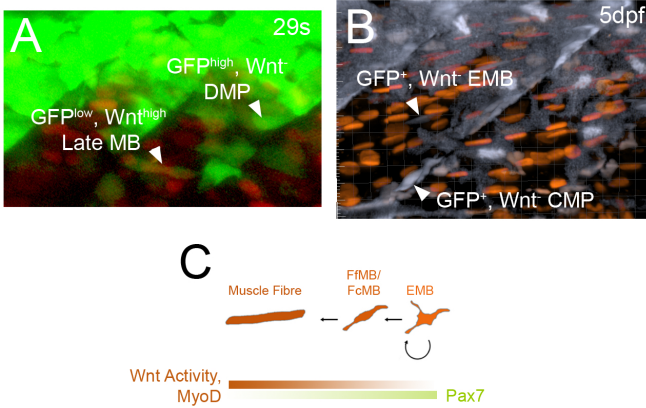


**Figure 19.2:** The vertical myoseptum is a zone of low canonical Wnt signaling activity. Intravital imaging of a transcriptional Wnt signaling reporter (*wtcf::NLS-mCherry*; A kind gift from Dr. Enrico Moro, University of Padova, Italy) in *pax7::GFP* background shows that the vertical myoseptum is a zone of low canonical Wnt signaling activity during embryonic stages (A) as well as in the larva (B). Interestingly, not only DMP and CMPs display low canonical Wnt signaling activity, but also EMBs, which are found inside the myotome. The differentiation of DMPs to fibre-forming myoblasts (FMB) during embryonic stages is accompanied by a rapid upregulation of Wnt signaling activity and a coinciding down-regulation of Pax7. These data suggest that the general view on the role of Wnt signaling in amniote myogenesis can be extended to teleost muscle development.

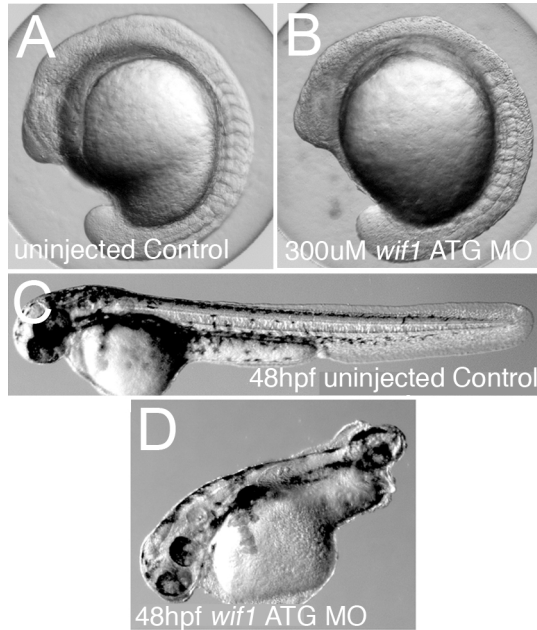


**Figure 19.3:** Morphology of *wif1* ATG morphants at mid-segmentation stage and 48hpf. In comparison to uninjected control (A) embryos, *wif1*<sup>ATG</sup> MO injected embryos (B) exhibit slightly irregular somites during midsegmentation stage. At 48hpf severe somite patterning defects are observed in *wif1*<sup>ATG</sup> morphants (D), which are not seen in uninjected control embryos (C).

to the severe phenotype of the axial musculature in 2day-old *wif1*<sup>ATG</sup> morphants (Figures 19.3 and 19.4). Likewise, the subtle cranial defects apparent during early embryogenesis are now very prominent. Interestingly, splice-blocking morpholinos, whose effectivity was assessed on cDNA-level, did not elicit a detectable phenotype. This is most likely attributable to residual maternal message. For this reason, further analysis was based on *wif1*<sup>ATG</sup> hypomorphic morphants. These are characterized by blocky somites, which fail to acquire the typical chevron-shaped morphology, absent or defective horizontal myoseptum, as well as irregular vertical myosepta (Figure 19.4). These traits are indicative of defects in Hh signaling. It is conceivable that Wif1 deposited at the vertical myoseptum serves two major functions:

- suppression of Wnt signaling
- facilitating the mobility of lipid-modified Wnt and Hh ligands along the extent of the vertical myoseptum The latter might allow notochord-derived Hh ligands (*shh*, *ehh*) to reach the distantly located MSCs.

The strong phenotype of the *wif1* ATG morphants contrasts with the effect of splice blocking *wif1* morpholinos, which was reported previously, but also reattempted as part of this work (Yin et al., 2012). A previous study using splice-blocking *wif1* MOs did not detect any phenotype similar to the observations described here, but described defects in swim bladder formation in succession to *wif1* knockdown (Yin et al., 2012). Further experiments will be needed to address this issue. As a *wif1* TILLING allele has been identified, but will not become available until 2013, efforts in the near future will thus

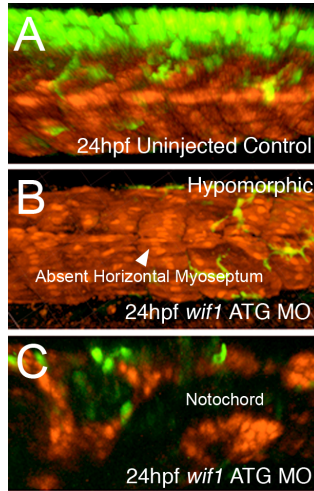


**Figure 19.4:** Somite patterning defects in 24hpf *wif1* ATG morphants. MO was injected in *pax7::GFP;myoD::NLS-mCherry* transgenic embryos. (A) Control, (B) hypomorphic and (C) regular *wif1*<sup>ATG</sup> morphants exhibit mild and severe somite patterning defects. The *myoD::NLS-mCherry* BAC transgenic line was generated by Dr. Jana Krauss (MPI für Entwicklungsbiologie, Tübingen)

largely depend on the *wif1*<sup>ATG</sup> MO, whose effectivity should be more stringently assessed using the Wif1 antibody. While the absence of a phenotype in *wif1*<sup>-/-</sup> mice does not answer the question of whether or not Wif1's function is redundant, it indicates that its role in adult physiology is secondary at best. In part this might be explained by the presence of other soluble Wnt inhibitors of the sFRP class (Surmann-Schmitt et al., 2009).

## 19.2 A2CEY7 is a novel candidate component of the Hedgehog signaling pathway

In order to assess the possible importance of Gas1b during myogenesis, a *gas1b*<sup>ATG</sup> MO was injected into zebrafish embryos. As depicted in Figure 11.1 *gas1b* morphants exhibit a very strong early embryonic phenotype (16-18hpf), that includes strong reduction of cranial tissue, accumulation of spheroid cells on top of hindbrain, necrosis in the head and anterior trunk as well as a dysmorphic trunk with blocky somites. This phenotype is unlike the relatively mild phenotype of *cdon* morphants, which primarily affects the head and eyes at this stage (Figure 11.1). Strikingly, *A2CEY7* and *CD81/tspan28* morphants, display phenotypes, which closely resemble the one of *gas1b* morphants (Figure 11.1). As Gas1 is a well established component of the Hh signaling pathway (Allen et al., 2007; Martinelli and Fan, 2007a, b), it seemed reasonable to assume that also A2CEY7 and CD81 may operate in this pathway. A2CEY7 is an as yet uncharacterized protein containing a Reeler domain, which spans most of the protein. Several prediction methods unanimously predicted a highly probable GPI-anchor site. While regular BLAST against the Uniprot database did not retrieve amniote homologs, sensitive remote homology detection using HHpred (MPI toolkit, Biegert et al., 2006) identified a weak homology to human Stromal Cell Derived Factor Receptor 2 (Acc. NP001013682).

In order to circumvent the very strong and early phenotype of *A2CEY7* ATG morphants both a splice blocking morpholino,

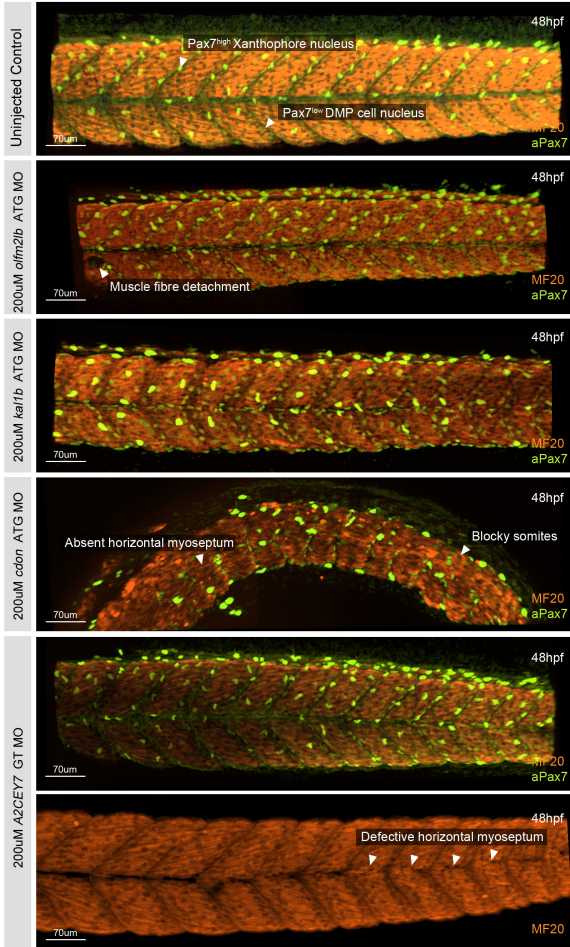


**Figure 19.5:** Anti-Pax7, Anti-MF20 immunohistochemistry reveals changes in MSC number and overall muscle histology in selected 2dpf morphants. *olfml2Bb*<sup>ATG</sup> morphants do not show an obvious change in the number of Pax7<sup>+</sup> MSCs or of gross muscle morphology. Small lesions to the musculature can, however, be observed in these morphants at this stage. No deviation from the uninjected control situation could be detected in response to *kal1b*<sup>ATG</sup> MO injection. A prominent phenotype consisting mainly of blocky somites, absence of horizontal myoseptum and a strong reduction in Pax7<sup>+</sup> MSC is caused by knockdown of the Hh coreceptor Cdon. These defects are accompanied by cranial defects. Similarly, very weak hypomorphic A2CEY7 morphants display partial absence of horizontal myoseptum, which points to a possible role in Hh signaling.

which leaves the maternal mRNA intact, and subeffective doses of ATG morpholino were employed. The corresponding hypomorphic morphants did not show an early phenotype and developed with no detectable change in the number of Pax7<sup>+</sup> MSC at 2dpf, however, the horizontal myoseptum was missing in many segments of hypomorphic *A2CEY7* morphants indicating defective Hh signaling (Figure 19.5). Similarly, *cdon* ATG morphants display defective formation of the horizontal myoseptum at 2dpf, blocky somites, severe growth defects, disorganized muscle fibres and curved trunk apart from defects in the cranium. Importantly, the number of Pax7<sup>+</sup> MSCs in 48hpf *cdon* morphants seems to be strongly reduced (Figure 19.5). Whether this apparent reduction is a primary consequence of the knockdown of *cdon* or a secondary effect of the somite patterning defects that arise in *cdon* morphants remains to be elucidated. Taken together these findings may suggest

- that MSC express a number of cell surface and secreted proteins, which are known regulators of Hh signaling, e.g. *cdon*, *gas1b*, *wif1*.
- that secreted, GPI-anchored A2CEY7 and possibly also the tetraspanin CD81 might be novel and essential components of the Hh pathway.
- that the Hh coreceptor, Cdon, is required for proper patterning of the myotome and the development of the horizontal myoseptum.
- that Cdon might be required cell autonomously to regulate muscle stem cell number.

— Wenn du, als Jüngling, deinen Vater ehrst,  
So wirst du gern von ihm empfangen;  
Wenn du, als Mann, die Wissenschaft vermehrest,  
So kann dein Sohn, zu höh'rem Ziel gelangen.—

Goethe, Faust

# 20

## Auto- and paracrine Csf1-FMS signaling regulates *pax7* expression during teleost neural crest and muscle development

COLONY STIMULATING FACTOR 1 (Csf1, M-Csf) is the prototypical ligand for c-FMS/Csf1r receptor tyrosine kinase, the product of the *c-fms* oncogene. Different Csf1 isoforms – a cell surface-bound, a soluble glycoprotein and soluble proteoglycan isoform – are derived from a full-length precursor by proteolytic processing (Douglass et al., 2008; Pixley and

Stanley, 2004). Elegant experiments, which restored a particular isoform in *csf1*<sup>-/-</sup> mice, clearly demonstrated that these distinct isoforms serve different purposes. Apart from being a classical cytokine governing proliferation, survival, and differentiation of mononuclear phagocytes (Pixley and Stanley, 2004), Csf1 has been implicated in a variety of biological phenomena, including chemotaxis (Cammer et al., 2009), Paneth cell specification (Huynh et al., 2009), and spermatogonial stem cell self-renewal (Oatley et al., 2009). Both the *csf1* and *fms/csf1r* genes, which encode the Csf1-Fms ligand-receptor pair, underwent duplication at the base of teleost evolution (Wang et al., 2008). One of the *csf1* ligands, *csf1b*, turned out to be the second most strongly upregulated gene in the ‘teleost MSC profiling’. This raised the question whether this reflects *csf1b* expression in MSCs/MPs or whether *csf1b* is in fact expressed by Pax7<sup>+</sup> xanthophores, which might be present as a contamination in the sorted Pax7<sup>+</sup> MSC/MP cell population that was used for the ‘teleost MSC profiling’. Csf1 is secreted by rat myoblasts in cell culture (Borycki et al., 1995b). Moreover, knockdown of *csf1r* in L6 $\alpha$  rat myoblasts induces G1-growth arrest supporting a role for this cytokine in the myogenic context (Borycki et al., 1995a).

Forward genetic screens have identified several *pfeffer/panther* alleles, which carry molecular lesions in the *csf1ra/fmsA* gene. In *pfeffer* mutants xanthophore precursors, which are marked by strong expression of *pax7*, *csf1ra/fmsa*, and *gch2*, apoptose during their migration (Minchin and Hughes, 2008; Odenthal et al., 1996; Parichy et al., 2000). This leads to an almost complete disappearance of xanthophores in *pfeffer* mutants. Whether the apparent reduction in melanophore number in

adult *pfeffer* mutants is a direct consequence of *csf1ra* mutation or a secondary effect is currently unclear. While it is conceivable that xanthophores derived signals might positively regulate melanophore differentiation and/or survival, the regulation of *Mitf* by *Csf1-Csf1r* signaling in mice (Weilbaecher et al., 2001) suggests that in teleosts *Csf1-Csf1r* signaling might regulate *Mitfa*, which is a master regulator of melanophore differentiation (Lister et al., 1999). Apart from the defect in xanthophore development, only slight changes in bone development have been reported for *pfeffer* mutants (Chatani et al., 2011). The close spatial correlation between MSCs, which are located at the vertical myosepta, and xanthophores, which likewise cluster along this structure, might be related to the secretion of *Csf1b* by MSCs. In this scenario MSC-derived *Csf1b* would act in an autocrine fashion on MSCs and in a paracrine fashion as a chemoattractant on xanthophores.

## 20.1 Functional and topological divergence of *Csf1-FMS* ligand-receptor genes

The analysis of *csf1a* and *csf1b* expression is difficult as the mRNA encoding both ligands is expressed at very low levels (Figure 20.1). What can be safely said is that both ligands are expressed in at least partially overlapping domains in the cranium and CNS at 48hpf. In the trunk, however, expression patterns diverged as evident from Figure 20.1 (*in situ* hybridization of *csf1a/b* was performed by Dr. Katrin Henke, MPI für Entwicklungsbiologie, Tübingen). *csf1a* is expressed in a dorsal and ventral stripe as well as along the length of the ho-

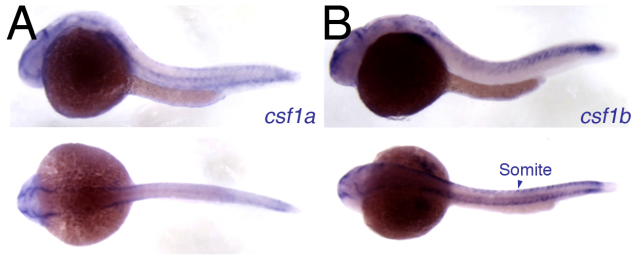


**Figure 20.1:** Divergent expression patterns of teleost *csf1* paralogs. 24hpf *alb in situ* hybridisation for *csf1a* (A) and *csf1b* (B) shows that apart from shared expression domains in the CNS expression patterns in the trunk diverged considerably. While *csf1a* in the trunk is expressed in mainly dorsally, ventrally and medially along the horizontal myoseptum, *csf1b* is expressed in the somite and most prominently in the posterior younger somites. The *in situ* hybridisation for *csf1a* and *csf1b* was performed by Katrin Henke (MPI für Entwicklungsbiologie).

horizontal myoseptum, whereas *csf1b* seems to be expressed in dorsal myotomes of newly formed somites. Despite their divergent expression patterns both ligands are able to bind the FMSa/Csf1rA receptor (unpublished observation of Alessandro Mongera and Dr. Christian Söllner, MPI für Entwicklungsbiologie, Tübingen). It was therefore surprising to find that in the context of xanthogenesis both ligands diverged not only topologically but also functionally. Upon morpholino-mediated knockdown of *csf1a* xanthophores, which are normally found to be distributed in a dorsal to ventral gradient (Figure 20.2 A and D), form a dense stripe of xanthophores, that covers the dorsal hemisegment (Figure 20.2 B and E). It is not clear, at present, how depletion of Csf1a leads to the development of this phenotype. Two alternative explanations might account

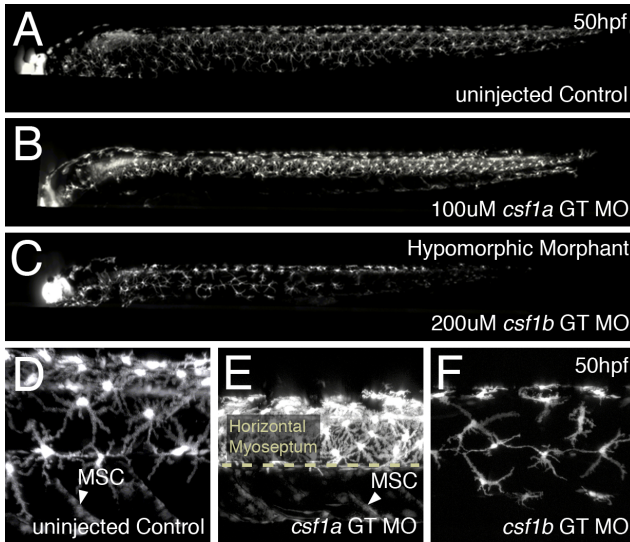


**Figure 20.2:** Functional divergence of Csf1 ligand paralogs in teleost fish. Morpholinos targeting the splicing of *csf1a* and *csf1b* were injected into *pax7::GFP* transgenic embryos. (A,D) Uninjected control. (B,E) *csf1a*<sup>GT</sup> morphants exhibit xanthophore migration defect and cluster exclusively on the dorsal hemisegment and do not cross the horizontal myoseptum (C,F) *csf1b*<sup>GT</sup> morphants are early embryonic lethal (not shown) their hypomorphic counterparts, which were obtained by injecting a subeffective dose of MO, exhibit strong reduction in xanthophore number and reduced myotome growth.

for this defect. First, in absence of *Csf1a* xanthophores might be unable to cross the horizontal myoseptum. In this scenario *Csf1a* would provide positional information and the phenotype would be caused by a migration defect. Second, *Csf1a*-FMS signaling might regulate the spacing between xanthophores by mediating contact-inhibition. In this scenario, lack of *Csf1a* would lead xanthophores to cluster. In contrast to this patterning or migration defect, *csf1b* knockdown using an ATG or GT morpholino leads to a severe early embryonic lethal phenotype. Hypomorphic *csf1b*<sup>GT</sup> morphants show a strong reduction in the number of xanthophores with no apparent deficit in migration or patterning (Figure 20.2C and F). As such hypomorphic *csf1b* morphants phenocopy *pfeffer* mutant embryos.

## 20.2 *Csf1*-FMS signaling regulates *Pax7* expression

The expression of *Csf1* by teleost and mammalian MSCs points to an important function of MSC-derived *Csf1* (Figures 10.2, 10.3, and Table 17.1). At this point the *pax7::GFP* transgenic line does not only provide a read out for the number of distinct *Pax7*<sup>+</sup> cells, but also allows the strength of *pax7* expression to be assessed in these distinct cell types. To this end the central cell body of xanthophores or other *Pax7*<sup>+</sup> cells can be segmented by isosurface rendering. Various traits of this isosurface including mean intensity can then be read out.

In this way the mean strength of *pax7::GFP* reporter expression was read out for xanthophores and MSCs in 4dpf trans-

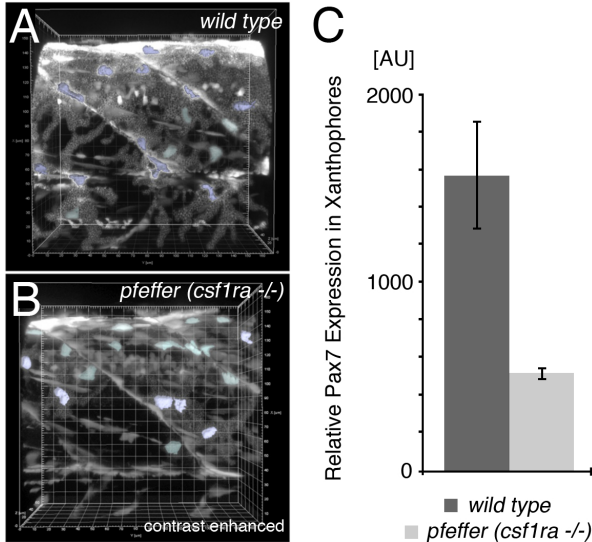


**Figure 20.3:** Csf1-Csf1r signaling regulates Pax7 expression. The relative strength of Pax7 expression was assessed using *pax7::GFP* transgenic embryos in *wt* (A) or *cs1ra<sup>-/-</sup>* background (B, *pfeffer* mutant). For this purpose isosurfaces were rendered including the central somata of xanthophores (light blue isosurfaces) and MSCs (light green isosurfaces). An approximately 4-fold reduction of Pax7 expression was observed in neural crest derived xanthophores (C) but not in cells of the myogenic lineage. This strongly suggests that Csf1-Csf1r signaling via Csf1ra/FMSa, which is known to be strongly expressed in xanthophores, regulates Pax7 expression in these cells. It is conceivable that likewise Csf1-Csf1rb/FMSb or both receptors in parallel regulate Pax7 expression in the myogenic lineage.

genic *wt* and *pfeffer* larvae (Figure 20.3 A and B). In absence of FMSa, the mean *pax7::GFP* reporter strength in the remaining xanthophores turned out to be reduced by a factor of 3-4 (Figure 20.3 C). Taken together with the observation that Csf1b depletion phenocopies the *pfeffer* phenotype, this indicates that Csf1b-FMSa signaling regulates *pax7* expression in xanthophores. No significant difference of *pax7* expression strength was observed between *wt* and *pfeffer* mutants in MSCs. This might indicate that Csf1-FMS signaling does not influence *pax7* in the myogenic lineage. In light of the conserved expression of Csf1 by teleost and mammalian MSCs (Table 17.1), it seems reasonable to assume that Csf1-FMS signaling regulates *pax7* expression also in the myogenic lineage. In this case Csf1b-FMSa and/or Csf1b-FMSb might regulate *pax7* expression in teleost MSCs. These observations can be summarized as follows. As a result of genome duplication the Csf1-FMS ligand-receptor pair is present in duplicate in the teleost genome.

Through the use of morpholinos, mutants and inhibitors it is possible to block distinct aspects of Csf1-FMS signaling. The *pfeffer* mutant for instance, which is a null mutant for *csf1ra/fmsA*, displays a selective loss of Csf1b-FMSa and Csf1a-FMSa, but leaves signaling via FMSb intact. Interestingly, the knockdown of *csf1a* and *csf1b* elicits very different phenotypes. The knockdown of *csf1b* phenocopies the *pfeffer* mutant phenotype indicating that Csf1b-FMSa and not Csf1a-FMSa signaling is essential for xanthophore differentiation and survival. Apart from this *csf1b* morphants exhibit reduced length and height of the trunk (Figure 20.2 C and F), which may be caused by reduced growth of the axial musculature. These de-

fects are less pronounced in *csf1a* morphants (Figure 20.2 B and E).

These observations may be tentatively put together into a working model of autocrine and paracrine Csf1-FMS signaling between cells of the myogenic and neural crest cell lineage (Figure 20.4). In this model MSC-derived Csf1b regulates Pax7 expression via FMSa and/or FMSb in MSCs (autocrine signaling). It is conceivable that Csf1b is a Pax7 target gene, which would mean that they are part of an autocrine feedback-loop. Apart

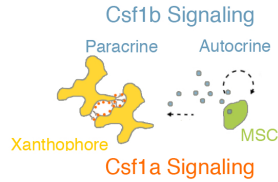


**Figure 20.4:** Working model of the autocrine and paracrine Csf1-FMS signaling cross-talk between MSCs and xanthophores.

from this autocrine signaling, Csf1b binds to the FMSa receptor on xanthophores (paracrine signaling) and likewise positively regulates Pax7 expression. The strong reduction of Pax7 expression in xanthophores in *pfeffer* mutants suggests that FMSb is not expressed in xanthophores. In light of this, it is interesting to note the very prominent clustering phenotype that xanthophores display in absence of Csf1a. It seems possible, that Csf1a and FMSa are both present on the xanthophore cell surface. Csf1a-FMSa might as such well mediate contact inhibition between xanthophores and thereby regulate the spacing between xanthophores. In absence of Csf1a this contact inhibition is lost and xanthophores cluster on the dorsal aspect forming a tight stripe of xanthophores. Future analysis will be needed to test predictions derived from this model.



— *Ein schöner Traum, indessen sie entweicht.*  
*Ach! zu des Geistes Flügeln wird so leicht*  
*Kein körperlicher Flügel sich gesellen.—*

Goethe, Faust

# 21

## Concluding Remarks

THE WORK presented here shows, that the zebrafish's unique advantages as a vertebrate model system can be harnessed to study the muscle stem cells as well as the cellular dynamics and molecular regulation of myogenesis in the living animal. Despite the fact that more than 300 million years have past since the divergence of the teleost and amniote lineage key aspects of myogenesis such as the genetic regulatory networks governing myogenic commitment or myoblast fusion have been conserved throughout vertebrate evolution (Baugh and Hunter, 2006; Bryson-Richardson and Currie, 2008; Cleto et al., 2003; Rochlin et al., 2010; Seipel and Schmid, 2005; Shaffer and

Gillis, 2010; Vandekerckhove and Weber, 1984). Thus far it remained uncertain, however, whether the dermomyotomal origin of amniote MSCs represents an evolutionary novelty or an ancient vertebrate trait. The observation that teleost MSCs originate in a Pax7<sup>+</sup> epithelial layer that covers the teleost myotome early during embryogenesis now resolves this issue showing that this structure is indeed homologous to the amniote dermomyotome. The presence of a dermomyotome in teleosts and amniotes suggests that the dermomyotome is a vertebrate synapomorphy, as hypothesized before (Devoto et al., 2006; Feng et al., 2006). Likewise, transcriptional profiling of teleost MSCs unearthed a number of cytoplasmic and secreted proteins, whose expression characterizes teleost and mammalian MSCs. These observations imply that not only the genetics of myogenic commitment, but also the ontogeny of muscle stem cells and the mechanisms ensuring their maintenance are highly conserved inside the vertebrate subphylum. This indicates that the zebrafish can be used as a model system for the study of principles relating to the self-renewal and commitment of human MSCs.

The generation and characterisation of a *pax7::GFP* transgenic line, which drives robust GFP expression in Pax7<sup>+</sup> cells, thus establishes a new model system for the analysis of vertebrate myogenesis in general and MSCs in particular. Using this tool, MSCs and their progeny can now be accessed in the living animal by intravital confocal microscopy. In this way myogenesis can be studied at the single cell level with a spatial resolution in the submicron range and a temporal resolution of seconds to minutes. The *pax7::GFP* transgenic line is an excellent tool to study diverse aspects of myogenesis such as MSC self-renewal,

myoblast migration and fusion, and muscle regeneration. Likewise, it will enable chemical biology screening efforts, which aim at the identification of small molecule compounds that modulate MSC self-renewal or commitment. Such molecules are sought after for their possible use in the treatment of serious human illness such as muscular dystrophies or other muscle wasting diseases such as Cachexia which is a comorbidity of cancer, HIV, tuberculosis, and other pathologies.

The inability to clearly differentiate stem cells from their committed progenitors based on molecular markers is a major general limitation in stem cell research. While the present study achieved the distinction of MSC from their committed progeny based on a large number of 'complex criteria', such as developmental origin, clonal relationship, anatomical location, cell morphology, cell migration behavior, and cell membrane dynamics, it fell short of showing that these distinct populations express different molecular markers. Owing to the lack of antibodies recognizing well established or newly identified markers the question of whether or not there are molecular makers distinguishing MSCs, CMPs, EMBs could simply not be addressed. As a number of new antibodies raised against zebrafish proteins became available recently, this point is likely to be resolved in the near future.

The identification of the actual MSC compartment in teleost embryos and larva in turn allowed the dynamics under distinct experimental conditions to be investigated. In the course of the main project this paradigm has been exploited to show an essential function for *Tnw* as an MSC-derived MSC niche component. Several other candidate genes have, however, been

identified in the ‘teleost MSC profiling’. As Pax7<sup>+</sup> MPs comprise a heterogenous population of myogenic progenitors including MSCs and at least two downstream committed progenitor compartments it is expected that the dataset not only contains genes implicated in MSC stemness but also other aspects of myogenesis, such as myogenic commitment and differentiation, myoblast survival and fusion, or muscle fibre attachment. Thus it came as no surprise that the functional analysis of a significant share of MSC-secreted molecules tentatively implicated a number of candidate genes in these different contexts. This initial characterization forms a solid base for future projects.

Notably, several candidate genes appear to be involved in more than just one aspect of myogenesis. The knockdown of Tnw for instance indicated that MSC-secreted Tnw functions as an MSC-derived niche component. A function that is likely attributable to its interaction with ligands of the Notch signaling pathway, whose importance for MSC self-renewal is well documented in mammals. At the same time, however, severe defects of the vertical myosepta are a consequence of Tnw’s depletion. Whether this is a genuine primary effect of the depletion of Tnw or results from the reduction in MSC number, which by necessity will be associated with reduced synthesis of other MSC-derived ECM components, is current not clear. It is conceivable, however, that Tnw and other MSC-derived components of the ECM serve multiple functions.

The complexity of these interactions questions the suitability of the ‘top-down’ single gene approach to study the relationship between stem cells and their niche. An exciting part of

this project are therefore the first steps towards a ‘systems level’ analysis of the extracellular protein-protein interactions between MSCs and their niche. As discussed in Chapter 11, the current AVEXIS library size is too small, to construct networks, which can be studied using network theory concepts. Future efforts will be needed to arrive at this point. Nevertheless, the AVEXIS screen is a key part of this project as it identified a number of novel interactions, which are likely to be of pivotal importance to MSC self-renewal. Apart from this some of the interactions identified such as the interaction between Tnw and Delta ligands represent novel attractive targets for the therapy of human cancer. The extracellular nature of these targets is a particular advantage as it renders them accessible to therapeutic antibodies or aptamers.



## Part V

# Materials and Methods



— *Wie könnt Ihr Euch darum betreiben!*  
*Tut nicht ein braver Mann genug,*  
*Die Kunst, die man ihm übertrug,*  
*Gewissenhaft und pünktlich auszuüben? —*

Goethe, Faust

# 22

## Experimental Procedures

### 22.1 Fish strains

Fish were kept in 10h dark, 14h light cycle at 29°C. The following strains were used as *wild type*: Tübingen (Tü), TE, WIK. The mutants *pfeffer*<sup>(tm236b)</sup> and *albino* (*alb*) were used. Apart from the Tg(*pax7*:EGFP)<sup>sa</sup> BAC transgenic line. Further transgenic lines were used in this study.

The Tg(*flk1*:EGFP)<sup>s843</sup> line (Jin et al., 2005) labels the vasculature. Dr. Enrico Moro (University of Padova, Italy) kindly provided the Tg(*xtcf*::NLS-Cherry) transgenic line, which was used as a transcriptional reporter for canonical Wnt signal-

ing. The Tg(*myoD*::NLS-Cherry) BAC transgenic line was generated by Dr. Jana Krauss (MPI für Entwicklungsbiologie, Tübingen) and used to visualize slow muscle fibres.

## 22.2 Generation of Tg(*pax7*:EGFP)<sup>sa</sup> BAC transgenic line

CH211-287M7 was identified by screening the CHORI BAC library with probe for *pax7a*. This BAC was modified using the Genebridges GmbH (Dresden, Germany) protocol and inserted a GFP-SV40polyA-FRT-KanR-FRT cassette replacing the proteogenic part of exon1. The BAC DNA was dialyzed O/N at 4°C against 2l TE using 3,5K MWCO Slide-A-Lyzer dialysis cassettes (Thermo Scientific, Waltham, MA) and digested with *NotI* O/N before injection at a concentration of 10ng/ul. One transgenic founder was identified. In the main text of the manuscript and figures this line is referred to as *pax7*::GFP.

## 22.3 Non-invasive intravital 4D imaging

Imaging was performed on a LSM510 Meta Axioplan2.0 (Carl Zeiss, Jena, Germany) at RT and on a LSM5 Live Axiobserver2.1 (Carl Zeiss, Jena, Germany) equipped with incubation set to 29°C. The LD C-Apochromat 40x/1,20 W Korr or LD LCI Plan-Apochromat 25x/0,8 Imm Korr DIC M27 multi immersion lens in combination with Immersol W (Carl Zeiss, Jena, Germany) was used for intravital imaging. Live

samples were mounted in glass bottom culture dishes (MatTek, No.1) using 0.75% low melting agarose in E2 containing 0.04% Mesab (3-amino benzoic ethyl ester methanesulfonate). Acquired imaging data were processed and analyzed using Imaris (Bitplane, Zürich, Switzerland). Details of particular imaging experiments are summarized in Table 22.1.

## 22.4 Direct Isolation of Pax7<sup>+</sup> MSCs/MPs by FAC-sorting

For each replicate about 1,000 *pax7::GFP* transgenic larvae were consecutively (in groups of about 50) deeply anesthetized with Mesab (3-amino benzoic ethyl ester methanesulfonate), decapitated and put on ice until the whole cohort was processed. The larval trunks were then dissociated using 15ml Accumax (Millipore, Billerica, MA) for 45-60min in a 50ml Falcon tube (BD Biosciences, Heidelberg, Germany). The resulting suspension was filtered through 100 $\mu$ m sieves (BD Biosciences, Heidelberg, Germany) spun down at 1,000x g at 4°C using a swing-out rotor, carefully resuspended in 1mM EDTA/PBS and again filtered through 40 $\mu$ m sieves (BD Biosciences, Heidelberg, Germany). Cytometry and FACS was performed on a BD FACSAria using FSC-A, SSC-A gating followed by gating according to GFP expression (488nm excitation, FITC emission). Each population was subject to further gating as to remove debris and aggregates.

**Table 22.1:** Supplemental movies.

| Movie, related to Fig. | Stage | Duration  | Interval | Comment  |
|------------------------|-------|-----------|----------|--|
| Movie S1, 9-4A         | 19hpf | 13h:40min | 5min     | Primary myogenesis: formation of the teleost dermomyotome                |
| Movie S2, 9-4B         | 19hpf | 2h:40min  | 5min     | Primary myogenesis: DMP cell undergoing differentiation                  |
| Movie S3, 9-5          | 48hpf | 35h:40min | 20min    | Transition phase: amplification of DMP cell pool                         |
| Movie S4, 9-8          | 4dpf  | 14h:20min | 15min    | Secondary myogenesis: CMFs and EMFs                                      |
| Movie S5, 9-7          | 4dpf  | 22h40min  | 10min    | Secondary myogenesis: quiescence of DMFs                                 |
| Movie S6, 13-7         | 4dpf  | 13h30min  | 10min    | Secondary myogenesis: loss of quiescence of DMFs in <i>tnw</i> morphants |
| Animation S1, 9-6      | 4dpf  | -         | -        | Secondary myogenesis: dorsal hemisegment including isosurfaces.          |
| Animation S2, 9-9      | 4dpf  | -         | -        | Secondary myogenesis: CMFs and EMFs in normal shading projection         |

## 22.5 Microarray Profiling

Cell pellets from the FAC-sorting were used for extracting RNA with TRIzol Reagent (Invitrogen, Darmstadt, Germany) following the manufacturer's instructions. The RNA was then used as a template for cDNA synthesis and cRNA dye labeling using the Agilent Low Input Quick Amp Labeling Kit (Agilent Technologies, Waldbronn, Germany). Cy-3 and Cy-5 labeled cRNA was hybridized to the Agilent Zebrafish V2 microarray containing 44,000 probes to 22,000 genes, according to the manufacturer's protocol. Four biological replicates were conducted comparing GFP-positive to GFP-negative cells from the FACS experiment. The slides were scanned with a GenePix 4000b scanner (Axon Instruments, Hamburg, Germany). All data were processed and analyzed as in (Reischauer et al., 2009) with the R environment and the Limma microarray analysis module in Bioconductor (Gentleman et al., 2004; Smyth, 2004). The false discovery rate (FDR) method was used to control for multiple hypothesis testing (Benjamini and Hochberg, 1995). All data will be made available through the ArrayExpress expression repository <http://www.ebi.ac.uk/arrayexpress/>.

## 22.6 Raising and Affinity Purification of Zebrafish Pax7 Antibody

Recombinant zebrafish Pax7 C-terminus immunogen corresponding (aa300-469; Uniprot Accession O57418) was expressed in *E. coli* DE3RIPL strain using pET28a vector and purified under denaturing condition by FPLC using Ni-NTA Super-

flow resin (QIAGEN, Hilden, Germany). A rabbit was immunized two times with 0.5mg recombinant protein using 4 subcutaneous and 2 intramuscular (*M. femoris*) injections. Bleeding was started two weeks after a second booster immunization respectively. The Pax7 C-terminus antibody ( $\alpha$ Pax7<sup>MPIEB</sup>) was affinity purified from crude serum using immunogen, which was purified under native conditions by FPLC using Ni-NTA Superflow resin (QIAGEN, Hilden, Germany) and coupled to HiTrap<sup>TM</sup> NHS-activated columns following manufacturers instructions (GE Healthcare, München, Germany).

## 22.7 Antibody Staining

Embryo or larva were fixed for 1h at RT in 4% PFA, 0.1% Tween-20 in PBS, rinsed twice with PBS, washed with 1% Triton-X100, 1%DMSO in PBS (PDT) for 15min at RT, quenching of free aldehyde groups was performed with 100mM glycine in PDT for 15min RT, samples were washed once again with PDT, and then subject to blocking in 1% bovine serum albumine, 10% normal goat serum in PDT for 1h at RT or overnight at 4°C. Embryos older than 24hpf were treated with ice-cold acetone for 5-20min depending on developmental stage (48-96hpf). Primary rabbit  $\alpha$ Pax7<sup>MPIEB</sup> antibody raised against the Pax7 C-terminus was used at a concentration of 0.1 $\mu$ g/ml in blocking buffer. After incubation with the primary antibody samples were rinsed twice with PBS, washed four times 15min each at RT with PDT. Secondary antibodies were used according to manufacturer's instructions.

## 22.8 Histology

GIEMSA-stained transverse sections were prepared as described before (Sonawane et al., 2005).

## 22.9 *in situ* Hybridization

*in situ* hybridization was performed as described before with minor modifications (Nüsslein-Volhard, 2002).

## 22.10 Morpholino Injections

MOs were resuspended in water at 65°C for 10min, then spun in microcentrifuge at full speed to pellet non-dissolved aggregates and stored in screw cap tubes at room temperature in the dark. MO concentration was measured by determining the absorption at 265nm of 1:50 dilution of MO in 0.1M HCl using NanoDrop ND-1000 spectrophotometer (Thermo Scientific, Wilmington, USA). Injection needles (BM120IF-10) were purchased from BioMedical Instruments (Zöllnitz, Germany) and average injection volume was determined to be 1.10 +/-0.10 nl (n=20) by measuring bolus diameter after injection of water droplets into immersion oil (Immersol F, Carl Zeiss, Jena, Germany). MOs were diluted in 0.025% Phenol red in water and. Morpholinos (MO) and 5 mismatch morpholinos (5MM) listed in Table 22.2 were used in this study. The MOs and corresponding 5 mismatch MOs (5MM) were injected using air pressure microinjection setups directly into zebrafish zygotes using the

indicated doses. The most stringent control for a particular MO is considered to be a MO of the same sequence carrying 5 mismatches (5MM). The inclusion of 5MM controls, however, doubles the cost of the MO screen. As the injection of 0,025% phenol red/water, in which all other MOs were diluted, did not yield any detectable phenotype uninjected embryos were used as a reference for the MO screen.

## **22.11 Extracellular protein-protein interaction screen (AVEXIS)**

The AVEXIS assay (Bushell et al. 2008) has been used to identify binding partners for Tnw and other MSC-secreted proteins. Recombinant bait and prey proteins have been produced by using the HEK293 large scale transient expression system (NRC Technology). Table 22.4 lists all of the protein constructs used in the screen. The tissue culture supernatants containing the secreted recombinant proteins were harvested at day 6, quantified and normalized as described (Bushell et al., 2008). The AVEXIS screen was performed by binding mono-biotinylated bait proteins to activated streptavidin coated 96-well micro titer plates (Nunc, Denmark) followed by one-hour incubation at room temperature. After three HBS (adipo washes the bait proteins were incubated for one hour with normalized beta-lactamase tagged prey proteins. Non-bound prey proteins have been removed by two HBST (HBS containing 0,05% Tween-20) followed by two HBS washes. 50 $\mu$ l of nitrocefin (100g/ml) have been added to each well and the absorbance has been measured at 486nm after

**Table 22.2:** Morpholinos used in this study.

| Target                               | Dose [ng] | Sequence                   |
|--------------------------------------|-----------|----------------------------|
| <i>tnw</i> <sup>e1i1</sup> MO        | 0.8-1.6   | TGCAGATGCCTTACCCGAGAATATT  |
| <i>tnw</i> <sup>e1i1</sup> 5MM       | 0.8-1.6   | TGgAcATGCgTTACCCgAcAATATT  |
| <i>tnw</i> <sup>e2i2</sup> MO        | 1.6-2.4   | CTTCATGTTTGGACTACTACCTGCC  |
| <i>tnw</i> <sup>e2i2</sup> 5MM       | 1.6-2.4   | CTTgATcTTTcGACTACTACgTcCC  |
| <i>tnw</i> <sup>e3i3</sup> MO        | 2.4-3.2   | TCACACAGAAGTCATTCTTACCCAT  |
| <i>tnw</i> <sup>e3i3</sup> 5MM       | 2.4-3.2   | TCACAgAcAAcTCATTgTTAgCCAT  |
| <i>thbs4b</i> <sup>ATG</sup> MO      | 0.4-1.2   | CCGGCCATCCTTCAATCACAACCTT  |
| <i>thbs4b</i> <sup>e1i1</sup> MO     | 0.4-1.2   | GAAACTTCGTGTGTACTCACCGATT  |
| <i>kal1b</i> <sup>ATG</sup> MO       | 1.0-3.2   | AGCAGAGATTCCTCAAAAGCAGCAT  |
| <i>fmod</i> <sup>ATG</sup> MO        | 1.6-2.4   | AAAGCAGGAGAGCAATTAGCCGCAT  |
| <i>olfml2bb</i> <sup>ATG</sup> MO    | 2.4-3.2   | ATGAAGATTCCCTCAAGAAGAGCTGC |
| <i>wif1</i> <sup>ATG</sup> MO        | 2.4-3.2   | GCGTCCTGAAAGCCATCCTTTGGTT  |
| <i>wif1</i> GT MO                    | 2.4-3.2   | GAAACTACGCAAACATTACCAATT   |
| <i>wif1</i> GT MO                    | 2.4-3.2   | AAGAATAAAAGCCACCCAGATGCTT  |
| <i>seraf/vdwe</i> <sup>ATG</sup> MO  | 2.4-3.2   | TACAGCAAAGCCCTGCCATTTTCAT  |
| <i>seraf/vdwe</i> <sup>e1i1</sup> MO | 2.4-3.2   | TGCAATGCAGAAcAACTCACCAAAT  |
| <i>seraf/vdwe</i> MO                 | 2.4-3.2   | AGTTTGCTGAAATGAACACATGAAT  |
| <i>seraf/vdwe</i> <sup>e2i2</sup> MO | 2.4-3.2   | TGTGATTA AAAAGTTACCTCTGTGA |
| <i>wfdc1</i> <sup>ATG</sup> MO       | 2.4-3.2   | GACAGCCCTGCATGATCCCGCTCAT  |
| <i>HFREP-1</i> <sup>GT</sup> MO      | 2.4-3.2   | TTATGTGGCGCATTACCTTTATCGT  |
| <i>HFREP-1</i> <sup>ATG</sup> MO     | 2.4-3.2   | TGGCATGACCTGGTAATAGTAGAAC  |
| <i>csf1a</i> <sup>ATG</sup> MO       | 1.6-2.4   | GTTTCATCTGGCTGACCTGAACAAAT |
| <i>csf1a</i> <sup>ATG</sup> 5MM      | 1.6-2.4   | GTTgATgTGcCTcACCTcAACAAAT  |
| <i>csf1a</i> <sup>GT</sup> MO        | 1.6-2.4   | AGATGGACTTTGTGTACCTCAATCTC |
| <i>csf1b</i> <sup>GT</sup> MO        | 1.6-2.4   | ATTGTGATTGGACTTCTCACCAGTT  |
| <i>csf1b</i> <sup>ATG</sup> MO       | 0.8-1.6   | TGTAGGGTTGTTTCATCTGGCTACC  |
| <i>csf1b</i> <sup>ATG</sup> 5MM      | 0.8-1.6   | TGaAcGGTTCcTTCATgTcGCTCAC  |
| <i>csf1ra</i> <sup>ATG</sup> MO      | 2.4-3.2   | AAGAGCGGAAGAACATCTCAGAGC   |
| <i>csf1ra</i> <sup>ATG</sup> 5MM     | 2.4-3.2   | AAcAcCGCcAAcAACATCTCAcAGC  |
| <i>prtga</i> <sup>ATG</sup> MO       | 2.4-3.2   | AAAGACGCCATTTACTCTGTACTC   |
| <i>cdon</i> <sup>ATG</sup> MO        | 2.4-3.2   | ATAATCTCAGGCCACCGTCTCCAT   |
| <i>CD81</i> <sup>ATG</sup> MO        | 1.6-2.4   | TGCAGCCTTCCACGCCACGCCCAT   |
| <i>gas1b</i> <sup>ATG</sup> MO       | 1.6-2.4   | TTGCCATTCCCTTCATGTGCCCGCAT |
| <i>A2CEY7</i> <sup>ATG</sup> MO      | 1.6-2.4   | ACACAGTCTTCATCATTCTGCTAC   |
| <i>A2CEY7</i> <sup>GT</sup> MO       | 1.6-2.4   | TCATCCAGATCATCTCCTACCTGTT  |
| <i>rgmb</i> <sup>ATG</sup> MO        | 1.6-2.4   | GCCACCATGGGTATGGGGAGAGCAG  |
| <i>rgmb</i> <sup>GT</sup> MO         | 1.6-2.4   | AAGTGTAAGAGCGGTGTTTACCTATG |
| <i>swiprosin2</i> <sup>ATG</sup> MO  | 1.6-2.4   | GTTTCAGAGGTTGTGTGCTCGCTCAT |

one and three hours of incubation at room temperature using a Quant plate reader (BIO-TEK Instruments, INC.). Interactions correspond to wells showing an absorbance reading of 0.1 after one-hour incubation, these are wells in which the substrate turnover led to a color change from yellow to red. The interacting proteins have been re-expressed and the interactions have been retested and confirmed in a validation screen (Figure 13.8B). Interactions between Tnw and Delta ligands could only be detected in one orientation, an observation, which is congruent with the fact that the only further interaction found in the AVEXIS screen involving Delta ligands is likewise only detectable in one orientation, in which Delta ligands are presented as monomeric bait proteins (unpublished results). The most likely explanation for this phenomenon seems to be homotypic binding amongst Delta ligands, which has been reported before (Wright et al., 2011), and is likely to compete with binding to other proteins. While the generation of bait and prey protein constructs was performed by the author, the expression in HEK293 cells and screening against the AVEXIS library was performed by Dr. Christian Söllner.

## Part VI

# Supplemental Data



**Table 22.3:** ‘Teleost MSC microarray profiling’ dataset

| ID           | logFC | adj. p-value | Gene symbol         |
|--------------|-------|--------------|---------------------|
| A_15_P108902 | -4.5  | 0.0022       | <i>myog</i>         |
| A_15_P140551 | -4.2  | 0.0022       | <i>myog</i>         |
| A_15_P161511 | -3.5  | 0.0022       | <i>zgc:158436</i>   |
| A_15_P335870 | -3.5  | 0.0022       | <i>zgc:158436</i>   |
| A_15_P416575 | -3.5  | 0.0022       | <i>pax7</i>         |
| A_15_P119443 | -3.4  | 0.0022       | <i>tmsb</i>         |
| A_15_P105522 | -3.2  | 0.0022       | <i>thbs4</i>        |
| A_15_P584917 | -3.1  | 0.0022       | <i>sb:cb560</i>     |
| A_15_P151411 | -3.1  | 0.0015       | <i>myf5</i>         |
| A_15_P209871 | -3.0  | 0.0022       | <i>wu:fj19b07</i>   |
| A_15_P157711 | -3.0  | 0.0022       | <i>LOC563523</i>    |
| A_15_P172406 | -3.0  | 0.0022       | <i>gch2</i>         |
| A_15_P151221 | -2.8  | 0.0022       | <i>thbs4</i>        |
| A_15_P102035 | -2.7  | 0.0022       | <i>lmnb1</i>        |
| A_15_P107372 | -2.7  | 0.0018       | <i>wu:fj19b07</i>   |
| A_15_P108946 | -2.6  | 0.0023       | <i>kal1b</i>        |
| A_15_P105497 | -2.6  | 0.0022       | <i>zgc:92343</i>    |
| A_15_P107369 | -2.5  | 0.0022       | <i>zgc:113456</i>   |
| A_15_P212091 | -2.5  | 0.0023       | <i>pax3</i>         |
| A_15_P186046 | -2.4  | 0.0022       | <i>rbp7b</i>        |
| A_15_P103020 | -2.4  | 0.0022       | <i>zgc:153112</i>   |
| A_15_P117410 | -2.4  | 0.0024       | <i>her2</i>         |
| A_15_P161696 | -2.4  | 0.0022       | <i>uncx4.1</i>      |
| A_15_P102602 | -2.3  | 0.0022       | <i>hey1</i>         |
| A_15_P186541 | -2.3  | 0.0022       | <i>LOC562554</i>    |
| A_15_P101384 | -2.3  | 0.0023       | <i>zgc:92518</i>    |
| A_15_P102590 | -2.3  | 0.0022       | <i>hsp90a.1</i>     |
| A_15_P101831 | -2.3  | 0.0022       | <i>pax3</i>         |
| A_15_P193566 | -2.3  | 0.0022       | <i>LOC100005261</i> |
| A_15_P152741 | -2.2  | 0.0023       | <i>hey2</i>         |
| A_15_P208781 | -2.2  | 0.0023       | <i>zgc:158671</i>   |
| A_15_P144471 | -2.1  | 0.0022       | <i>cilp</i>         |
| A_15_P210071 | -2.1  | 0.0022       | <i>tuba8l3</i>      |
| A_15_P102236 | -2.1  | 0.0022       | <i>pax7</i>         |
| A_15_P132386 | -2.0  | 0.0022       | <i>lmnb1</i>        |
| A_15_P116030 | -2.0  | 0.0022       | <i>myf5</i>         |
| A_15_P410100 | -2.0  | 0.0022       | <i>zgc:158482</i>   |
| A_15_P120710 | -2.0  | 0.0024       |                     |
| A_15_P152231 | -1.9  | 0.0022       | <i>dut</i>          |
| A_15_P168776 | -1.9  | 0.0024       | <i>zgc:113499</i>   |

Continued on following page.

| ID           | logFC | adj. p-value | Gene symbol       |
|--------------|-------|--------------|-------------------|
| A_15_P147706 | -1.9  | 0.0023       | <i>LOC562682</i>  |
| A_15_P205971 | -1.8  | 0.0022       | <i>zic1</i>       |
| A_15_P120190 | -1.8  | 0.0024       | <i>apex1</i>      |
| A_15_P307466 | -1.8  | 0.0024       |                   |
| A_15_P116526 | -1.8  | 0.0024       | <i>kbtbd10</i>    |
| A_15_P471265 | -1.8  | 0.0022       |                   |
| A_15_P198921 | -1.7  | 0.0023       | <i>tnw</i>        |
| A_15_P419550 | -1.7  | 0.0022       | <i>gch2</i>       |
| A_15_P269301 | -1.7  | 0.0024       | <i>LOC792773</i>  |
| A_15_P529807 | -1.7  | 0.0022       | <i>GRIP2</i>      |
| A_15_P120512 | -1.7  | 0.0022       | <i>oep</i>        |
| A_15_P134851 | -1.7  | 0.0023       |                   |
| A_15_P110305 | -1.7  | 0.0023       | <i>zic1</i>       |
| A_15_P207866 | -1.7  | 0.0023       | <i>zgc:158623</i> |
| A_15_P151491 | -1.6  | 0.0024       | <i>mcm2</i>       |
| A_15_P109152 | -1.6  | 0.0022       | <i>nr2f11</i>     |
| A_15_P200931 | -1.6  | 0.0022       | <i>LOC795902</i>  |
| A_15_P104490 | -1.6  | 0.0024       | <i>wif1</i>       |
| A_15_P103444 | -1.6  | 0.0022       | <i>mcm4</i>       |
| A_15_P172956 | -1.6  | 0.0022       | <i>MGC162334</i>  |
| A_15_P445060 | -1.6  | 0.0022       |                   |
| A_15_P109736 | -1.6  | 0.0022       |                   |
| A_15_P110500 | -1.6  | 0.0022       | <i>rgmb</i>       |
| A_15_P151891 | -1.6  | 0.0023       | <i>zgc:113307</i> |
| A_15_P103323 | -1.6  | 0.0022       | <i>lpl</i>        |
| A_15_P173576 | -1.5  | 0.0022       | <i>zgc:85677</i>  |
| A_15_P187936 | -1.5  | 0.0024       | <i>LOC798510</i>  |
| A_15_P153176 | -1.5  | 0.0024       | <i>flj20508l</i>  |
| A_15_P100639 | -1.5  | 0.0024       | <i>asf1b</i>      |
| A_15_P169966 | -1.5  | 0.0023       | <i>mcm5</i>       |
| A_15_P460655 | -1.5  | 0.0024       |                   |
| A_15_P121188 | -1.5  | 0.0023       | <i>zgc:56121</i>  |
| A_15_P109939 | -1.5  | 0.0023       | <i>zgc:65780</i>  |
| A_15_P195676 | -1.5  | 0.0023       | <i>entpd1</i>     |
| A_15_P116435 | -1.5  | 0.0023       | <i>fgfr4</i>      |
| A_15_P335349 | -1.5  | 0.0023       |                   |
| A_15_P102773 | -1.5  | 0.0022       | <i>rcc1</i>       |
| A_15_P105141 | -1.4  | 0.0024       | <i>zgc:110092</i> |
| A_15_P104275 | -1.4  | 0.0023       | <i>nhp2l1</i>     |
| A_15_P208956 | -1.4  | 0.0022       | <i>fabp3</i>      |
| A_15_P476650 | -1.4  | 0.0022       |                   |
| A_15_P209511 | -1.4  | 0.0023       |                   |

Continued on following page.

| ID           | logFC | adj. p-value | Gene symbol       |
|--------------|-------|--------------|-------------------|
| A_15_P213871 | -1.4  | 0.0022       | <i>zgc:85677</i>  |
| A_15_P101988 | -1.4  | 0.0024       | <i>zgc:56699</i>  |
| A_15_P169321 | -1.4  | 0.0024       | <i>tspan13</i>    |
| A_15_P296106 | -1.4  | 0.0023       | <i>flj20508l</i>  |
| A_15_P184561 | -1.4  | 0.0023       |                   |
| A_15_P349300 | -1.4  | 0.0023       | <i>LOC564151</i>  |
| A_15_P109391 | -1.4  | 0.0022       | <i>mcm3</i>       |
| A_15_P219226 | -1.4  | 0.0022       | <i>zgc:113499</i> |
| A_15_P544287 | -1.4  | 0.0025       | <i>rpa2</i>       |
| A_15_P154211 | -1.4  | 0.0024       | <i>rrm2</i>       |
| A_15_P103048 | -1.4  | 0.0023       | <i>rac3</i>       |
| A_15_P140167 | -1.4  | 0.0025       | <i>ddx52</i>      |
| A_15_P537237 | -1.4  | 0.0023       | <i>nol5a</i>      |
| A_15_P544287 | -1.4  | 0.0025       | <i>zgc:158623</i> |
| A_15_P168986 | -1.4  | 0.0024       | <i>rnaseh2a</i>   |
| A_15_P194016 | -1.4  | 0.0025       | <i>cdon</i>       |
| A_15_P304326 | -1.3  | 0.0022       | <i>uhrf1</i>      |
| A_15_P117020 | -1.3  | 0.0022       | <i>tcf12</i>      |
| A_15_P107014 | -1.3  | 0.0022       | <i>snrpd1</i>     |
| A_15_P114974 | -1.3  | 0.0023       | <i>six4.1</i>     |
| A_15_P118554 | -1.3  | 0.0023       |                   |
| A_15_P120199 | -1.3  | 0.0023       |                   |
| A_15_P176781 | -1.3  | 0.0024       | <i>mybbp1a</i>    |
| A_15_P596817 | -1.3  | 0.0023       |                   |
| A_15_P204261 | -1.3  | 0.0024       | <i>mef2d</i>      |
| A_15_P117621 | -1.3  | 0.0023       | <i>zgc:110727</i> |
| A_15_P272131 | -1.3  | 0.0022       |                   |
| A_15_P111496 | -1.3  | 0.0022       | <i>surf6l</i>     |
| A_15_P179111 | -1.3  | 0.0023       | <i>LOC792773</i>  |
| A_15_P180791 | -1.3  | 0.0024       |                   |
| A_15_P149131 | -1.3  | 0.0025       | <i>zgc:153991</i> |
| A_15_P351050 | -1.3  | 0.0023       |                   |
| A_15_P114679 | -1.3  | 0.0024       | <i>rfc3</i>       |
| A_15_P169246 | -1.3  | 0.0023       | <i>mjge8</i>      |
| A_15_P281466 | -1.3  | 0.0023       |                   |
| A_15_P496837 | -1.3  | 0.0023       |                   |
| A_15_P276521 | -1.3  | 0.0024       | <i>zgc:153707</i> |
| A_15_P190106 | -1.3  | 0.0025       | <i>LOC571720</i>  |
| A_15_P143526 | -1.3  | 0.0024       | <i>MGC158750</i>  |
| A_15_P104404 | -1.3  | 0.0023       | <i>tcf12</i>      |
| A_15_P133676 | -1.3  | 0.0024       | <i>eftud2</i>     |
| A_15_P147966 | -1.2  | 0.0024       | <i>zgc:112501</i> |

Continued on following page.

| ID           | logFC | adj. p-value | Gene symbol             |
|--------------|-------|--------------|-------------------------|
| A_15_P207476 | -1.2  | 0.0023       | <i>dpysl5b</i>          |
| A_15_P119868 | -1.2  | 0.0024       |                         |
| A_15_P367640 | -1.2  | 0.0023       | <i>eftud2</i>           |
| A_15_P111895 | -1.2  | 0.0023       | <i>eya1</i>             |
| A_15_P181008 | -1.2  | 0.0024       | <i>nola2</i>            |
| A_15_P105109 | -1.2  | 0.0023       | <i>cd81</i>             |
| A_15_P118954 | -1.2  | 0.0024       | <i>sf3b3</i>            |
| A_15_P590617 | -1.2  | 0.0024       |                         |
| A_15_P120275 | -1.2  | 0.0023       | <i>ssb</i>              |
| A_15_P114882 | -1.2  | 0.0024       | <i>myca</i>             |
| A_15_P104158 | -1.2  | 0.0023       | <i>fabp3</i>            |
| A_15_P349525 | -1.2  | 0.0024       | <i>si:dkey-15j16.4</i>  |
| A_15_P209306 | -1.2  | 0.0024       | <i>zgc:56486</i>        |
| A_15_P169436 | -1.2  | 0.0023       | <i>zgc:153534</i>       |
| A_15_P198926 | -1.2  | 0.0024       |                         |
| A_15_P118844 | -1.2  | 0.0023       | <i>tomm40l</i>          |
| A_15_P195931 | -1.2  | 0.0025       | <i>alcam</i>            |
| A_15_P109049 | -1.2  | 0.0024       |                         |
| A_15_P113995 | -1.2  | 0.0024       | <i>her8a</i>            |
| A_15_P175756 | -1.2  | 0.0023       | <i>ass1</i>             |
| A_15_P435930 | -1.1  | 0.0023       |                         |
| A_15_P208706 | -1.1  | 0.0024       | <i>zgc:158231</i>       |
| A_15_P116794 | -1.1  | 0.0023       |                         |
| A_15_P423665 | -1.1  | 0.0023       | <i>fabp3</i>            |
| A_15_P103700 | -1.1  | 0.0024       | <i>six4.2</i>           |
| A_15_P570327 | -1.1  | 0.0023       | <i>zgc:158231</i>       |
| A_15_P116482 | -1.1  | 0.0023       | <i>si:ch211-152m4.1</i> |
| A_15_P164056 | -1.1  | 0.0024       | <i>zgc:110551</i>       |
| A_15_P117142 | -1.1  | 0.0025       | <i>snrpb</i>            |
| A_15_P201966 | -1.1  | 0.0024       | <i>col5a2</i>           |
| A_15_P120511 | -1.1  | 0.0024       | <i>snrpf1</i>           |
| A_15_P424610 | -1.1  | 0.0024       |                         |
| A_15_P133996 | -1.1  | 0.0024       | <i>ppig</i>             |
| A_15_P161736 | -1.1  | 0.0025       | <i>gas1b</i>            |
| A_15_P102607 | -1.1  | 0.0024       | <i>rbb4l</i>            |
| A_15_P194611 | -1.1  | 0.0024       | <i>dlc</i>              |
| A_15_P174396 | -1.1  | 0.0024       | <i>top2a</i>            |
| A_15_P149541 | -1.1  | 0.0025       | <i>lpl</i>              |
| A_15_P192911 | -1.1  | 0.0024       | <i>prtga</i>            |
| A_15_P158891 | -1.1  | 0.0024       | <i>LOC797547</i>        |
| A_15_P546122 | -1.1  | 0.0024       | <i>LOC100002019</i>     |
| A_15_P121213 | -1.1  | 0.0024       | <i>uck2b</i>            |

Continued on following page.

| <b>ID</b>    | <b>logFC</b> | <b>adj. p-value</b> | <b>Gene symbol</b> |
|--------------|--------------|---------------------|--------------------|
| A_15_P109021 | -1.1         | 0.0024              | <i>nol6</i>        |
| A_15_P149381 | -1.1         | 0.0024              | <i>zgc:112254</i>  |
| A_15_P432875 | -1.1         | 0.0024              | <i>col6a</i>       |
| A_15_P100792 | -1.0         | 0.0024              | <i>prmt5</i>       |
| A_15_P420895 | -1.0         | 0.0024              |                    |
| A_15_P120915 | -1.0         | 0.0025              | <i>cirh1a</i>      |
| A_15_P495557 | -1.0         | 0.0024              | <i>col5a</i>       |
| A_15_P134301 | -1.0         | 0.0024              | <i>brig1</i>       |
| A_15_P104470 | -1.0         | 0.0024              | <i>caxc5</i>       |
| A_15_P103456 | -1.0         | 0.0024              | <i>LOC570288</i>   |
| A_15_P212376 | -1.0         | 0.0024              | <i>LOC553478</i>   |
| A_15_P178446 | -1.0         | 0.0024              | <i>LOC558911</i>   |
| A_15_P118913 | -1.0         | 0.0025              | <i>def</i>         |
| A_15_P102810 | -1.0         | 0.0025              | <i>LOC561131</i>   |
| A_15_P210696 | -1.0         | 0.0025              | <i>dt1p1a10l</i>   |
| A_15_P106777 | -1.0         | 0.0024              | <i>sox9a</i>       |

Continued on following page.

**Table 22.4:** AVEXIS screen of Tnw(5xFn-FG) deletion construct vs. bait protein library.

| <b>Bait protein</b>  | <b>AU</b> |
|--|-----------|
| Islr2  | 0.065     |
| Pleiotrophin   | 0.077     |
| Egf3   | 0.067     |
| Calreticulin like  | 0.064     |
| DeltaC   | 0.066     |
| Ret1 receptor tyrosine kinase                                | 0.066     |
| Transmembrane protein 59-like                                | 0.067     |
| Hemochromatosis type 2                                       | 0.070     |
| RGM domain family member A                                   | 0.063     |
| Protocadherin 18a  | 0.071     |
| Midkine-related growth factor a                              | 0.076     |
| Midkine-related growth factor b                              | 0.069     |
| Spondin 2a extracellular matrix protein                      | 0.069     |
| Calumenin a  | 0.072     |
| Protogenin homolog b   | 0.073     |
| Prion protein related sequence 1                             | 0.070     |
| Eph-like receptor tyrosine kinase 8                          | 0.099     |
| Otoconin 90  | 0.072     |
| Frizzled-related protein                                     | 0.074     |
| Semaphorin 3d  | 0.068     |
| Neuropilin 1b  | 0.067     |
| Vasorin (TILLING allele)                                     | 0.070     |
| Lrig1  | 0.071     |
| si:ch211-170d8.2   | 0.068     |
| Eph receptor B4a   | 0.070     |
| Neuropeptide B   | 0.060     |
| Vasorin like   | 0.067     |
| Protocadherin 17   | 0.069     |
| Cspg4  | 0.072     |
| zgc:113574   | 0.068     |
| Cxcl12b  | 0.068     |
| Follistatin a  | 0.075     |
| Nerve growth factor receptor/p75                             | 0.071     |
| Transiently expressed axonal glycoprotein                    | 0.065     |
| Protocadherin 10b  | 0.070     |
| Meteorin glial cell differentiation regulator-like           | 0.095     |
| Secreted frizzled-related protein 1a                         | 0.070     |
| Hyaluronan proteoglycan link protein 1                       | 0.068     |
| Wingless-type MMTV integration site family member 11 related | 0.067     |

*Continued on following page.*

| <b>Protein</b>                                       | <b>AU</b> |
|--|-----------|
| Eph-like kinase 3                                    | 0.072     |
| Secreted acidic cysteine rich glycoprotein           | 0.063     |
| Tumor necrosis factor receptor superfamily member 21 | 0.066     |
| Draxin   | 0.067     |
| Arginine-rich mutated in early stage tumors          | 0.068     |
| Draxin V2  | 0.066     |
| zgc:110088   | 0.064     |
| Kallmann syndrome 1a sequence                        | 0.084     |
| Cysteine-rich with EGF-like domains 2                | 0.060     |
| Neuropilin 2b  | 0.066     |
| <b>Ek1</b>   | 0.169     |
| Wingless-type MMTV integration site family member 1  | 0.069     |
| Eph receptor A4a                                     | 0.088     |
| Cadherin 2neuronal                                   | 0.060     |
| Eph receptor A7                                      | 0.066     |
| Ephrin A2  | 0.078     |
| Protein tyrosine phosphatase receptor type A         | 0.067     |
| Ephrin A3b   | 0.087     |
| Ephrin A5b   | 0.069     |
| Ephrin B2a   | 0.063     |
| Ephrin B3  | 0.062     |
| Calreticulin   | 0.065     |
| Jam2   | 0.070     |
| Cadm2a   | 0.076     |
| Galanin V2   | 0.073     |
| Alcam  | 0.060     |
| Mpz  | 0.060     |
| Lrit2  | 0.061     |
| Neol   | 0.063     |
| Unc5b  | 0.073     |
| Fgfr2  | 0.069     |
| Ror1   | 0.065     |
| Wnt11  | 0.065     |
| Ryk  | 0.061     |
| Csf1b  | 0.065     |
| Wnt4b  | 0.069     |
| Gas1b  | 0.072     |
| Transmembrane glycoprotein A33                       | 0.064     |
| Fgfr4  | 0.072     |
| Csf1ra   | 0.068     |
| Lumican  | 0.068     |
| Seraf  | 0.096     |

*Continued on following page.*

| <b>Protein</b>                                     | <b>AU</b> |
|--|-----------|
| Dkk1   | 0.065     |
| Nlrr1  | 0.065     |
| Elfn2  | 0.065     |
| Ngl2   | 0.062     |
| Cntn1a   | 0.064     |
| <b>DeltaA</b>                                      | 0.114     |
| <b>DeltaB</b>                                      | 0.159     |
| Lrrc4c   | 0.063     |
| Mpzl   | 0.058     |
| Cadm4  | 0.062     |
| Follistatin-like 1a                                | 0.069     |
| Prepro-urotensin                                   | 0.062     |
| A2CEY7   | 0.066     |
| Fgf3   | 0.069     |
| zgc:110239   | 0.066     |
| Nenf   | 0.061     |
| LOC797163  | 0.068     |
| Galanin  | 0.063     |
| Pituitary tumor-transforming 1 interacting protein | 0.062     |
| Gremlin2   | 0.068     |
| Cocaine- and amphetamine-regulated transcript      | 0.068     |
| Clusterin  | 0.061     |
| Defensin beta-like 1                               | 0.07      |
| loc793120  | 0.071     |
| Cxcl12a  | 0.101     |
| Igfbp1a  | 0.072     |
| zgc161979  | 0.067     |
| Lndc1  | 0.089     |
| CD59   | 0.067     |
| Ccbe1  | 0.073     |
| <b>Wfdc1</b>                                       | 0.113     |
| Olfml2b  | 0.063     |
| Csf1a  | 0.07      |
| Cd59-like  | 0.066     |
| Slc22a7a   | 0.069     |
| Chromogranin                                       | 0.064     |
| Bmper  | 0.092     |
| Edn3b  | 0.077     |
| Edn3   | 0.066     |
| Ramp2  | 0.070     |
| <b>Igfbp7</b>                                      | 0.110     |
| Neurotrimin  | 0.066     |

*Continued on following page.*

| <b>Protein</b>        | <b>AU</b>    |
|-----------------------|--------------|
| Biglycan b            | 0.077        |
| Bcan                  | 0.079        |
| Mxra8a                | 0.075        |
| Nlrr1                 | 0.069        |
| Tnw (FG)              | 0.064        |
| Tnw (3.5xEGF-5xFn-FG) | 0.089        |
| Tnw (5xFn-FG)         | 0.069        |
| <b>Matrilin 4sv</b>   | <b>0.235</b> |

*Continued on following page.*



— *Den Göttern gleich ich nicht! Zu tief ist es gefühlt;  
Dem Wurme gleich ich, der den Staub durchwühlt;  
Den, wie er sich im Staube nährend lebt,  
Des Wandrers Tritt vernichtet und begräbt.* —

Goethe, Faust

# 23

## Author contributions

The work presented here was carried out in the lab of Prof. Dr. Christiane Nüsslein-Volhard at the Max-Planck-Institut für Entwicklungsbiologie in Tübingen. It was jointly supervised by Dr. Jana Krauss and Prof. Dr. Christiane Nüsslein-Volhard. Apart from this the members of the PhD advisory committee, Prof. Dr. Rolf Reuter (Eberhard-Karls-Universität, Tübingen), Prof. Dr. Gerd Jürgens (Eberhard-Karls-Universität and Max-Planck-Institut für Entwicklungsbiologie, Tübingen), Dr. Gaspár Jekely (Max-Planck-Institut für Entwicklungsbiologie, Tübingen), and Dr. Mitchell Paul Levesque (Max-Planck-Institut für Entwicklungsbiologie, Tübingen) accom-

panied this project with constructive criticism. All experiments were planned, conducted and analyzed by the author unless explicitly stated otherwise in the main text. Collaborations with Dr. Mitchell Paul Levesque, a former member of the lab, now at UZH (Zürich) and Dr. Christian Söllner ((Max-Planck-Institut für Entwicklungsbiologie, Tübingen) were pivotal to the success of this project. Specifically, Dr. Mitchell Paul Levesque has performed the statistical analysis of microarray data. Dr. Christian Söllner and his former lab head Dr. Gavin Wright (Sanger, Cambridge, UK) have generously provided the AVEXIS library. While the author has cloned MSC-derived candidate proteins into suitable AVEXIS expression vectors and added them to the AVEXIS library, Dr. Christian Söllner expressed these proteins and performed the AVEXIS screen. Dr. Jana Krauss generated the Tg(*myod*::NLS-Cherry BAC transgenic line and performed the *in situ* hybridisation of *tnw* in 4dpf old larva. Dr. Katrin Henke a former member of the lab provided the *in situ* hybridization of *csf1a/b*. Alessandro Mongera (Max-Planck-Institut für Entwicklungsbiologie, Tübingen) cloned the *csf1a/b* AVEXIS expression constructs.

— O sähest du, voller Mondenschein  
zum letzten Mal auf meine Pein,  
Den ich so manche Mitternacht  
an diesem Pult herangewacht: —

Goethe, Faust

# 24

## Bibliography

Abmayr, S.M., and Pavlath, G.K. (2012). Myoblast fusion: lessons from flies and mice. *Development* 139, 641-656.

Adams, J.C., and Lawler, J. (1994). Cell-type specific adhesive interactions of skeletal myoblasts with thrombospondin-1. *Mol Biol Cell* 5, 423-437.

Adams, J.C., and Lawler, J. (2011). The thrombospondins. *Cold Spring Harb Perspect Biol* 3, a009712.

Afonin, B., Ho, M., Gustin, J.K., Meloty-Kapella, C., and Domingo, C.R. (2006). Cell behaviors associated with somite segmentation and rotation in *Xenopus laevis*. *Dev Dyn* 235, 3268-3279.

Allen, B.L., Tenzen, T., and McMahon, A.P. (2007). The Hedgehog-binding proteins Gas1 and Cdo cooperate to positively regulate Shh signaling during mouse development. *Genes Dev* 21, 1244-1257.

Altman, J., and Das, G.D. (1965). Autoradiographic and histological evidence of postnatal hippocampal neurogenesis in rats. *J Comp Neurol* 124, 319-335.

Anakwe, K., Robson, L., Hadley, J., Buxton, P., Church, V., Allen, S., Hartmann, C., Harfe, B., Nohno, T., Brown, A.M., et al. (2003). Wnt signalling regulates myogenic differentiation in the developing avian wing. *Development* 130, 3503-3514.

Artavanis-Tsakonas, S., and Muskavitch, M.A. (2010). Notch: the past, the present, and the future. *Curr Top Dev Biol* 92, 1-29.

Artavanis-Tsakonas, S., Rand, M.D., and Lake, R.J. (1999). Notch signaling: cell fate control and signal integration in development. *Science* 284, 770-776.

Barker, N., van Es, J.H., Kuipers, J., Kujala, P., van den Born, M., Cozijnsen, M., Haegebarth, A., Korving, J., Begthel, H., Peters, P.J., et al. (2007). Identification of stem cells in small intestine and colon by marker gene *Lgr5*. *Nature* 449, 1003-1007.

Bassett, D.I., Bryson-Richardson, R.J., Daggett, D.F., Gautier, P., Keenan, D.G., and Currie, P.D. (2003). Dystrophin is required for the formation of stable muscle attachments in the zebrafish embryo. *Development* 130, 5851-5860.

Baugh, L.R., and Hunter, C.P. (2006). MyoD, modularity, and myogenesis: conservation of regulators and redundancy in *C. elegans*. *Genes Dev* 20, 3342-3346.

Ben-Yair, R., and Kalcheim, C. (2005). Lineage analysis of the avian dermomyotome sheet reveals the existence of single cells with both dermal and muscle progenitor fates. *Development* 132, 689-701.

Benezra, R., Davis, R.L., Lockshon, D., Turner, D.L., and Weintraub, H. (1990). The protein Id: a negative regulator of helix-loop-helix DNA binding proteins. *Cell* 61, 49-59.

Bentley, A.A., and Adams, J.C. (2010). The evolution of thrombospondins and their ligand-binding activities. *Mol Biol Evol* 27, 2187-2197.

- Bentzinger, C.F., Wang, Y.X., and Rudnicki, M.A. (2012). Building muscle: molecular regulation of myogenesis. *Cold Spring Harb Perspect Biol* 4.
- Beres, B.J., George, R., Lougher, E.J., Barton, M., Verrelli, B.C., McGlade, C.J., Rawls, J.A., and Wilson-Rawls, J. (2011). Numb regulates Notch1, but not Notch3, during myogenesis. *Mech Dev* 128, 247-257.
- Bergmann, O., Bhardwaj, R.D., Bernard, S., Zdunek, S., Barnabe-Heider, F., Walsh, S., Zupicich, J., Alkass, K., Buchholz, B.A., Druid, H., et al. (2009). Evidence for cardiomyocyte renewal in humans. *Science* 324, 98-102.
- Berkes, C.A., and Tapscott, S.J. (2005). MyoD and the transcriptional control of myogenesis. *Semin Cell Dev Biol* 16, 585-595.
- Bertini, E., D'Amico, A., Gualandi, F., and Petrini, S. (2011). Congenital muscular dystrophies: a brief review. *Semin Pediatr Neurol* 18, 277-288.
- Betancur, P., Bronner-Fraser, M., and Sauka-Spengler, T. (2010). Assembling neural crest regulatory circuits into a gene regulatory network. *Annu Rev Cell Dev Biol* 26, 581-603.
- Biegert, A., Mayer, C., Remmert, M., Soding, J., and Lupas, A.N. (2006). The MPI Bioinformatics Toolkit for protein sequence analysis. *Nucleic Acids Res* 34, W335-339.
- Bill, B.R., Petzold, A.M., Clark, K.J., Schimmenti, L.A., and Ekker, S.C. (2009). A primer for morpholino use in zebrafish. *Zebrafish* 6, 69-77.
- Biressi, S., and Rando, T.A. (2010). Heterogeneity in the muscle satellite cell population. *Semin Cell Dev Biol* 21, 845-854.
- Bismuth, K., and Relaix, F. (2010). Genetic regulation of skeletal muscle development. *Exp Cell Res* 316, 3081-3086.
- Biteau, B., Hochmuth, C.E., and Jasper, H. (2011). Maintaining tissue homeostasis: dynamic control of somatic stem cell activity. *Cell Stem Cell* 9, 402-411.

Bjornson, C.R., Cheung, T.H., Liu, L., Tripathi, P.V., Steeper, K.M., and Rando, T.A. (2012). Notch signaling is necessary to maintain quiescence in adult muscle stem cells. *Stem Cells* 30, 232-242.

Blanpain, C., and Fuchs, E. (2006). Epidermal stem cells of the skin. *Annu Rev Cell Dev Biol* 22, 339-373.

Blanpain, C., Horsley, V., and Fuchs, E. (2007). Epithelial stem cells: turning over new leaves. *Cell* 128, 445-458.

Bonaguidi, M.A., Wheeler, M.A., Shapiro, J.S., Stadel, R.P., Sun, G.J., Ming, G.L., and Song, H. (2011). In vivo clonal analysis reveals self-renewing and multipotent adult neural stem cell characteristics. *Cell* 145, 1142-1155.

Boonen, K.J., and Post, M.J. (2008). The muscle stem cell niche: regulation of satellite cells during regeneration. *Tissue Eng Part B Rev* 14, 419-431.

Borello, U., Coletta, M., Tajbakhsh, S., Leyns, L., De Robertis, E.M., Buckingham, M., and Cossu, G. (1999). Transplacental delivery of the Wnt antagonist *Frzb1* inhibits development of caudal paraxial mesoderm and skeletal myogenesis in mouse embryos. *Development* 126, 4247-4255.

Borycki, A.G., Foucrier, J., Saffar, L., and Leibovitch, S.A. (1995a). Repression of the CSF-1 receptor (c-fms proto-oncogene product) by antisense transfection induces G1-growth arrest in L6 alpha 1 rat myoblasts. *Oncogene* 10, 1799-1811.

Borycki, A.G., Smadja, F., Stanley, R., and Leibovitch, S.A. (1995b). Colony-stimulating factor 1 (CSF-1) is involved in an autocrine growth control of rat myogenic cells. *Exp Cell Res* 218, 213-222.

Brack, A.S., Conboy, I.M., Conboy, M.J., Shen, J., and Rando, T.A. (2008). A temporal switch from notch to Wnt signaling in muscle stem cells is necessary for normal adult myogenesis. *Cell Stem Cell* 2, 50-59.

Brack, A.S., Conboy, M.J., Roy, S., Lee, M., Kuo, C.J., Keller, C., and Rando, T.A. (2007). Increased Wnt signaling during aging alters muscle stem cell fate and increases fibrosis. *Science* 317, 807-810.

Braun, T., and Gautel, M. (2011). Transcriptional mechanisms regulating skeletal muscle differentiation, growth and homeostasis. *Nat Rev Mol Cell Biol* 12, 349-361.

Bresnick, E.H., Katsumura, K.R., Lee, H.Y., Johnson, K.D., and Perkins, A.S. (2012). Master regulatory GATA transcription factors: mechanistic principles and emerging links to hematologic malignancies. *Nucleic Acids Res.*

Brockes, J.P., Kumar, A., and Velloso, C.P. (2001). Regeneration as an evolutionary variable. *J Anat* 199, 3-11.

Bryson-Richardson, R.J., and Currie, P.D. (2008). The genetics of vertebrate myogenesis. *Nat Rev Genet* 9, 632-646.

Buas, M.F., Kabak, S., and Kadesch, T. (2009). Inhibition of myogenesis by Notch: evidence for multiple pathways. *J Cell Physiol* 218, 84-93.

Buas, M.F., Kabak, S., and Kadesch, T. (2010). The Notch effector Hey1 associates with myogenic target genes to repress myogenesis. *J Biol Chem* 285, 1249-1258.

Buas, M.F., and Kadesch, T. (2010). Regulation of skeletal myogenesis by Notch. *Exp Cell Res* 316, 3028-3033.

Buckingham, M., and Relaix, F. (2007). The role of Pax genes in the development of tissues and organs: Pax3 and Pax7 regulate muscle progenitor cell functions. *Annu Rev Cell Dev Biol* 23, 645-673.

Buckingham, M., and Vincent, S.D. (2009). Distinct and dynamic myogenic populations in the vertebrate embryo. *Curr Opin Genet Dev* 19, 444-453.

Burda, P., Laslo, P., and Stopka, T. (2010). The role of PU.1 and GATA-1 transcription factors during normal and leukemogenic hematopoiesis. *Leukemia : official journal of the Leukemia Society of America, Leukemia Research Fund, UK* 24, 1249-1257.

Bushell, K.M., Sollner, C., Schuster-Boeckler, B., Bateman, A., and Wright, G.J. (2008). Large-scale screening for novel low-affinity extracellular protein interactions. *Genome Res* 18, 622-630.

Buttitta, L.A., and Edgar, B.A. (2007). Mechanisms controlling cell cycle exit upon terminal differentiation. *Curr Opin Cell Biol* 19, 697-704.

Cairns, J. (1975). Mutation selection and the natural history of cancer. *Nature* 255, 197-200.

Cajal, S.R.y. (1906). *Studien über die Hirnrinde des Menschen* (Johann Ambrosius Barth).

Cammer, M., Gevrey, J.C., Lorenz, M., Dovas, A., Condeelis, J., and Cox, D. (2009). The mechanism of CSF-1-induced Wiskott-Aldrich syndrome protein activation in vivo: a role for phosphatidylinositol 3-kinase and Cdc42. *J Biol Chem* 284, 23302-23311.

Carlson, B.M. (2010). *Stem Cell Anthology* (London: Academic Press).

Casanova, J. (2012). Stemness as a cell default state. *EMBO Rep.* 13, 396 - 397

Cavazzana-Calvo, M., Hacein-Bey, S., de Saint Basile, G., Gross, F., Yvon, E., Nusbaum, P., Selz, F., Hue, C., Certain, S., Casanova, J.L., et al. (2000). Gene therapy of human severe combined immunodeficiency (SCID)-X1 disease. *Science* 288, 669-672.

Cerletti, M., Jurga, S., Witczak, C.A., Hirshman, M.F., Shadrach, J.L., Goodyear, L.J., and Wagers, A.J. (2008). Highly efficient, functional engraftment of skeletal muscle stem cells in dystrophic muscles. *Cell* 134, 37-47.

Charge, S.B., and Rudnicki, M.A. (2004). Cellular and molecular regulation of muscle regeneration. *Physiol Rev* 84, 209-238.

Chatani, M., Takano, Y., and Kudo, A. (2011). Osteoclasts in bone modeling, as revealed by in vivo imaging, are essential for organogenesis in fish. *Dev Biol* 360, 96-109.

Cheng, H., and Leblond, C.P. (1974). Origin, differentiation and renewal of the four main epithelial cell types in the mouse small intestine. V. Unitarian Theory of the origin of the four epithelial cell types. *The American journal of anatomy* 141, 537-561.

Chevallier, A., Kieny, M., and Mauger, A. (1977). Limb-somite relationship: origin of the limb musculature. *J Embryol Exp Morphol* 41, 245-258.

Chillakuri, C.R., Sheppard, D., Lea, S.M., and Handford, P.A. (2012). Notch receptor-ligand binding and activation: Insights from molecular studies. *Semin Cell Dev Biol*.

Chiquet, M., and Fambrough, D.M. (1984a). Chick myotendinous antigen. I. A monoclonal antibody as a marker for tendon and muscle morphogenesis. *J Cell Biol* 98, 1926-1936.

Chiquet, M., and Fambrough, D.M. (1984b). Chick myotendinous antigen. II. A novel extracellular glycoprotein complex consisting of large disulfide-linked subunits. *J Cell Biol* 98, 1937-1946.

Chiquet-Ehrismann, R., and Tucker, R.P. (2004). Connective tissues: signalling by tenascins. *Int J Biochem Cell Biol* 36, 1085-1089.

Christ, B., Jacob, H.J., and Jacob, M. (1977). Experimental analysis of the origin of the wing musculature in avian embryos. *Anat Embryol (Berl)* 150, 171-186.

Christ, B., and Scaal, M. (2008). Formation and differentiation of avian somite derivatives. *Advances in experimental medicine and biology* 638, 1-41.

Ciciliot, S., and Schiaffino, S. (2010). Regeneration of mammalian skeletal muscle. Basic mechanisms and clinical implications. *Curr Pharm Des* 16, 906-914.

Cleto, C.L., Vandenberghe, A.E., MacLean, D.W., Pannunzio, P., Tortorelli, C., Meedel, T.H., Satou, Y., Satoh, N., and Hastings, K.E. (2003). Ascidian larva reveals ancient origin of vertebrate-skeletal-muscle troponin I characteristics in chordate locomotory muscle. *Mol Biol Evol* 20, 2113-2122.

Cohen, M., Georgiou, M., Stevenson, N.L., Miodownik, M., and Baum, B. (2010). Dynamic filopodia transmit intermittent Delta-Notch signaling to drive pattern refinement during lateral inhibition. *Dev Cell* 19, 78-89.

Collins, C.A., Olsen, I., Zammit, P.S., Heslop, L., Petrie, A., Partridge, T.A., and Morgan, J.E. (2005). Stem cell function, self-renewal, and behavioral heterogeneity of cells from the adult muscle satellite cell niche. *Cell* 122, 289-301.

Conboy, M.J., Karasov, A.O., and Rando, T.A. (2007). High incidence of non-random template strand segregation and asymmetric fate determination in dividing stem cells and their progeny. *PLoS Biol* 5, e102.

Davis, R.L., Weintraub, H., and Lassar, A.B. (1987). Expression of a single transfected cDNA converts fibroblasts to myoblasts. *Cell* 51, 987-1000.

De Jousineau, C., Soule, J., Martin, M., Anguille, C., Montcourrier, P., and Alexandre, D. (2003). Delta-promoted filopodia mediate long-range lateral inhibition in *Drosophila*. *Nature* 426, 555-559.

Devoto, S.H., Melancon, E., Eisen, J.S., and Westerfield, M. (1996). Identification of separate slow and fast muscle precursor cells in vivo, prior to somite formation. *Development* 122, 3371-3380.

Devoto, S.H., Stoiber, W., Hammond, C.L., Steinbacher, P., Haslett, J.R., Barresi, M.J., Patterson, S.E., Adiarte, E.G., and Hughes, S.M. (2006). Generality of vertebrate developmental patterns: evidence for a dermomyotome in fish. *Evol Dev* 8, 101-110.

Doe, C.Q., and Goodman, C.S. (1985). Early events in insect neurogenesis. II. The role of cell interactions and cell lineage in the determination of neuronal precursor cells. *Dev Biol* 111, 206-219.

Dooley, K., and Zon, L.I. (2000). Zebrafish: a model system for the study of human disease. *Curr Opin Genet Dev* 10, 252-256.

Dor, Y., Brown, J., Martinez, O.I., and Melton, D.A. (2004). Adult pancreatic beta-cells are formed by self-duplication rather than stem-cell differentiation. *Nature* 429, 41-46.

Douglass, T.G., Driggers, L., Zhang, J.G., Hoa, N., Delgado, C., Williams, C.C., Dan, Q., Sanchez, R., Jeffes, E.W., Wepsic, H.T., et al. (2008). Macrophage colony stimulating factor: not just for macrophages anymore! A gateway into complex biologies. *International immunopharmacology* 8, 1354-1376.

Dumont, E., Ralliere, C., and Rescan, P.Y. (2008). Identification of novel genes including Dermo-1, a marker of dermal differentiation, expressed in trout somitic external cells. *J Exp Biol* 211, 1163-1168.

Edmondson, D.G., Cheng, T.C., Cserjesi, P., Chakraborty, T., and Olson, E.N. (1992). Analysis of the myogenin promoter reveals an indirect pathway for positive autoregulation mediated by the muscle-specific enhancer factor MEF-2. *Mol Cell Biol* 12, 3665-3677.

Eisen, J.S., and Smith, J.C. (2008). Controlling morpholino experiments: don't stop making antisense. *Development* 135, 1735-1743.

Ellisen, L.W., Bird, J., West, D.C., Soreng, A.L., Reynolds, T.C., Smith, S.D., and Sklar, J. (1991). TAN-1, the human homolog of the *Drosophila* notch gene, is broken by chromosomal translocations in T lymphoblastic neoplasms. *Cell* 66, 649-661.

Enver, T., Pera, M., Peterson, C., and Andrews, P.W. (2009). Stem cell states, fates, and the rules of attraction. *Cell Stem Cell* 4, 387-397.

Erwin, D.H., and Davidson, E.H. (2009). The evolution of hierarchical gene regulatory networks. *Nat Rev Genet* 10, 141-148.

Fausto, N. (2000). Liver regeneration. *J Hepatol* 32, 19-31.

Feng, X., Adiarte, E.G., and Devoto, S.H. (2006). Hedgehog acts directly on the zebrafish dermomyotome to promote myogenic differentiation. *Dev Biol* 300, 736-746.

Fortini, M.E., and Artavanis-Tsakonas, S. (1994). The suppressor of hairless protein participates in notch receptor signaling. *Cell* 79, 273-282.

Fortunel, N.O., Otu, H.H., Ng, H.H., Chen, J., Mu, X., Chevassut, T., Li, X., Joseph, M., Bailey, C., Hatzfeld, J.A., et al. (2003). Comment on " 'Stemness': transcriptional profiling of embryonic and adult stem cells" and "a stem cell molecular signature". *Science* 302, 393; author reply 393.

Friedmann, T., and Roblin, R. (1972). Gene therapy for human genetic disease? *Science* 175, 949-955.

Fuchs, E., Tumber, T., and Guasch, G. (2004). Socializing with the neighbors: stem cells and their niche. *Cell* 116, 769-778.

Fukada, S., Uezumi, A., Ikemoto, M., Masuda, S., Segawa, M., Tanimura, N., Yamamoto, H., Miyagoe-Suzuki, Y., and Takeda, S. (2007). Molecular signature of quiescent satellite cells in adult skeletal muscle. *Stem Cells* 25, 2448-2459.

Fukada, S., Yamaguchi, M., Kokubo, H., Ogawa, R., Uezumi, A., Yoneda, T., Matev, M.M., Motohashi, N., Ito, T., Zolkiewska, A., et al. (2011). *Hes1* and *Hes3* are essential to generate undifferentiated quiescent satellite cells and to maintain satellite cell numbers. *Development* 138, 4609-4619.

Fukushige, T., Brodigan, T.M., Schriefer, L.A., Waterston, R.H., and Krause, M. (2006). Defining the transcriptional redundancy of early body-wall muscle development in *C. elegans*: evidence for a unified theory of animal muscle development. *Genes Dev* 20, 3395-3406.

Gaspera, B.D., Armand, A.S., Sequeira, I., Chesneau, A., Mazabraud, A., Lecolle, S., Charbonnier, F., and Chanoine, C. (2012). Myogenic waves and myogenic programs during *Xenopus* embryonic myogenesis. *Dev Dyn.* 24, 995-1007.

Gautel, M. (2011). The sarcomeric cytoskeleton: who picks up the strain? *Curr Opin Cell Biol* 23, 39-46.

Gayraud-Morel, B., Chretien, F., Jory, A., Sambasivan, R., Negroni, E., Flamant, P., Soubigou, G., Coppee, J.Y., Di Santo, J., Cumano, A., et al. (2012). *Myf5* haploinsufficiency reveals distinct cell fate potentials for adult skeletal muscle stem cells. *J Cell Sci.* 125, 1738-49.

Gazave, E., Lapebie, P., Richards, G.S., Brunet, F., Ereskovsky, A.V., Degnan, B.M., Borchiellini, C., Vervoort, M., and Renard, E. (2009). Origin and evolution of the Notch signalling pathway: an overview from eukaryotic genomes. *BMC Evol Biol* 9, 249.

Gilbert, P.M., Havenstrite, K.L., Magnusson, K.E., Sacco, A., Leonardi, N.A., Kraft, P., Nguyen, N.K., Thrun, S., Lutolf, M.P., and Blau, H.M. (2010). Substrate elasticity regulates skeletal muscle stem cell self-renewal in culture. *Science* 329, 1078-1081.

Glise, B., Miller, C.A., Crozatier, M., Halbisen, M.A., Wise, S., Olson, D.J., Vincent, A., and Blair, S.S. (2005). Shifted, the *Drosophila* ortholog of Wnt inhibitory factor-1, controls the distribution and movement of Hedgehog. *Dev Cell* 8, 255-266.

Goldspink, G., Wessner, B., and Bachl, N. (2008). Growth factors, muscle function and doping. *Curr Opin Pharmacol* 8, 352-357.

Gopinath, S.D., and Rando, T.A. (2008). Stem cell review series: aging of the skeletal muscle stem cell niche. *Aging Cell* 7, 590-598.

Gorfinkiel, N., Sierra, J., Callejo, A., Ibanez, C., and Guerrero, I. (2005). The *Drosophila* ortholog of the human Wnt inhibitor factor Shifted controls the diffusion of lipid-modified Hedgehog. *Dev Cell* 8, 241-253.

Gros, J., Manceau, M., Thome, V., and Marcelle, C. (2005). A common somitic origin for embryonic muscle progenitors and satellite cells. *Nature* 435, 954-958.

Gulino, A., Di Marcotullio, L., and Screpanti, I. (2010). The multiple functions of Numb. *Exp Cell Res* 316, 900-906.

Hacein-Bey-Abina, S., Garrigue, A., Wang, G.P., Soulier, J., Lim, A., Morillon, E., Clappier, E., Caccavelli, L., Delabesse, E., Beldjord, K., et al. (2008). Insertional oncogenesis in 4 patients after retrovirus-mediated gene therapy of SCID-X1. *J Clin Invest* 118, 3132-3142.

Hacein-Bey-Abina, S., Von Kalle, C., Schmidt, M., McCormack, M.P., Wulfraat, N., Leboulch, P., Lim, A., Osborne, C.S., Pawliuk, R., Morillon, E., et al. (2003). LMO2-associated clonal T cell proliferation in two patients after gene therapy for SCID-X1. *Science* 302, 415-419.

Hammond, C.L., Hinitz, Y., Osborn, D.P., Minchin, J.E., Tettamanti, G., and Hughes, S.M. (2007). Signals and myogenic regulatory factors restrict pax3 and pax7 expression to dermomyotome-like tissue in zebrafish. *Dev Biol* 302, 504-521.

Han, R., and Campbell, K.P. (2007). Dysferlin and muscle membrane repair. *Curr Opin Cell Biol* 19, 409-416.

Hernandez-Hernandez, J.M., Delgado-Olguin, P., Aguillon-Huerta, V., Furlan-Magaril, M., Recillas-Targa, F., and Coral-Vazquez, R.M. (2009). Sox9 represses alpha-sarcoglycan gene expression in early myogenic differentiation. *J Mol Biol* 394, 1-14.

Holland, L.Z., Schubert, M., Kozmik, Z., and Holland, N.D. (1999). Amphipax3/7, an amphioxus paired box gene: insights into chordate myogenesis, neurogenesis, and the possible evolutionary precursor of definitive vertebrate neural crest. *Evol Dev* 1, 153-165.

Holland, N.D., and Holland, L.Z. (2006). Stage- and tissue-specific patterns of cell division in embryonic and larval tissues of amphioxus during normal development. *Evol Dev* 8, 142-149.

Holley, S.A. (2007). The genetics and embryology of zebrafish metamerism. *Dev Dyn* 236, 1422-1449.

Hollway, G.E., Bryson-Richardson, R.J., Berger, S., Cole, N.J., Hall, T.E., and Currie, P.D. (2007). Whole-somite rotation generates muscle progenitor cell compartments in the developing zebrafish embryo. *Dev Cell* 12, 207-219.

Hsieh, J.C., Kodjabachian, L., Rebbert, M.L., Rattner, A., Smallwood, P.M., Samos, C.H., Nusse, R., Dawid, I.B., and Nathans, J. (1999). A new secreted protein that binds to Wnt proteins and inhibits their activities. *Nature* 398, 431-436.

Huynh, D., Dai, X.M., Nandi, S., Lightowler, S., Trivett, M., Chan, C.K., Bertoncello, I., Ramsay, R.G., and Stanley, E.R. (2009). Colony stimulating factor-1 dependence of paneth cell development in the mouse small intestine. *Gastroenterology* 137, 136-144, 144 e131-133.

Im, W.B., Phelps, S.F., Copen, E.H., Adams, E.G., Slightom, J.L., and Chamberlain, J.S. (1996). Differential expression of dystrophin isoforms in strains of mdx mice with different mutations. *Hum Mol Genet* 5, 1149-1153.

Ingham, P.W., and Kim, H.R. (2005). Hedgehog signalling and the specification of muscle cell identity in the zebrafish embryo. *Exp Cell Res* 306, 336-342.

Itzkovitz, S., Blat, I.C., Jacks, T., Clevers, H., and van Oudenaarden, A. (2012). Optimality in the development of intestinal crypts. *Cell* 148, 608-619.

Ivanova, N.B., Dimos, J.T., Schaniel, C., Hackney, J.A., Moore, K.A., and Lemischka, I.R. (2002). A stem cell molecular signature. *Science* 298, 601-604.

Jarriault, S., Brou, C., Logeat, F., Schroeter, E.H., Kopan, R., and Israel, A. (1995). Signalling downstream of activated mammalian Notch. *Nature* 377, 355-358.

Jen, Y., Weintraub, H., and Benezra, R. (1992). Overexpression of Id protein inhibits the muscle differentiation program: in vivo association of Id with E2A proteins. *Genes Dev* 6, 1466-1479.

Johnston, I.A., Bower, N.I., and Macqueen, D.J. (2011). Growth and the regulation of myotomal muscle mass in teleost fish. *J Exp Biol* 214, 1617-1628.

Johnston, I.A.H., W.S.; Randall, D.A. (2000). *Muscle Development and Growth: v.18 (Fish Physiology)* (Academic Press Inc.).

Jouliia-Ekaza, D., and Cabello, G. (2006). Myostatin regulation of muscle development: molecular basis, natural mutations, physiopathological aspects. *Exp Cell Res* 312, 2401-2414.

Jürgens, G., Wieschaus, E., Nüsslein-Volhard, C., Kluding, H. (1984). Mutations affecting the pattern of the larval cuticle in *Drosophila melanogaster*. *Development Genes and Evolution* 193, 283-295.

Kari, G., Rodeck, U., and Dicker, A.P. (2007). Zebrafish: an emerging model system for human disease and drug discovery. *Clin Pharmacol Ther* 82, 70-80.

Kauffman, S.A. (1969). Metabolic stability and epigenesis in randomly constructed genetic nets. *J Theor Biol* 22, 437-467.

Keller, C.A., Grill, M.A., and Abmayr, S.M. (1998). A role for nautilus in the differentiation of muscle precursors. *Dev Biol* 202, 157-171.

Kelsh, R.N. (2006). Sorting out Sox10 functions in neural crest development. *Bioessays* 28, 788-798.

Kiel, M.J., He, S., Ashkenazi, R., Gentry, S.N., Teta, M., Kushner, J.A., Jackson, T.L., and Morrison, S.J. (2007). Haematopoietic stem cells do not asymmetrically segregate chromosomes or retain BrdU. *Nature* 449, 238-242.

Kimble, J.E., and White, J.G. (1981). On the control of germ cell development in *Caenorhabditis elegans*. *Dev Biol* 81, 208-219.

Knoblich, J.A. (2008). Mechanisms of asymmetric stem cell division. *Cell* 132, 583-597.

Kopan, R., Nye, J.S., and Weintraub, H. (1994). The intracellular domain of mouse Notch: a constitutively activated repressor of myogenesis directed at the basic helix-loop-helix region of MyoD. *Development* 120, 2385-2396.

Kozmik, Z., Holland, N.D., Kreslova, J., Oliveri, D., Schubert, M., Jonasova, K., Holland, L.Z., Pestarino, M., Benes, V., and Candiani, S. (2007). Pax-Six-Eya-Dach network during amphioxus development: conservation in vitro but context specificity in vivo. *Dev Biol* 306, 143-159.

Kretzschmar, K., and Watt, F.M. (2012). Lineage tracing. *Cell* 148, 33-45.

Kuang, S., Gillespie, M.A., and Rudnicki, M.A. (2008). Niche regulation of muscle satellite cell self-renewal and differentiation. *Cell Stem Cell* 2, 22-31.

Kuang, S., Kuroda, K., Le Grand, F., and Rudnicki, M.A. (2007). Asymmetric self-renewal and commitment of satellite stem cells in muscle. *Cell* 129, 999-1010.

Langlands, K., Yin, X., Anand, G., and Prochownik, E.V. (1997). Differential interactions of Id proteins with basic-helix-loop-helix transcription factors. *J Biol Chem* 272, 19785-19793.

Lansdorp, P.M. (2007). Immortal strands? Give me a break. *Cell* 129, 1244-1247.

Lee, S.J., and McPherron, A.C. (1999). Myostatin and the control of skeletal muscle mass. *Curr Opin Genet Dev* 9, 604-607.

Lee, S.J., and McPherron, A.C. (2001). Regulation of myostatin activity and muscle growth. *Proc Natl Acad Sci U S A* 98, 9306-9311.

Leimeister, C., Externbrink, A., Klamt, B., and Gessler, M. (1999). Hey genes: a novel subfamily of hairy- and Enhancer of split related genes specifically expressed during mouse embryogenesis. *Mech Dev* 85, 173-177.

Lepper, C., and Fan, C.M. (2010). Inducible lineage tracing of Pax7-descendant cells reveals embryonic origin of adult satellite cells. *Genesis* 48, 424-436.

Leychkis, Y., Munzer, S.R., and Richardson, J.L. (2009). What is stemness? *Stud Hist Philos Biol Biomed Sci* 40, 312-320.

Liepinsh, E., Banyai, L., Patthy, L., and Otting, G. (2006). NMR structure of the WIF domain of the human Wnt-inhibitory factor-1. *J Mol Biol* 357, 942-950.

Lindstrom, M., Pedrosa-Domellof, F., and Thornell, L.E. (2010). Satellite cell heterogeneity with respect to expression of MyoD, myogenin, Dlk1 and c-Met in human skeletal muscle: application to a cohort of power lifters and sedentary men. *Histochem Cell Biol* 134, 371-385.

Lister, J.A., Robertson, C.P., Lepage, T., Johnson, S.L., and Raible, D.W. (1999). nacre encodes a zebrafish microphthalmia-related protein that regulates neural-crest-derived pigment cell fate. *Development* 126, 3757-3767.

Lopez-Garcia, C., Klein, A.M., Simons, B.D., and Winton, D.J. (2010). Intestinal stem cell replacement follows a pattern of neutral drift. *Science* 330, 822-825.

Louvi, A., and Artavanis-Tsakonas, S. (2012). Notch and disease: A growing field. *Semin Cell Dev Biol*.

Lu, J., Webb, R., Richardson, J.A., and Olson, E.N. (1999). MyoR: a muscle-restricted basic helix-loop-helix transcription factor that antagonizes the actions of MyoD. *Proc Natl Acad Sci U S A* 96, 552-557.

Lun, Y., Sawadogo, M., and Perry, M. (1997). Autoactivation of *Xenopus* MyoD transcription and its inhibition by USF. *Cell Growth Differ* 8, 275-282.

Luo, D., Renault, V.M., and Rando, T.A. (2005). The regulation of Notch signaling in muscle stem cell activation and postnatal myogenesis. *Semin Cell Dev Biol* 16, 612-622.

Macarthur, B.D., Ma'ayan, A., and Lemischka, I.R. (2009). Systems biology of stem cell fate and cellular reprogramming. *Nat Rev Mol Cell Biol* 10, 672-681.

Malinauskas, T. (2008). Docking of fatty acids into the WIF domain of the human Wnt inhibitory factor-1. *Lipids* 43, 227-230.

Malinauskas, T., Aricescu, A.R., Lu, W., Siebold, C., and Jones, E.Y. (2011). Modular mechanism of Wnt signaling inhibition by Wnt inhibitory factor 1. *Nature structural & molecular biology* 18, 886-893.

Mankoo, B.S., Skuntz, S., Harrigan, I., Grigorieva, E., Candia, A., Wright, C.V., Arnheiter, H., and Pachnis, V. (2003). The concerted action of Meox homeobox genes is required upstream of genetic pathways essential for the formation, patterning and differentiation of somites. *Development* 130, 4655-4664.

Mansouri, A., and Gruss, P. (1998). Pax3 and Pax7 are expressed in commissural neurons and restrict ventral neuronal identity in the spinal cord. *Mech Dev* 78, 171-178.

Mansouri, A., Stoykova, A., Torres, M., and Gruss, P. (1996). Dysgenesis of cephalic neural crest derivatives in Pax7<sup>-/-</sup> mutant mice. *Development* 122, 831-838.

Marschallinger, J., Obermayer, A., Sanger, A.M., Stoiber, W., and Steinbacher, P. (2009). Postembryonic fast muscle growth of teleost fish depends upon a nonuniformly distributed population of mitotically active Pax7<sup>+</sup> precursor cells. *Dev Dyn* 238, 2442-2448.

Marshman, E., Booth, C., and Potten, C.S. (2002). The intestinal epithelial stem cell. *Bioessays* 24, 91-98.

Martina, E., Chiquet-Ehrismann, R., and Brellier, F. (2010). Tenascin-W: an extracellular matrix protein associated with osteogenesis and cancer. *Int J Biochem Cell Biol* 42, 1412-1415.

Martinelli, D.C., and Fan, C.M. (2007a). Gas1 extends the range of Hedgehog action by facilitating its signaling. *Genes Dev* 21, 1231-1243.

Martinelli, D.C., and Fan, C.M. (2007b). The role of Gas1 in embryonic development and its implications for human disease. *Cell Cycle* 6, 2650-2655.

Mathé, G. (1959). Transfusions et greffes de moelle osseuse homologue chez des humains irradiés à haute dose accidentellement. *Revue française d'études cliniques et biologiques* 4, 226-238.

Mauro, A. (1961). Satellite cell of skeletal muscle fibers. *J Biophys Biochem Cytol* 9, 493-495.

McKinnell, I.W., Ishibashi, J., Le Grand, F., Punch, V.G., Addicks, G.C., Greenblatt, J.F., Dilworth, F.J., and Rudnicki, M.A. (2008). Pax7 activates myogenic genes by recruitment of a histone methyltransferase complex. *Nat Cell Biol* 10, 77-84.

McPherron, A.C., Lawler, A.M., and Lee, S.J. (1997). Regulation of skeletal muscle mass in mice by a new TGF-beta superfamily member. *Nature* 387, 83-90.

McPherron, A.C., and Lee, S.J. (1997). Double muscling in cattle due to mutations in the myostatin gene. *Proc Natl Acad Sci U S A* 94, 12457-12461.

Megeney, L.A., Kablar, B., Garrett, K., Anderson, J.E., and Rudnicki, M.A. (1996). MyoD is required for myogenic stem cell function in adult skeletal muscle. *Genes Dev* 10, 1173-1183.

Melnikova, I.N., Bounpheng, M., Schatteman, G.C., Gilliam, D., and Christy, B.A. (1999). Differential biological activities of mammalian Id proteins in muscle cells. *Exp Cell Res* 247, 94-104.

Meregalli, M., Farini, A., Colleoni, F., Cassinelli, L., and Torrente, Y. (2012). The Role of Stem Cells in Muscular Dystrophies. *Curr Gene Ther*.

Mikkers, H., and Frisen, J. (2005). Deconstructing stemness. *EMBO J* 24, 2715-2719.

Minchin, J.E., and Hughes, S.M. (2008). Sequential actions of Pax3 and Pax7 drive xanthophore development in zebrafish neural crest. *Dev Biol* 317, 508-522.

Miura, T., Kishioka, Y., Wakamatsu, J., Hattori, A., and Nishimura, T. (2010). Interaction between myostatin and extracellular matrix components. *Anim Sci J* 81, 102-107.

Molkentin, J.D., Black, B.L., Martin, J.F., and Olson, E.N. (1995). Cooperative activation of muscle gene expression by MEF2 and myogenic bHLH proteins. *Cell* 83, 1125-1136.

Montarras, D., Morgan, J., Collins, C., Relaix, F., Zaffran, S., Cumano, A., Partridge, T., and Buckingham, M. (2005). Direct isolation of satellite cells for skeletal muscle regeneration. *Science* 309, 2064-2067.

Morgan, T.H. (1917). The theory of the gene. *American Naturalist* 51, 513-544.

Morrison, J.I., Loof, S., He, P., and Simon, A. (2006). Salamander limb regeneration involves the activation of a multipotent skeletal muscle satellite cell population. *J Cell Biol* 172, 433-440.

Morrison, S.J., and Kimble, J. (2006). Asymmetric and symmetric stem-cell divisions in development and cancer. *Nature* 441, 1068-1074.

Morrison, S.J., and Spradling, A.C. (2008). Stem cells and niches: mechanisms that promote stem cell maintenance throughout life. *Cell* 132, 598-611.

Mosher, D.F., and Adams, J.C. (2012). Adhesion-modulating/matricellular ECM protein families: a structural, functional and evolutionary appraisal. *Matrix biology : journal of the International Society for Matrix Biology* 31, 155-161.

Moss, F.P., and Leblond, C.P. (1971). Satellite cells as the source of nuclei in muscles of growing rats. *Anat Rec* 170, 421-435.

Mourikis, P., Sambasivan, R., Castel, D., Rocheteau, P., Bizzarro, V., and Tajbakhsh, S. (2012). A critical requirement for notch signaling in maintenance of the quiescent skeletal muscle stem cell state. *Stem Cells* 30, 243-252.

Naidu, P.S., Ludolph, D.C., To, R.Q., Hinterberger, T.J., and Konieczny, S.F. (1995). Myogenin and MEF2 function synergistically to activate the MRF4 promoter during myogenesis. *Mol Cell Biol* 15, 2707-2718.

Nüsslein-Volhard, C., Dahm, R., (2002). *Zebrafish - A Practical Approach* (Oxford University Press).

Nüsslein-Volhard, C., Wieschaus, E., Kluding, H. (1984). Mutations affecting the pattern of the larval cuticle in *Drosophila melanogaster*. *Development Genes and Evolution* 193, 267-282.

Nye, J.S., Kopan, R., and Axel, R. (1994). An activated Notch suppresses neurogenesis and myogenesis but not gliogenesis in mammalian cells. *Development* 120, 2421-2430.

Oatley, J.M., Oatley, M.J., Avarbock, M.R., Tobias, J.W., and Brinster, R.L. (2009). Colony stimulating factor 1 is an extrinsic stimulator of mouse spermatogonial stem cell self-renewal. *Development* 136, 1191-1199.

Odenthal, J., Rossnagel, K., Haffter, P., Kelsh, R.N., Vogelsang, E., Brand, M., van Eeden, F.J., Furutani-Seiki, M., Granato, M., Hamerschmidt, M., et al. (1996). Mutations affecting xanthophore pigmentation in the zebrafish, *Danio rerio*. *Development* 123, 391-398.

Ohlstein, B., and Spradling, A. (2006). The adult *Drosophila* posterior midgut is maintained by pluripotent stem cells. *Nature* 439, 470-474.

Ordahl, C.P., and Christ, B. (1997). Avian somite transplantation: a review of basic methods. *Methods in cell biology* 52, 3-27.

Oskarsson, T., Acharyya, S., Zhang, X.H., Vanharanta, S., Tavazoie, S.F., Morris, P.G., Downey, R.J., Manova-Todorova, K., Brogi, E., and Massague, J. (2011). Breast cancer cells produce tenascin C as a metastatic niche component to colonize the lungs. *Nat Med* 17, 867-874.

Otto, A., Schmidt, C., and Patel, K. (2006). Pax3 and Pax7 expression and regulation in the avian embryo. *Anat Embryol (Berl)* 211, 293-310.

Pallafacchina, G., Francois, S., Regnault, B., Czarny, B., Dive, V., Cumanò, A., Montarras, D., and Buckingham, M. (2010). An adult tissue-specific stem cell in its niche: a gene profiling analysis of in vivo quiescent and activated muscle satellite cells. *Stem Cell Res* 4, 77-91.

Parichy, D.M., Ransom, D.G., Paw, B., Zon, L.I., and Johnson, S.L. (2000). An orthologue of the kit-related gene *fms* is required for development of neural crest-derived xanthophores and a subpopulation of adult melanocytes in the zebrafish, *Danio rerio*. *Development* 127, 3031-3044.

Parker, M.H., Perry, R.L., Fauteux, M.C., Berkes, C.A., and Rudnicki, M.A. (2006). MyoD synergizes with the E-protein HEB beta to induce myogenic differentiation. *Mol Cell Biol* 26, 5771-5783.

Pellettieri, J., and Sanchez Alvarado, A. (2007). Cell turnover and adult tissue homeostasis: from humans to planarians. *Annual review of genetics* 41, 83-105.

Pittet, M.J., and Weissleder, R. (2011). Intravital imaging. *Cell* 147, 983-991.

Pixley, F.J., and Stanley, E.R. (2004). CSF-1 regulation of the wandering macrophage: complexity in action. *Trends in cell biology* 14, 628-638.

Potten, C.S. (1981). Cell replacement in epidermis (keratopoiesis) via discrete units of proliferation. *Int Rev Cytol* 69, 271-318.

Potten, C.S., Booth, C., and Pritchard, D.M. (1997). The intestinal epithelial stem cell: the mucosal governor. *International journal of experimental pathology* 78, 219-243.

Potten, C.S., and Loeffler, M. (1990). Stem cells: attributes, cycles, spirals, pitfalls and uncertainties. Lessons for and from the crypt. *Development* 110, 1001-1020.

Potten, C.S., Owen, G., and Booth, D. (2002). Intestinal stem cells protect their genome by selective segregation of template DNA strands. *J Cell Sci* 115, 2381-2388.

Poulson, D.F. (1937). Chromosomal Deficiencies and the Embryonic Development of *Drosophila Melanogaster*. *Proc Natl Acad Sci U S A* 23, 133-137.

Poulson, D.F. (1940). The effects of certain X-chromosome deficiencies in the embryonic development of *Drosophila melanogaster*. *Journal of Experimental Zoology* 83.

Ramalho-Santos, M., Yoon, S., Matsuzaki, Y., Mulligan, R.C., and Melton, D.A. (2002). "Stemness": transcriptional profiling of embryonic and adult stem cells. *Science* 298, 597-600.

Rebay, I., Fleming, R.J., Fehon, R.G., Cherbas, L., Cherbas, P., and Artavanis-Tsakonas, S. (1991). Specific EGF repeats of Notch mediate interactions with Delta and Serrate: implications for Notch as a multi-functional receptor. *Cell* 67, 687-699.

Relaix, F., Rocancourt, D., Mansouri, A., and Buckingham, M. (2005). A Pax3/Pax7-dependent population of skeletal muscle progenitor cells. *Nature* 435, 948-953.

Rocheteau, P., Gayraud-Morel, B., Siegl-Cachedenier, I., Blasco, M.A., and Tajbakhsh, S. (2012). A subpopulation of adult skeletal muscle stem cells retains all template DNA strands after cell division. *Cell* 148, 112-125.

Rochlin, K., Yu, S., Roy, S., and Baylies, M.K. (2010). Myoblast fusion: when it takes more to make one. *Dev Biol* 341, 66-83.

Rudnicki, M.A., Braun, T., Hinuma, S., and Jaenisch, R. (1992). Inactivation of MyoD in mice leads to up-regulation of the myogenic HLH gene Myf-5 and results in apparently normal muscle development. *Cell* 71, 383-390.

Rudnicki, M.A., and Jaenisch, R. (1995). The MyoD family of transcription factors and skeletal myogenesis. *Bioessays* 17, 203-209.

Rudnicki, M.A., Schnegelsberg, P.N., Stead, R.H., Braun, T., Arnold, H.H., and Jaenisch, R. (1993). MyoD or Myf-5 is required for the formation of skeletal muscle. *Cell* 75, 1351-1359.

Ruiz, C., Huang, W., Hegi, M.E., Lange, K., Hamou, M.F., Fluri, E., Oakeley, E.J., Chiquet-Ehrismann, R., and Orend, G. (2004). Growth promoting signaling by tenascin-C [corrected]. *Cancer Res* 64, 7377-7385.

Sacco, A., Doyonnas, R., Kraft, P., Vitorovic, S., and Blau, H.M. (2008). Self-renewal and expansion of single transplanted muscle stem cells. *Nature* 456, 502-506.

Sacco, A., Mourkioti, F., Tran, R., Choi, J., Llewellyn, M., Kraft, P., Shkreli, M., Delp, S., Pomerantz, J.H., Artandi, S.E., et al. (2010). Short telomeres and stem cell exhaustion model Duchenne muscular dystrophy in mdx/mTR mice. *Cell* 143, 1059-1071.

Sanchez-Arrones, L., Cardozo, M., Nieto-Lopez, F., and Bovolenta, P. (2012). Cdon and Boc: Two transmembrane proteins implicated in cell-cell communication. *Int J Biochem Cell Biol* 44, 698-702.

Sangiorgi, E., and Capecchi, M.R. (2008). Bmi1 is expressed in vivo in intestinal stem cells. *Nat Genet* 40, 915-920.

Sasai, Y., Kageyama, R., Tagawa, Y., Shigemoto, R., and Nakanishi, S. (1992). Two mammalian helix-loop-helix factors structurally related to *Drosophila hairy* and *Enhancer of split*. *Genes Dev* 6, 2620-2634.

Sato, T., van Es, J.H., Snippert, H.J., Stange, D.E., Vries, R.G., van den Born, M., Barker, N., Shroyer, N.F., van de Wetering, M., and Clevers, H. (2011). Paneth cells constitute the niche for Lgr5 stem cells in intestinal crypts. *Nature* 469, 415-418.

Scherberich, A., Tucker, R.P., Samandari, E., Brown-Luedi, M., Martin, D., and Chiquet-Ehrismann, R. (2004). Murine tenascin-W: a novel mammalian tenascin expressed in kidney and at sites of bone and smooth muscle development. *J Cell Sci* 117, 571-581.

Schienda, J., Engleka, K.A., Jun, S., Hansen, M.S., Epstein, J.A., Tabin, C.J., Kunkel, L.M., and Kardon, G. (2006). Somitic origin of limb muscle satellite and side population cells. *Proc Natl Acad Sci U S A* 103, 945-950.

Schofield, R. (1978). The relationship between the spleen colony-forming cell and the haemopoietic stem cell. *Blood Cells* 4, 7-25.

Schroeder, T. (2010). Hematopoietic stem cell heterogeneity: subtypes, not unpredictable behavior. *Cell Stem Cell* 6, 203-207.

Schuster-Gossler, K., Cordes, R., and Gossler, A. (2007). Premature myogenic differentiation and depletion of progenitor cells cause severe muscle hypotrophy in Delta1 mutants. *Proc Natl Acad Sci U S A* 104, 537-542.

Seger, C., Hargrave, M., Wang, X., Chai, R.J., Elworthy, S., and Ingham, P.W. (2011). Analysis of Pax7 expressing myogenic cells in zebrafish muscle development, injury, and models of disease. *Dev Dyn* 240, 2440-2451.

Seipel, K., and Schmid, V. (2005). Evolution of striated muscle: jellyfish and the origin of triploblasty. *Dev Biol* 282, 14-26.

Seo, H.C., Saetre, B.O., Havik, B., Ellingsen, S., and Fjose, A. (1998). The zebrafish Pax3 and Pax7 homologues are highly conserved, encode multiple isoforms and show dynamic segment-like expression in the developing brain. *Mech Dev* 70, 49-63.

Shaffer, J.F., and Gillis, T.E. (2010). Evolution of the regulatory control of vertebrate striated muscle: the roles of troponin I and myosin binding protein-C. *Physiol Genomics* 42, 406-419.

Shinin, V., Gayraud-Morel, B., and Tajbakhsh, S. (2009). Template DNA-strand co-segregation and asymmetric cell division in skeletal muscle stem cells. *Methods Mol Biol* 482, 295-317.

Simons, B.D., and Clevers, H. (2011). Strategies for homeostatic stem cell self-renewal in adult tissues. *Cell* 145, 851-862.

Slack, J.M. (2002). Conrad Hal Waddington: the last Renaissance biologist? *Nat Rev Genet* 3, 889-895.

Snippert, H.J., and Clevers, H. (2011). Tracking adult stem cells. *EMBO Rep* 12, 113-122.

Snippert, H.J., van der Flier, L.G., Sato, T., van Es, J.H., van den Born, M., Kroon-Veenboer, C., Barker, N., Klein, A.M., van Rheenen, J., Simons, B.D., et al. (2010). Intestinal crypt homeostasis results from neutral competition between symmetrically dividing Lgr5 stem cells. *Cell* 143, 134-144.

Spalding, K.L., Arner, E., Westermark, P.O., Bernard, S., Buchholz, B.A., Bergmann, O., Blomqvist, L., Hoffstedt, J., Naslund, E., Britton, T., et al. (2008). Dynamics of fat cell turnover in humans. *Nature* 453, 783-787.

Spalding, K.L., Bhardwaj, R.D., Buchholz, B.A., Druid, H., and Frisen, J. (2005). Retrospective birth dating of cells in humans. *Cell* 122, 133-143.

Spradling, A.C., Nystul, T., Lighthouse, D., Morris, L., Fox, D., Cox, R., Tootle, T., Frederick, R., and Skora, A. (2008). Stem cells and their niches: integrated units that maintain *Drosophila* tissues. *Cold Spring Harb Symp Quant Biol* 73, 49-57.

Steffen, L.S., Guyon, J.R., Vogel, E.D., Beltre, R., Pusack, T.J., Zhou, Y., Zon, L.I., and Kunkel, L.M. (2007). Zebrafish orthologs of human muscular dystrophy genes. *BMC Genomics* 8, 79.

Steinbacher, P., Haslett, J.R., Six, M., Gollmann, H.P., Sanger, A.M., and Stoiber, W. (2006). Phases of myogenic cell activation and possible role of dermomyotome cells in teleost muscle formation. *Dev Dyn* 235, 3132-3143.

Steinhauser, M.L., Bailey, A.P., Senyo, S.E., Guillermier, C., Perlstein, T.S., Gould, A.P., Lee, R.T., and Lechene, C.P. (2012). Multi-isotope imaging mass spectrometry quantifies stem cell division and metabolism. *Nature* 481, 516-519.

Stellabotte, F., Dobbs-McAuliffe, B., Fernandez, D.A., Feng, X., and Devoto, S.H. (2007). Dynamic somite cell rearrangements lead to distinct waves of myotome growth. *Development* 134, 1253-1257.

Summers, A.P., and Koob, T.J. (2002). The evolution of tendon-morphology and material properties. *Comp Biochem Physiol A Mol Integr Physiol* 133, 1159-1170.

Summerton, J., Stein, D., Huang, S.B., Matthews, P., Weller, D., and Partridge, M. (1997). Morpholino and phosphorothioate antisense oligomers compared in cell-free and in-cell systems. *Antisense Nucleic Acid Drug Dev* 7, 63-70.

- Summerton, J., and Weller, D. (1997). Morpholino antisense oligomers: design, preparation, and properties. *Antisense Nucleic Acid Drug Dev* 7, 187-195.
- Sun, D., Li, H., and Zolkiewska, A. (2008). The role of Delta-like 1 shedding in muscle cell self-renewal and differentiation. *J Cell Sci* 121, 3815-3823.
- Surmann-Schmitt, C., Widmann, N., Dietz, U., Saeger, B., Eitzinger, N., Nakamura, Y., Rattel, M., Latham, R., Hartmann, C., von der Mark, H., et al. (2009). Wif-1 is expressed at cartilage-mesenchyme interfaces and impedes Wnt3a-mediated inhibition of chondrogenesis. *J Cell Sci* 122, 3627-3637.
- Suster, M.L., Abe, G., Schouw, A., and Kawakami, K. (2011). Transposon-mediated BAC transgenesis in zebrafish. *Nat Protoc* 6, 1998-2021.
- Suster, M.L., Kikuta, H., Urasaki, A., Asakawa, K., and Kawakami, K. (2009). Transgenesis in zebrafish with the tol2 transposon system. *Methods Mol Biol* 561, 41-63.
- Tai, P.W., Fisher-Aylor, K.I., Himeda, C.L., Smith, C.L., Mackenzie, A.P., Helterline, D.L., Angello, J.C., Welikson, R.E., Wold, B.J., and Hauschka, S.D. (2011). Differentiation and fiber type-specific activity of a muscle creatine kinase intronic enhancer. *Skeletal muscle* 1, 25.
- Tanaka, E.M., and Reddien, P.W. (2011). The cellular basis for animal regeneration. *Dev Cell* 21, 172-185.
- Tapscott, S.J., and Weintraub, H. (1991). MyoD and the regulation of myogenesis by helix-loop-helix proteins. *J Clin Invest* 87, 1133-1138.
- Thisse, B., Heyer, V., Lux, A., Alunni, V., Degrave, A., Seiliez, I., Kirchner, J., Parkhill, J.P., and Thisse, C. (2004). Spatial and temporal expression of the zebrafish genome by large-scale in situ hybridization screening. *Methods in cell biology* 77, 505-519.
- Thisse, B.T., C (2004). Fast release clones: A high throughput expression analysis. ZFIN direct data submission (<http://zfin.org>).
- Thomas, E. (2005). Bone marrow transplantation from the personal viewpoint. *Int J Hematol* 81, 89-93.

Tian, H., Biehs, B., Warming, S., Leong, K.G., Rangell, L., Klein, O.D., and de Sauvage, F.J. (2011). A reserve stem cell population in small intestine renders Lgr5-positive cells dispensable. *Nature* 478, 255-259.

Till, J.E., and McCulloch, E.A. (1961). A direct measurement of the radiation sensitivity of normal mouse bone marrow cells. *Radiat Res* 14, 213-222.

Tsivitse, S. (2010). Notch and Wnt signaling, physiological stimuli and postnatal myogenesis. *Int J Biol Sci* 6, 268-281.

Tumbar, T., Guasch, G., Greco, V., Blanpain, C., Lowry, W.E., Rendl, M., and Fuchs, E. (2004). Defining the epithelial stem cell niche in skin. *Science* 303, 359-363.

Uemura, T., Shepherd, S., Ackerman, L., Jan, L.Y., and Jan, Y.N. (1989). *numb*, a gene required in determination of cell fate during sensory organ formation in *Drosophila* embryos. *Cell* 58, 349-360.

Vandekerckhove, J., and Weber, K. (1984). Chordate muscle actins differ distinctly from invertebrate muscle actins. The evolution of the different vertebrate muscle actins. *J Mol Biol* 179, 391-413.

Vasyutina, E., Lenhard, D.C., Wende, H., Erdmann, B., Epstein, J.A., and Birchmeier, C. (2007). RBP-J (Rbpsiuh) is essential to maintain muscle progenitor cells and to generate satellite cells. *Proc Natl Acad Sci U S A* 104, 4443-4448.

Velloso, C.P. (2008). Regulation of muscle mass by growth hormone and IGF-I. *Br J Pharmacol* 154, 557-568.

Vilquin, J.T., Catelain, C., and Vauchez, K. (2011). Cell therapy for muscular dystrophies: advances and challenges. *Curr Opin Organ Transplant* 16, 640-649.

von Holst, A. (2008). Tenascin C in stem cell niches: redundant, permissive or instructive? *Cells Tissues Organs* 188, 170-177.

Voog, J., and Jones, D.L. (2010). Stem cells and the niche: a dynamic duo. *Cell Stem Cell* 6, 103-115.

Waddington, C.H. (1957). The strategy of the genes. A discussion of some aspects of theoretical biology. With an appendix by H. Kacser. (London: G. Allen and Unwin).

Wakamatsu, Y., Osumi, N., and Weston, J.A. (2004). Expression of a novel secreted factor, Seraf indicates an early segregation of Schwann cell precursors from neural crest during avian development. *Dev Biol* 268, 162-173.

Wang, J., Zhang, K., Xu, L., and Wang, E. (2011). Quantifying the Waddington landscape and biological paths for development and differentiation. *Proc Natl Acad Sci U S A* 108, 8257-8262.

Wang, T., Hanington, P.C., Belosevic, M., and Secombes, C.J. (2008). Two macrophage colony-stimulating factor genes exist in fish that differ in gene organization and are differentially expressed. *J Immunol* 181, 3310-3322.

Weber, P., Montag, D., Schachner, M., and Bernhardt, R.R. (1998). Zebrafish tenascin-W, a new member of the tenascin family. *J Neurobiol* 35, 1-16.

Weilbaecher, K.N., Motyckova, G., Huber, W.E., Takemoto, C.M., Hemesath, T.J., Xu, Y., Hershey, C.L., Dowland, N.R., Wells, A.G., and Fisher, D.E. (2001). Linkage of M-CSF signaling to Mitf, TFE3, and the osteoclast defect in Mitf(mi/mi) mice. *Mol Cell* 8, 749-758.

Weinberg, E.S., Allende, M.L., Kelly, C.S., Abdelhamid, A., Murakami, T., Andermann, P., Doerre, O.G., Grunwald, D.J., and Riggelman, B. (1996). Developmental regulation of zebrafish MyoD in wild-type, no tail and spadetail embryos. *Development* 122, 271-280.

Weintraub, H., Davis, R., Tapscott, S., Thayer, M., Krause, M., Ben-zra, R., Blackwell, T.K., Turner, D., Rupp, R., Hollenberg, S., et al. (1991a). The myoD gene family: nodal point during specification of the muscle cell lineage. *Science* 251, 761-766.

Weintraub, H., Dwarki, V.J., Verma, I., Davis, R., Hollenberg, S., Snider, L., Lassar, A., and Tapscott, S.J. (1991b). Muscle-specific transcriptional activation by MyoD. *Genes Dev* 5, 1377-1386.

Weissman, I.L. (2000). Stem cells: units of development, units of regeneration, and units in evolution. *Cell* 100, 157-168.

Wen, Y., Bi, P., Liu, W., Asakura, A., Keller, C., and Kuang, S. (2012). Constitutive Notch activation upregulates Pax7 and promotes the self-renewal of skeletal muscle satellite cells. *Mol Cell Biol*.

Wharton, K.A., Johansen, K.M., Xu, T., and Artavanis-Tsakonas, S. (1985). Nucleotide sequence from the neurogenic locus notch implies a gene product that shares homology with proteins containing EGF-like repeats. *Cell* 43, 567-581.

Wieschaus, E., Nüsslein-Volhard, C., Jürgens, G. (1984). Mutations affecting the pattern of the larval cuticle in *Drosophila melanogaster*. *Development Genes and Evolution* 193, 296-307.

Wolpert, L. (1971). Positional information and pattern formation. *Curr Top Dev Biol* 6, 183-224.

Wolpert, L.B., R; Jessell, T; Lawrence, P; Meyerowitz, E; Smith, J; (2002). *Principles of development* (2nd ed.) (Oxford university press).

Xie, T., and Spradling, A.C. (1998). decapentaplegic is essential for the maintenance and division of germline stem cells in the *Drosophila* ovary. *Cell* 94, 251-260.

Xie, T., and Spradling, A.C. (2000). A niche maintaining germ line stem cells in the *Drosophila* ovary. *Science* 290, 328-330.

Yan, K.S., Chia, L.A., Li, X., Ootani, A., Su, J., Lee, J.Y., Su, N., Luo, Y., Heilshorn, S.C., Amieva, M.R., et al. (2012). The intestinal stem cell markers *Bmi1* and *Lgr5* identify two functionally distinct populations. *Proc Natl Acad Sci U S A* 109, 466-471.

Yaron, A., and Sprinzak, D. (2012). The cis side of juxtacrine signaling: a new role in the development of the nervous system. *Trends in neurosciences* 35, 230-239.

Yin, A., Korzh, V., and Gong, Z. (2012). Perturbation of zebrafish swimbladder development by enhancing Wnt signaling in *Wif1* morphants. *Biochim Biophys Acta* 1823, 236-244.

Youn, B.W., and Malacinski, G.M. (1981). Somitogenesis in the amphibian *Xenopus laevis*: scanning electron microscopic analysis of intrasomitic cellular arrangements during somite rotation. *J Embryol Exp Morphol* 64, 23-43.

Zhang, J.M., Chen, L., Krause, M., Fire, A., and Paterson, B.M. (1999). Evolutionary conservation of MyoD function and differential utilization of E proteins. *Dev Biol* 208, 465-472.

Zhao, C., Deng, W., and Gage, F.H. (2008). Mechanisms and functional implications of adult neurogenesis. *Cell* 132, 645-660.



— Vom Eise befreit sind Strom und Bäche,  
durch des Frühlings holden belebenden Blick —

Goethe, Faust

# 25

## Curriculum vitae

**Sören Alsheimer**

Diplom-Biologe

Neckarhalde 20 | 72070 | Tübingen

Geboren am 9. Mai 1980 in Frankfurt am Main

deutsch

ledig

### Tabellarischer Lebenslauf

- **1990-1999** Heinrich-von-Gagern Gymnasium in Frankfurt am Main, humanistisches Gymnasium mit neusprachlichem Zweig
- **1990-1999** Ehrenamtliche Tätigkeit für die Vogelschutzwarte für Hessen, Rheinland-Pfalz und Saarland, Frankfurt am Main
- **1999** Abitur einschließlich Latinum und Graecum am Heinrich-von-Gagern Gymnasium in Frankfurt am Main (Note: 2,0)
- **1999-2000** Wehrdienst bei 4.Transportbatallion/370 in Diez an der Lahn
- **2000-2005** Studium der Biologie, Goethe Universität Frankfurt am Main
- **2002** Diplom-Vorprüfung
- **2004-2005** Diplomarbeit „Plant Processing Bodies are Dynamic mRNP Decay Complexes“ bei Prof. Dr. Lutz Nover, Botanisches Institut der Goethe Universität Frankfurt am Main
- **2005** Diplom in Biologie mit Schwerpunkten Mikrobiologie, Genetik sowie Zell- und Entwicklungsbiologie, Goethe Universität Frankfurt am Main
- **2005-2006** Studium der Medizin, Goethe Universität Frankfurt am Main
- **2006-heute** Promotion bei Prof. Dr. Christiane Nüsslein-Volhard am Max-Planck-Institut für Entwicklungsbiologie, Tübingen
- **2006-2009** Stipendiat der Max-Planck-Gesellschaft
- **2009-heute** Wissenschaftlicher Angestellter der Max-Planck-Gesellschaft
- **2006-2009** Doktorandenvertreter für die Doktoranden des Max-Planck-Instituts für Entwicklungsbiologie und Friedrich-Miescher-Laboratoriums, Tübingen
- **2007-2008** Doktorandenvertreter für die Doktoranden der biomedizinischen Sektion der Max-Planck-Gesellschaft und Mitglied des Vorstands von ‘PhDnet’ der Doktorandenvertretung der Max-Planck-Gesellschaft

**Beiträge zu internationalen Konferenzen**

- **5th Post-transcriptional Regulation of Plant Gene Expression (PTRoPGE) Symposium**  
8 - 12 June | 2005 | Austin | Texas | USA  
Poster: 'Plant Processing Bodies are Dynamic mRNP Decay Complexes'
- **The Molecular and Cellular Mechanisms Regulating Skeletal Muscle Development and Regeneration**  
EMBO Conference Series  
24 - 29 September | 2008 | Sant Feliu de Guixols | Spanien  
Poster: 'Myogenesis live: Using a pax7GFP zebrafish transgenic line to study the myogenic lineage in vivo'
- **Christiane Nüsslein-Volhard Alumni Meeting**  
5 - 10 July | 2009 | Schloss Ringberg | Deutschland  
Vortrag: 'Muscle Stem Cell Imaging'
- **Molecular and Cellular Basis of Regeneration and Tissue Repair**  
EMBO Conference Series  
26 - 30 September | 2010 | Sesimbra | Portugal  
Vortrag: 'In vivo Imaging of Muscle Stem Cells and Muscle Regeneration in Zebrafish'
- **The Molecular and Cellular Mechanisms, Regulating Skeletal Muscle, Development and Regeneration**  
EMBO Conference Series  
10 - 15 Mai | 2011 | Wiesbaden | Deutschland  
Vortrag: 'Muscle Stem Cells Secrete Tenascin W, a Key Component of Their Niche'
- **Fish Muscle Growth and Repair; Models Linking Biomedicine and Aquaculture**  
Company of Biologists Workshop  
26 - 29 Juni | 2011 | Wiston House | Vereinigtes Königreich  
Vortrag: 'Muscle Stem Cells Secrete Tenascin W, a Key Component of Their Niche'